CONTRACTOR REPORT BRL-CR-611

BRL

A STUDY OF THE EFFECTS OF THERMAL SHIELD TEMPERATURE CHANGES ON GUN TUBE CURVATURE

H. B. KINGSBURY
A. V. KALBAG

JUNE 1989

U.S. ARMY LABORATORY COMMAND

BALLISTIC RESEARCH LABORATORY
ABERDEEN PROVING GROUND, MARYLAND

DESTRUCTION NOTICE

Destroy this report when it is no longer needed. DO NOT return it to the originator.

Additional copies of this report may be obtained from the National Technical Information Service, U.S. Department of Commerce, Springfield, VA 22161.

The findings of this report are not to be construed as an official Department of the Army position, unless so designated by other authorized documents.

The use of trade names or manufacturers' names in this report does not constitute indorsement of any commercial product.

UNCLASSIFIED

SECURITY CLASSIFICATION OF THIS PAGE

REPORT DOCUMENTATION PAGE

Form Approved OMB No. 0704-0188

1a. REPORT SECURITY CLASSIFICATION UNCLASSIFIED	1b. RESTRICTIVE MARKINGS
2a. SECURITY CLASSIFICATION AUTHORITY	3. DISTRIBUTION/AVAILABILITY OF REPORT APPROVED FOR PUBLIC RELEASE; DISTRIBUTION UNLIMITED
2b. DECLASSIFICATION/DOWNGRADING SCHEDULE	
4. PERFORMING ORGANIZATION REPORT NUMBER(S) BRL-CR-611	5. MONITORING ORGANIZATION REPORT NUMBER(S)
6a. NAME OF PERFORMING ORGANIZATION University of Delaware Dept of Mechancial Engineering 6b. OFFICE SYMBOL (If applicable)	7a. NAME OF MONITORING ORGANIZATION
6c. ADDRESS (City, State, and ZIP Code) Newark, Delaware 19716	7b. ADDRESS (City, State, and ZIP Code)
8a. NAME OF FUNDING/SPONSORING ORGANIZATION Ballistic Research Laboratory Mechanical and Structures Branch 8b. OFFICE SYMBOL (If applicable) SLCBR-IB-M	9. PROCUREMENT INSTRUMENT IDENTIFICATION NUMBER
8c. ADDRESS (City, State, and ZIP Code) Ballistic Research Laboratory Aberdeen Proving Ground, MD 21005-5066	10. SOURCE OF FUNDING NUMBERS PROGRAM ELEMENT NO. / PROJECT NO. 1L16110 2AH43 / TASK NO. / WORK UNIT ACCESSION NO.
11. TITLE (Include Security Classification) (U) A STUDY OF THE EFFECTS OF THERMAL SHIELD TEMPERATURE CHANGES ON GUN TUBE CURVATURE	
12. PERSONAL AUTHOR(S) Herbert B. Kingsbury and Ashwin V. Kalbag	
13a. TYPE OF REPORT CR 13b. TIME COVERED FROM _____ TO _____	14. DATE OF REPORT (Year, Month, Day) ~~86 December~~
15. PAGE COUNT	
16. SUPPLEMENTARY NOTATION	

17. COSATI CODES			18. SUBJECT TERMS (Continue on reverse if necessary and identify by block number)
FIELD	GROUP	SUB-GROUP	Heat Transfer, Gun Tubes, Thermal Shroud, Initially Curved Gun Tube, Curved Beam, Accuracy, Jump, Dispersion

19. ABSTRACT (Continue on reverse if necessary and identify by block number)

The subject of this investigation is the deformation and consequent lack of aim that a gun tube undergoes as a result of its initial imperfections. By initial imperfections, we mean the non-straightness of the centroidal axis of the gun tube. In reality, the centroidal axis is a general space curve. For the sake of analysis, however, it is assumed to be helical in shape. The gun tube is modeled as a rod of linearly elastic material, encased in a perfectly straight cylindrical thermal shroud to protect it from non-uniform temperature changes. The interaction between these two elements, namely the shroud and the gun tube renders the problem of finding the muzzle end displacement of the gun tube statically indeterminate.

Two solutions to the problem are proposed herein, using different approaches. In the first, a more exact solution for the gun tube end displacement is obtained by formulating

(con't on back)

20. DISTRIBUTION/AVAILABILITY OF ABSTRACT ☒ UNCLASSIFIED/UNLIMITED ☐ SAME AS RPT. ☐ DTIC USERS	21. ABSTRACT SECURITY CLASSIFICATION UNCLASSIFIED
22a. NAME OF RESPONSIBLE INDIVIDUAL Tom Haug/Bruce Burns	22b. TELEPHONE (Include Area Code) 301-278-6132 / 22c. OFFICE SYMBOL SLCBR-IB-M

DD Form 1473, JUN 86 Previous editions are obsolete. SECURITY CLASSIFICATION OF THIS PAGE

UNCLASSIFIED

an expression for the complementary strain energy of deformation of the rod and then employing Castigliano's Second Theorem, or as it is better known, by the method of minimum complementary strain energy. In the second approach, the differential equations for the problem formulated by Kingsbury are employed and a general finite element of variable curvature and torsion is developed. This element is then used to compute a set of displacements for independent confirmation. The element formulated may be used to analyze tubes or rods of arbitrarily varying cross-section, curvature and torsion. The report includes surface plots from a parametric study of the end displacement as a function of initial curvature and torsion of the gun tube and the conclusions drawn therefrom. Code for a finite element program that uses the element developed has been provided for implementation by the reader.

ACKNOWLEDGEMENTS

I would like to thank my advisor, Dr. Herbert Kingsbury, for his guidance through the entire span of my research, for his numerous suggestions towards this thesis, and for his patience in times of my intellectual lethargy.

I would like to also thank the U.S. Army Ballistics Research Laboratory, Aberdeen, Maryland for the financial support I received during the year 1986. I am deeply indebted to all the faculty members of the department that contributed to my education. I also wish to express my gratitude towards all my friends at the University of Delaware who have made my stay a pleasant experience.

Lastly, I would especially like to thank my friend Denise Celestini, whose unwavering confidence in my abilities helped me see a way through many a passing cloud of self-doubt.

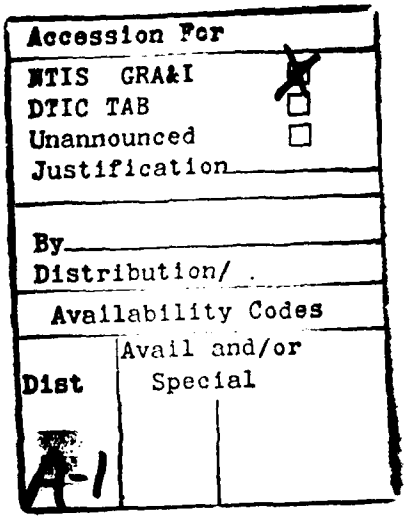

TABLE OF CONTENTS

LIST OF FIGURES

ABSTRACT

The subject of this investigation is the deformation and consequent lack of aim that a gun tube undergoes as a result of its initial imperfections. By initial imperfections, we mean the non-straightness of the centroidal axis of the gun tube. In reality, the centroidal axis is a general space curve. For the sake of analysis, however, it is assumed to be helical in shape. The gun tube is modeled as a rod of linearly elastic material, encased in a perfectly straight cylindrical thermal shroud to protect it from non-uniform temperature changes. The interaction between these two elements, namely, the shroud and the gun tube renders the problem of finding the muzzle end displacement of the gun tube statically indeterminate.

Two solutions to the problem are proposed herein, using different approaches. In the first, a more exact solution for the gun tube end displacement is obtained by formulating an expression for the complementary strain energy of deformation of the rod and then employing Castigliano's Second Theorem, or as it is better known, by the method of minimum complementary strain energy. In the second approach, the differential equations for the problem formulated by Kingsbury are employed and a general finite element of variable curvature and torsion is developed. This element is then used to compute a set of displacements for independent confirmation. The element formulated may be used to analyze tubes or rods of arbitrarily varying cross-section, curvature and torsion. The report includes surface plots from a parametric study of the end displacement as a function of initial curvature and torsion of the gun tube and the conclusions drawn therefrom. Code for a finite element program that uses the element developed has been provided for implementation by the reader.

CHAPTER 1

INTRODUCTION

1.1 Defining the Problem

The work described in the pages to follow is aimed at modeling the imperfections in the straightness of gun tubes. Gun tubes are often subjected to large variations in temperature which arise from several sources, for example, heating due to the firing of rounds of ammunition, cooling due to rainfall or wind, and the effect of field temperature. For this reason, they are encased in a protective outer cylinder called a thermal shroud, whose function is to distribute temperature changes uniformly.

The gun tube and its thermal shroud are attached to a common structural base near the receiver end of the gun and are again structurally connected near the muzzle. The latter connection allows relative motion of the end of the shroud to be transmitted to and to be constrained by the enclosed gun tube. Since the temperature changes are distributed uniformly around any circumference, the shroud does not undergo bending deformations due to thermal strains but expands or contracts axially.

When the gun tube and shroud assembly is subject to a change in temperature, say an increase, the shroud undergoes thermal expansion and thus exerts a force on the gun tube. If the gun tube were to be perfectly straight, this would merely cause it to extend along its centroidal axis, with no change in its aim. However, in reality, no gun tube is perfectly straight so that a change in temperature of the shroud may produce not only an extension of the tube in the direction of its length but also bending deformation, which affects its aim. We endeavor, then, to find the displacement and rotation of the end of the gun tube as a function of the imposed temperature change.

1.2 The Analytical Model

The centroidal axis of the gun tube would, in reality, be an arbitrary space curve. For the purpose of analysis, it is assumed to be helical in shape. It is also assumed that the cross-section of the helical rod is perfectly circular, so that the effects of out-of-roundness or twist of the tube are not considered.

The gun tube, then, is modeled as a helical rod of linearly elastic material, with a constant circular cross-section, which is contained within a thin-walled right circular cylinder representing the thermal shroud. Both the rod and the cylinder are considered fixed at one end to a massive common base. The common attachment at the other end of the rod is such that the relative motion of the end of the cylinder due to thermal strain, can be imparted to - and is constrained by - the rod at their point of intersection. Two cases of compatibility of gun tube and shroud end displacements are considered, the first in which the shroud is assumed to have zero lateral stiffness, and the second in which the shroud has a finite non-zero lateral stiffness. In the former case, the gun tube end displacements and rotations are not affected by the transverse rigidity of the cylinder. In both cases, however, these displacements and rotations are independent of the torsional rigidity of the cylinder.

1.3 Methods of Solution

Two solutions to the problem are proposed herein, using different approaches. In the first, more exact, solution, the end displacement is obtained by formulating an expression for the strain energy of deformation of the rod in terms of the components of the applied force and moment and then employing Castigliano's Second Theorem, or as it is better known, by the method of minimum complementary strain energy. In the second approach, the differential equations for the problem formulated by Kingsbury [Kingsbury 84] are employed and a general finite element of variable curvature and torsion is formulated using the variational method. This element is then used to independently confirm the results of the analytical model.

1.3.1 An Exact Solution

The required displacements are obtained most easily by employing an energy method; to be specific, by using Castigliano's Second Theorem which is stated as follows: If a linearly elastic structure is subjected to a set of loads, the displacement of any load in its direction is equal to the partial derivative of the complementary strain energy with respect to that load. In order to use Castigliano's theorem, an expression for the complementary strain energy of the rod must be formulated. This is done as follows: First, the helix representing the centroidal axis of the gun tube is parameterized in terms of the arc length and expressions are obtained for the vector tangent, binormal and principal normal to the curve at any point along its length. Second, expressions for the internal force and moment components along the local tangent, binormal and principal normal that result from applying a force and a moment to the end of the rod are obtained in terms of the applied force and moment. Thirdly, the complementary strain energy of the rod is written in terms of the internal force and moment components, and therefore, in terms of the applied force and moment. The required scalar displacements are finally obtained by differentiating the complementary strain energy with respect to each component of the applied force and moment.

Since the problem is statically indeterminate, the applied force is not known but is found by enforcing the compatibility of gun tube and shroud end displacements. This force is then used to compute the required displacements. A parametric study of the force and displacement components is performed in which each component is plotted as a function of the initial curvature and torsion of the helical rod. This is done for two cases of compatibility of displacements of the gun tube and the thermal shroud at the muzzle end; one in which the thermal shroud is assumed to have only axial stiffness and no transverse or rotational stiffness and the other in which the shroud has a finite non-zero transverse stiffness. Chapters 2 and 3 present the formulation of the strain energy and equilibrium equations while Chapter 4 deals with the imposition of compatibility of displacements of the muzzle ends of the gun tube and the thermal shroud, and consequent resolution of statical indeterminacy. Chapter 5 contains the above-mentioned parametric study.

1.3.2 A Finite Element Solution

In Chapter 6, an alternative solution is presented which involves the development of a finite beam element which is permitted to have variable curvature and torsion over its length. However, the rate of variation of the curvature and torsion is assumed to be constant in each element. By the use of an assemblage of such finite elements, rods of arbitrarily varying space curvatures can be analyzed.

The element is formulated using the variational method. The equations of motion of a space-curved rod have been formulated by Kingsbury [Kingsbury 84] as a set of four coupled differential equations in four unknown displacements. Every point on the rod has six degrees of freedom: three translations and three rotations. Two of these are expressed in terms of the four unknowns appearing in the differential equations.

The development proceeds as follows: First, a polynomial displacement field is assumed, which satisfies the differential equations exactly in the case in which curvature and torsion are identically zero, that is, in the case of a straight rod. Next, the constant coefficients appearing in the assumed polynomials are found in terms of the nodal values of displacements, and these polynomials are rewritten to yield the shape functions. Then, the expression for linear strain energy density of the rod developed by Tsay and Kingsbury [Tsay 86] is employed as follows. The displacements and their derivatives appearing in this expression are substituted with their equivalents in terms of the assumed displacement field and the strain energy density is integrated over the length of the rod to yield the strain energy of the rod. Finally, the strain energy is differentiated with respect to the nodal values of the displacements to obtain the elements of the stiffness matrix.

Lastly, the finite element is used to independently confirm the values for displacements obtained from the first method. Code for a finite element program has also been provided in Appendix D for implementation by the reader.

CHAPTER 2

INTERNAL FORCES IN THE HELICAL ROD

2.1 Parametric Representation of the Helix: Vector Tangent, Binormal and Principal Normal

2.1.1 Parametric Representation

The geometry of the helical rod is shown in Figure 2.1. Its shape is governed by two parameters: a, which is the length of the circular arc representing the projection of the helical centroidal axis of the rod on the XY plane, and ϕ, the angle subtended by this arc at the origin. The points on the helix can be described in terms of the arc length, s, by a position vector, $\mathbf{r}$, given by:

$$\mathbf{r} = \mathbf{r}(s) = \frac{a}{\phi}\cos\left(\frac{\phi s}{L}\right)\mathbf{i} + \frac{a}{\phi}\sin\left(\frac{\phi s}{L}\right)\mathbf{j} + \frac{b\,s}{L}\mathbf{k} \tag{2.1}$$

We also have the following expressions for the first and second derivatives of $\mathbf{r}$ with respect to s:

$$\mathbf{r}' = \frac{d\mathbf{r}}{ds} = -\frac{a}{L}\sin\left(\frac{\phi s}{L}\right)\mathbf{i} + \frac{a}{L}\cos\left(\frac{\phi s}{L}\right)\mathbf{j} + \frac{b}{L}\mathbf{k} \tag{2.2}$$

$$\mathbf{r}'' = \frac{d^2\mathbf{r}}{ds^2} = -\frac{a\phi}{L^2}\cos\left(\frac{\phi s}{L}\right)\mathbf{i} - \frac{a\phi}{L^2}\sin\left(\frac{\phi s}{L}\right)\mathbf{j} \tag{2.3}$$

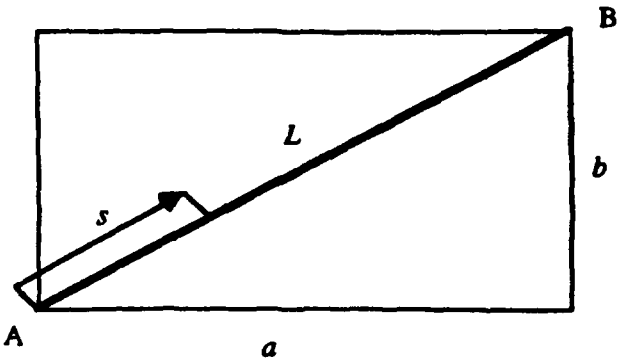

(i) The "Straightened" Helical Arc

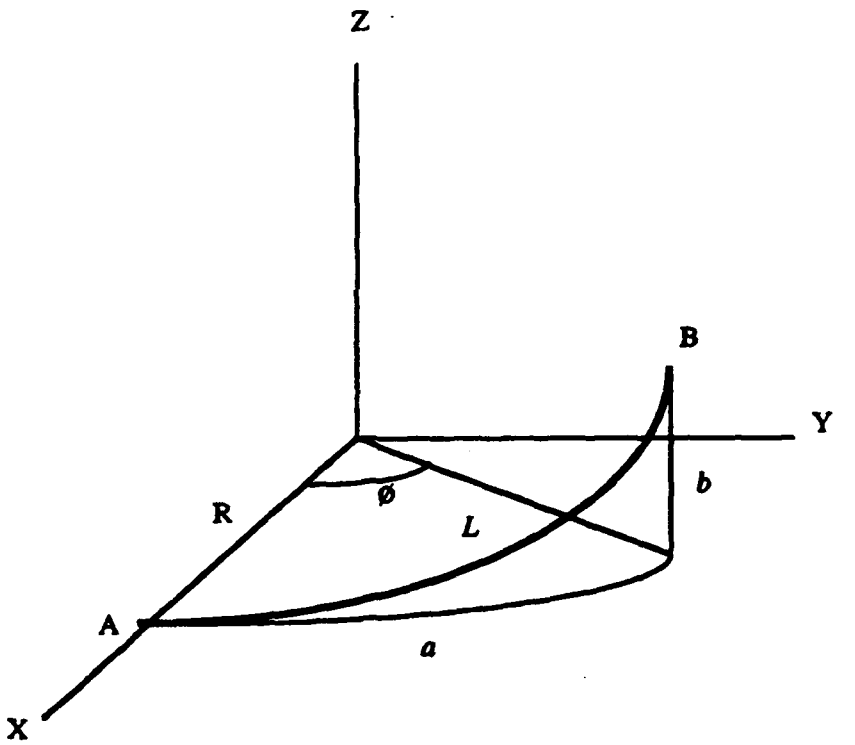

(ii) The Helical Arc and the Global Coordinate System

Figure 2-1: Geometry of the Helical Rod

2.1.2 Vector Tangent, Binormal and Principal Normal

These three characteristic vectors of a space curve form what is sometimes referred to as the *trihedral* associated with the curve [Sokolnikoff 66]. They are shown in Figure 2.2, and at any point along the curve, they are given in terms of the derivatives of the position vector, **r**, by the following relations:

Tangent $\vec{\tau}$:

$$\vec{\tau}(s) = \frac{\mathbf{r}'(s)}{|\mathbf{r}'(s)|} \tag{2.4}$$

Binormal $\vec{\beta}$:

$$\vec{\beta}(s) = \frac{\mathbf{r}'(s) \times \mathbf{r}''(s)}{|\mathbf{r}'(s) \times \mathbf{r}''(s)|} \tag{2.5}$$

Principal Normal $\vec{\nu}$:

$$\vec{\nu}(s) = \vec{\beta}(s) \times \vec{\tau}(s) \tag{2.6}$$

Substituting the derivatives in the above expressions, we find the following expressions for the three unit vectors:

$$\vec{\tau}(s) = -\frac{a}{L}\sin\left(\frac{\phi s}{L}\right)\mathbf{i} + \frac{a}{L}\cos\left(\frac{\phi s}{L}\right)\mathbf{j} + \frac{b}{L}\mathbf{k} \tag{2.7}$$

$$\vec{\beta}(s) = \frac{b}{L}\sin\left(\frac{\phi s}{L}\right)\mathbf{i} - \frac{b}{L}\cos\left(\frac{\phi s}{L}\right)\mathbf{j} + \frac{a}{L}\mathbf{k} \tag{2.8}$$

$$\vec{\nu}(s) = -\cos\left(\frac{\phi s}{L}\right)\mathbf{i} - \sin\left(\frac{\phi s}{L}\right)\mathbf{j} \tag{2.9}$$

The vector tangent, binormal and principal normal form a local coordinate system which varies with every point on the curve. We assume that the tangent points in the local

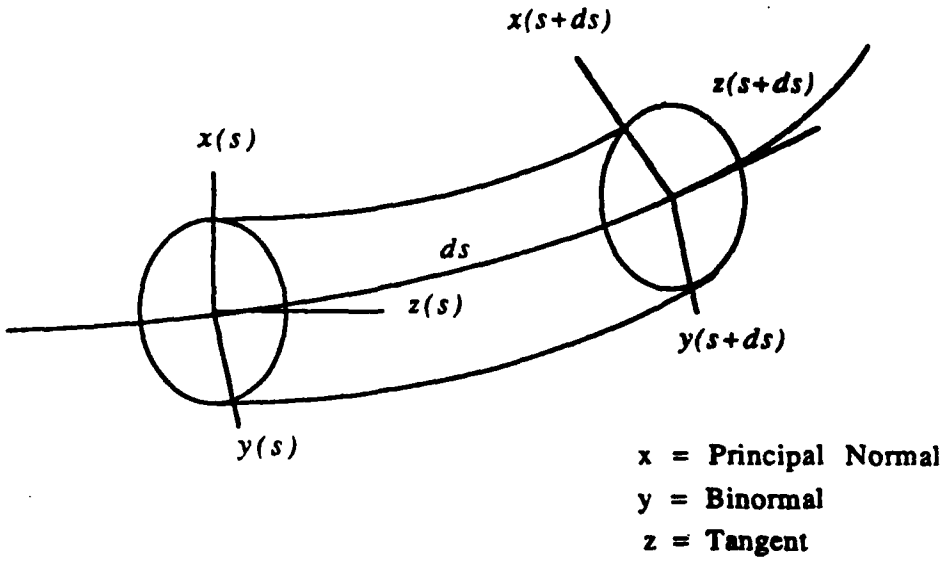

Figure 2-2: Vector Tangent, Binormal and Principal Normal

z or ς direction. Therefore, the principal normal and the binormal point in the local x (ξ) and y (η) directions respectively. In the next section, we shall use these three unit vectors to evaluate the components of the internal force and moment along the directions of the local ξ, η and ς axes.

2.2 Internal Force and Moment Components at a Generic Point

As mentioned in Chapter 1, the muzzle end of the gun tube is structurally connected to the thermal shroud in a manner that allows motion of the end of the shield to be transmitted to and also to be constrained by it. Also, the receiver end of the gun and the shroud are connected to a common massive base. In other words, for our analysis, we need to find the displacement of the free end of a helical rod, the other end being cantilevered. Having done this, we may then apply compatibility of displacements of the shroud and gun tube and find the force that results from their interaction. This

corresponds to the applied force **F** in the discussion to follow.

2.2.1 Internal Force and Moment

We now evaluate the internal force and moment components at a generic point. Figure 2.3 shows the forces acting on the free end of the rod and the corresponding reactions at the fixed end as represented in the global XYZ system.

The applied force at point B, that is, at $s = L$, is **F** given by:

$$\mathbf{F} = F_X\mathbf{i} - F_Y\mathbf{j} + F_Z\mathbf{k} \tag{2.10}$$

The applied moment at point B is **M** given by:

$$\mathbf{M} = M_X\mathbf{i} - M_Y\mathbf{j} + M_Z\mathbf{k} \tag{2.11}$$

The reactions at the fixed end A, that is, at $s = 0$, are a force $\mathbf{F}_R$, and a moment $\mathbf{M}_R$. $\mathbf{F}_R$ is found from force equilibrium as:

$$\mathbf{F}_R = -\mathbf{F} = -F_X\mathbf{i} - F_Y\mathbf{j} - F_Z\mathbf{k} \tag{2.12}$$

$\mathbf{M}_R$ is found from moment equilibrium by summing up moments about the point A, and is given as:

$$\begin{aligned}\mathbf{M}_R &= -\mathbf{M} - \triangle \times \mathbf{F}, \quad \text{where} \quad \triangle = \mathbf{r}(L) - \mathbf{r}(0), \\ &= \left[-M_X + F_Y b - \frac{F_Z a}{\phi}\sin\phi\right]\mathbf{i} - \left[M_Y + F_X b + \frac{F_Z a}{\phi}(1-\cos\phi)\right]\mathbf{j} \\ &\quad + \left[-M_Z + \frac{F_X a}{\phi}\sin\phi + \frac{F_Y a}{\phi}(1-\cos\phi)\right]\mathbf{k}\end{aligned} \tag{2.13}$$

Consider the free body shown in Figure 2.4. Now, from force equilibrium, we have

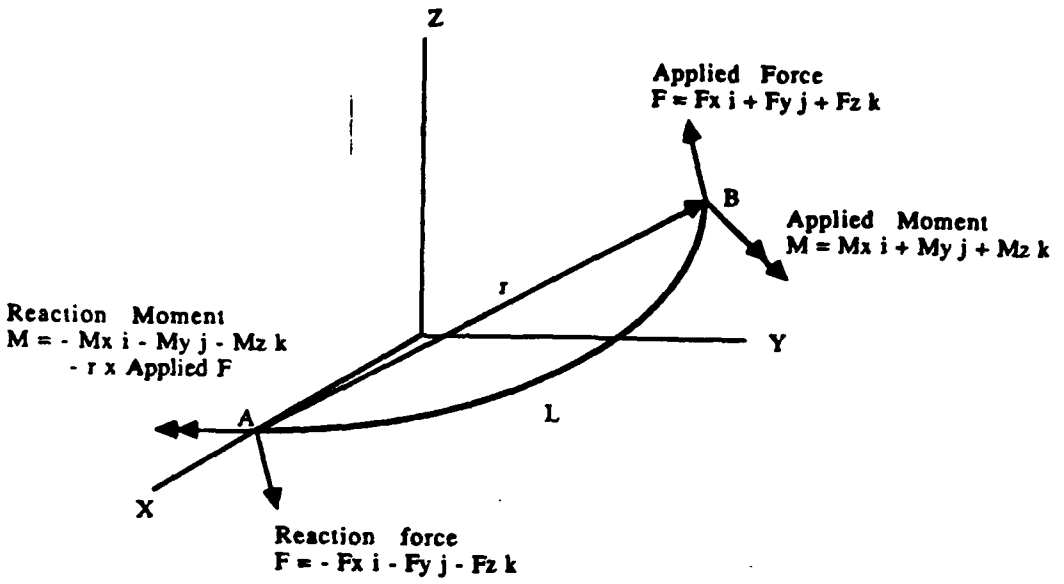

Figure 2-3: Forces on the Helical Rod

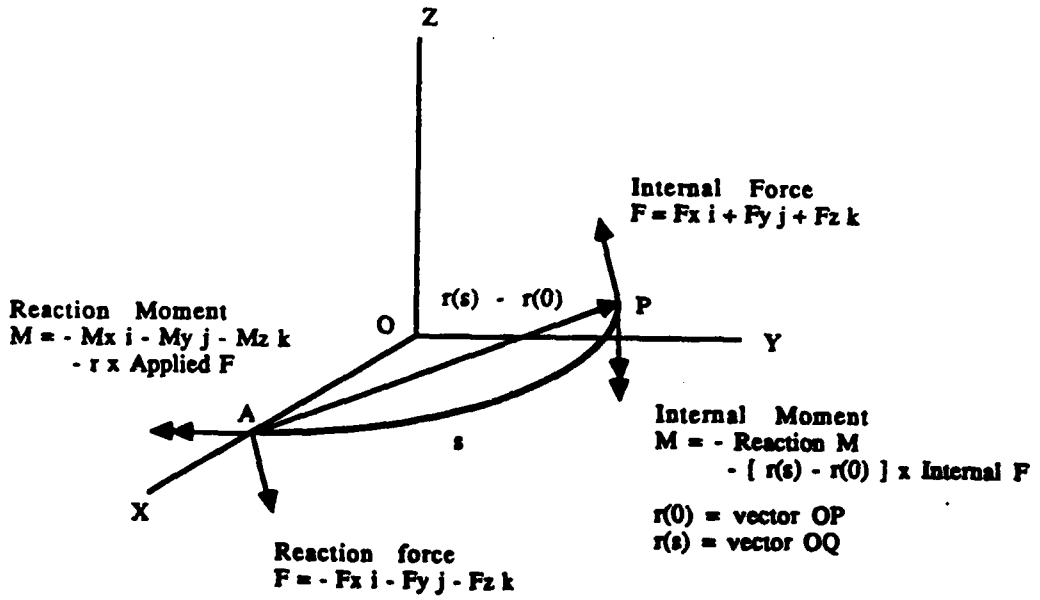

Figure 2-4: Free Body Diagram

the internal force at a generic point P, $\mathbf{F}_{int}$, in terms of the arc length along the rod, s, as:

$$\mathbf{F}_{int}(s) = -\mathbf{F}_R = F_X\mathbf{i} + F_Y\mathbf{j} + F_Z\mathbf{k} \tag{2.14}$$

Setting the sum of moments about the point A to zero (moment equilibrium), we find the internal moment at point P, $\mathbf{M}_{int}$, to be given as:

$$\mathbf{M}_{int}(s) = -\mathbf{M}_R - \triangle\mathbf{r}(s) \times \mathbf{F}_{int}(s) \tag{2.15}$$

where $\triangle\mathbf{r}(s)$ is the lever arm given by:

$$\triangle\mathbf{r}(s) = \mathbf{r}(s) - \mathbf{r}(0) \tag{2.16}$$

The complete expression for the internal moment acting at the generic point P, in terms of the arc length, s, is:

$$\begin{aligned}\mathbf{M}_{int}(s) = &\left[M_X - \frac{F_Y b}{L}(L-s) + \frac{F_Z a}{\phi}\left(\sin\phi - \sin\left(\frac{\phi s}{L}\right)\right)\right]\mathbf{i} \\ &+ \left[M_Y + \frac{F_X b}{L}(L-s) - \frac{F_Z a}{\phi}\left(\cos\phi - \cos\left(\frac{\phi s}{L}\right)\right)\right]\mathbf{j} \\ &+ \left[M_Z - \frac{F_X a}{\phi}\left(\sin\phi - \sin\left(\frac{\phi s}{L}\right)\right) + \frac{F_Y a}{\phi}\left(\cos\phi - \cos\left(\frac{\phi s}{L}\right)\right)\right]\mathbf{k}\end{aligned} \tag{2.17}$$

2.2.2 Local Components of Internal Force and Moment

The components of the internal force and moment, V_ξ, V_η, V_ς and M_ξ, M_η, M_ς respectively, may be found by taking the dot product of the vector in question with the unit vectors in the local $\xi\eta\varsigma$ coordinate system, namely, the vectors $\vec{\nu}$, $\vec{\beta}$ and $\vec{\tau}$. Therefore, we have the following scalar equations for the internal force and moment components as functions of the arc length s:

$$V_\xi(s) = -F_X\cos\left(\frac{\phi s}{L}\right) - F_Y\sin\left(\frac{\phi s}{L}\right) \tag{2.18}$$

$$V_\eta(s) = \frac{F_X b}{L}\sin\left(\frac{\phi s}{L}\right) - \frac{F_Y b}{L}\cos\left(\frac{\phi s}{L}\right) + \frac{F_Z a}{L} \tag{2.19}$$

$$V_\varsigma(s) = -\frac{F_X a}{L}\sin\left(\frac{\phi s}{L}\right) + \frac{F_Y a}{L}\cos\left(\frac{\phi s}{L}\right) + \frac{F_Z b}{L} \tag{2.20}$$

$$\begin{aligned} M_\xi(s) = &\left[- M_X + \frac{F_Y b}{L}(L-s) - \frac{F_Z a}{\phi}\left\{\sin\phi - \sin\left(\frac{\phi s}{L}\right)\right\}\right]\cos\left(\frac{\phi s}{L}\right) \\ &+ \left[- M_Y - \frac{F_X b}{L}(L-s) + \frac{F_Z a}{\phi}\left\{\cos\phi - \cos\left(\frac{\phi s}{L}\right)\right\}\right]\sin\left(\frac{\phi s}{L}\right) \end{aligned} \tag{2.21}$$

$$\begin{aligned} M_\eta(s) = &\left[M_X - \frac{F_Y b}{L}(L-s) + \frac{F_Z a}{\phi}\left\{\sin\phi - \sin\left(\frac{\phi s}{L}\right)\right\}\right]\frac{b}{L}\sin\left(\frac{\phi s}{L}\right) \\ &+ \left[- M_Y - \frac{F_X b}{L}(L-s) + \frac{F_Z a}{\phi}\left\{\cos\phi - \cos\left(\frac{\phi s}{L}\right)\right\}\right]\frac{b}{L}\cos\left(\frac{\phi s}{L}\right) \\ &+ \left[M_Z - \frac{F_X a}{\phi}\left\{\sin\phi - \sin\left(\frac{\phi s}{L}\right)\right\} + \frac{F_Y a}{\phi}\left\{\cos\phi - \cos\left(\frac{\phi s}{L}\right)\right\}\right]\frac{a}{L} \end{aligned} \tag{2.22}$$

$$\begin{aligned} M_\varsigma(s) = &\left[- M_X + \frac{F_Y b}{L}(L-s) - \frac{F_Z a}{\phi}\left\{\sin\phi - \sin\left(\frac{\phi s}{L}\right)\right\}\right]\frac{a}{L}\sin\left(\frac{\phi s}{L}\right) \\ &+ \left[M_Y + \frac{F_X b}{L}(L-s) - \frac{F_Z a}{\phi}\left\{\cos\phi - \cos\left(\frac{\phi s}{L}\right)\right\}\right]\frac{a}{L}\cos\left(\frac{\phi s}{L}\right) \\ &+ \left[M_Z - \frac{F_X a}{\phi}\left\{\sin\phi - \sin\left(\frac{\phi s}{L}\right)\right\} + \frac{F_Y a}{\phi}\left\{\cos\phi - \cos\left(\frac{\phi s}{L}\right)\right\}\right]\frac{b}{L} \end{aligned} \tag{2.23}$$

In the following chapter, we find an expression for the complementary strain energy of the deformed helical rod in terms of the above components of the internal force and moment acting at a cross-section, and then apply Castigliano's Second Theorem to find the displacements at the free end of the helical rod, and thereby, the elements of the corresponding flexibility matrix.

CHAPTER 3

THE STRAIN ENERGY OF THE ROD AND ITS END DISPLACEMENTS

3.1 Strain Energy of the Deformed Helical Rod

3.1.1 Components of Stress

The components of the internal force and moment at any cross-section are defined in terms of the local stress components by the following integrals evaluated over the area of that cross-section:

$$
\begin{aligned}
V_\xi &= \int_A \sigma_{\xi\varsigma}\, dA \\
V_\eta &= \int_A \sigma_{\eta\varsigma}\, dA \\
V_\varsigma &= \int_A \sigma_{\varsigma\varsigma}\, dA \\
M_\xi &= \int_A \eta\, \sigma_{\varsigma\varsigma}\, dA \\
M_\eta &= -\int_A \xi\, \sigma_{\varsigma\varsigma}\, dA \\
M_\varsigma &= \int_A (\xi\, \sigma_{\eta\varsigma} - \eta\, \sigma_{\xi\varsigma})\, dA
\end{aligned}
\tag{3.1}
$$

Even though we do not have relations for the components of stress, viz. $\sigma_{\xi\varsigma}$, $\sigma_{\eta\varsigma}$ and $\sigma_{\varsigma\varsigma}$, in terms of the components of the internal force and moment at a cross-section, we assume relations (analogous to known strength of materials relations) which are such that on substitution in the defining formulae, they yield identities. The assumed formulae for the stress components are:

$$\sigma_{\xi\varsigma} = -\frac{\eta M_\varsigma}{J_p} + \frac{V_\xi}{A}$$

$$\sigma_{\eta\varsigma} = \frac{\xi M_\varsigma}{J_p} + \frac{V_\eta}{A}$$

$$\sigma_{\varsigma\varsigma} = \frac{\eta M_\xi}{I_{\xi\xi}} - \frac{\xi M_\eta}{I_{\eta\eta}} + \frac{V_\varsigma}{A} \tag{3.2}$$

3.1.2 Strain Energy in Terms of Internal Force and Moment Components

We now derive an expression for the complementary strain energy of the deformed helical rod in terms of the local components of the internal force and moment acting at a cross-section. Assuming the material constituting the rod to be linearly elastic, the strain energy of the rod is:

$$U = \frac{1}{2}\int_V \epsilon^T \sigma \, dV \tag{3.3}$$

The stress and strain vectors in the above expression are:

$$\sigma^T = \begin{bmatrix} \sigma_{\xi\xi} & \sigma_{\eta\eta} & \sigma_{\varsigma\varsigma} & \sigma_{\xi\eta} & \sigma_{\eta\varsigma} & \sigma_{\xi\varsigma} \end{bmatrix}$$
$$\epsilon^T = \begin{bmatrix} \epsilon_{\xi\xi} & \epsilon_{\eta\eta} & \epsilon_{\varsigma\varsigma} & \epsilon_{\xi\eta} & \epsilon_{\eta\varsigma} & \epsilon_{\xi\varsigma} \end{bmatrix} \tag{3.4}$$

As per the assumptions made in the analysis of a general curved and twisted rod [Kingsbury 84], we have:

$$\epsilon_{\xi\xi} = \epsilon_{\eta\eta} = \epsilon_{\xi\eta} = 0 \tag{3.5}$$

With these assumptions, the applicable stress-strain relations are:

$$\sigma_{\varsigma\varsigma} = E\,\epsilon_{\varsigma\varsigma}$$
$$\sigma_{\xi\varsigma} = 2G\,\epsilon_{\xi\varsigma}$$
$$\sigma_{\eta\varsigma} = 2G\,\epsilon_{\eta\varsigma} \tag{3.6}$$

Substituting from equations (3.4), (3.5) and (3.6) into Equation (3.3), we get the following expression for the complementary strain energy:

$$U = \frac{1}{2}\left(\frac{1}{E}\int_V {\sigma_{ss}}^2\, dV + \frac{1}{2G}\int_V \{ {\sigma_{\xi s}}^2 + {\sigma_{\eta s}}^2 \}\, dV \right) \tag{3.7}$$

Since the bar is of constant circular cross-section of area A, we have the following section properties:

$$I_{\xi\xi} = I_{\eta\eta} = I$$

$$I_{\xi\eta} = 0$$

$$\int_A \xi\, dA = \int_A \eta\, dA = 0 \tag{3.8}$$

Substituting equations (3.2) and (3.8) into Equation (3.7), we arrive at the following expression for the complementary strain energy of the deformed helix in terms of the components of the internal force and moment represented in the local coordinate system:

$$U = \frac{1}{2EI}\int_L ({M_\xi}^2 + {M_\eta}^2)\, ds + \frac{1}{4GJ_p}\int_L {M_s}^2\, ds$$

$$- \frac{1}{4GA}\int_L ({V_\xi}^2 + {V_\eta}^2)\, ds + \frac{1}{2EA}\int_L {V_s}^2\, ds \tag{3.9}$$

It may be noted that the contributions to the shear stress components in equations (3.2) from the local force components V_ξ and V_η are assumed to be constant over the cross-section. More accurate results may be obtained by assuming a parabolic distribution of shear stress instead of an average value.

3.1.3 Strain Energy in Terms of Applied Force and Moment Components

In Chapter 2, we found expressions relating the local ($\xi\eta\varsigma$) components of the internal force and moment at a cross-section to the global (XYZ) components of the applied force **F** and moment **M**. We now combine those relations, namely, equations (2.18) - (2.23), with Equation (3.9), which is the expression for the complementary strain energy of the rod in terms of the components of the internal force and moment at a cross-section. Integrating the expression so obtained over the length of the rod, L, we find the complementary strain energy of the deformed rod in terms of the geometrical parameters, viz. a and ϕ, and the XYZ components of the applied force and moment. (Note that b is not an independent parameter, but is defined in terms of a, as $\sqrt{L^2 - a^2}$, L being held constant.) The complete expression for the complementary strain energy of the rod may be found in Appendix A. We are now equipped to calculate the displacements that occur at the free end of the rod.

3.2 Displacement of the Free End of the Rod

In this final section, we find expressions for the six scalar displacements (three translations and three rotations) of the free end of the rod using Castigliano's Second Theorem which may be stated briefly as: If a linearly elastic structure is subjected to a set of loads, then the displacement of a load in its direction is equal to the derivative of the complementary strain energy of deformation of the structure with respect to that load. We may write this mathematically as:

$$\Delta_P = \frac{\partial U}{\partial P} \tag{3.10}$$

Differentiating the complementary strain energy expression of Appendix A with respect to F_X, F_Y, F_Z, M_X, M_Y and M_Z respectively, we obtain the three end translations $\Delta X, \Delta Y, \Delta Z$, and the three end rotations $\Delta\theta_X, \Delta\theta_Y, \Delta\theta_Z$ as:

$$\triangle X = f_{11} F_X + f_{12} F_Y + f_{13} F_Z + f_{14} M_X + f_{15} M_Y + f_{16} M_Z$$

$$\triangle Y = f_{21} F_X + f_{22} F_Y + f_{23} F_Z + f_{24} M_X + f_{25} M_Y + f_{26} M_Z$$

$$\triangle Z = f_{31} F_X + f_{32} F_Y + f_{33} F_Z + f_{34} M_X + f_{35} M_Y + f_{36} M_Z$$

$$\triangle \theta_X = f_{41} F_X + f_{42} F_Y + f_{43} F_Z + f_{44} M_X + f_{45} M_Y + f_{46} M_Z$$

$$\triangle \theta_Y = f_{51} F_X + f_{52} F_Y + f_{53} F_Z + f_{54} M_X + f_{55} M_Y + f_{56} M_Z$$

$$\triangle \theta_Z = f_{61} F_X + f_{62} F_Y + f_{63} F_Z + f_{64} M_X + f_{65} M_Y + f_{66} M_Z \qquad (3.11)$$

where f_{ij} represent the elements of the 6×6 symmetric flexibility matrix. The complete expressions for these elements are listed below. For the sake of conciseness, the following notation is used: $c = \cos\phi$, $s = \sin\phi$, $C = a/L$, and $S = b/L$.

$$\begin{aligned} f_{11} = {} & \frac{L^3}{12EI}\left(\frac{1}{\phi^3}\{ 6C^4[3sc - 4s + 2\phi s^2 + \phi] + S^4[3\phi + 2\phi^3 - 3sc] \right. \\ & \left. + 6C^2S^2[4s - 3sc - \phi] + S^2[-3\phi + 2\phi^3 + 3sc]\} \right) \\ & - \frac{L^3}{24GJ_p}\left(\frac{C^2S^2}{\phi^3}[-15\phi - 12\phi s^2 - 2\phi^3 + 48s - 33sc] \right) \\ & - \frac{L}{2EA}\left(\frac{C^2}{\phi}[\phi - sc] \right) + \frac{L}{4GA}\left(\frac{C^2}{\phi}[\phi + sc] + 2S^2 \right) \end{aligned} \qquad (3.12)$$

$$\begin{aligned} f_{12} = {} & \frac{L^3}{4EI}\left(\frac{1}{\phi^3}\{ 2C^4[3s^2 - 2\phi sc + 2c - 2] + S^4[\phi^2 - s^2] \right. \\ & \left. + 2C^2S^2[-3s^2 + 2\phi s - 2c + 2] + S^2[s^2 - \phi^2]\} \right) \\ & - \frac{L^3}{8GJ_p}\left(\frac{C^2S^2}{\phi^3}[8 - 8c - 11s^2 + 4\phi sc + 4\phi s - \phi^2] \right) \\ & - \frac{L}{2EA}\left(\frac{C^2}{\phi}[s^2] \right) + \frac{L}{4GA}\left(\frac{C^2}{\phi}[s^2] \right) \end{aligned} \qquad (3.13)$$

$$f_{13} = \frac{L^3}{4EI}\left(\frac{1}{\phi^3}\{CS[\phi s-\phi^2 c]+2C^3S[-2+2c-2s^2+3\phi s] + CS^3[4-4c-\phi s-\phi^2 c]\}\right) - \frac{L^3}{8GJ_p}\left(\frac{C^3S}{\phi^3}[\phi^2 c+7\phi s-4s^2+8c-8]\right) - \frac{L}{EA}\left(\frac{CS}{\phi}[1-c]\right) + \frac{L}{2GA}\left(\frac{CS}{\phi}[1-c]\right) \quad (3.14)$$

$$f_{14} = \frac{L^2}{4EI}\left(\frac{1}{\phi^2}\{S[\phi-sc]+2C^2S[\phi+sc-2s]+S^3[sc-\phi]\}\right) - \frac{L^2}{8GJ_p}\left(\frac{C^2S}{\phi^2}[sc-4s+3\phi]\right) \quad (3.15)$$

$$f_{15} = \frac{L^2}{4EI}\left(\frac{1}{\phi^2}\{S[\phi^2-s^2]+2C^2S[s^2]+S^3[\phi^2+s^2]\}\right) - \frac{L^2}{8GJ_p}\left(\frac{C^2S}{\phi^2}[s^2-\phi^2]\right) \quad (3.16)$$

$$f_{16} = \frac{L^2}{EI}\left(\frac{1}{\phi^2}\{C^3[1-c-\phi s]+CS^2[c-1]\}\right) - \frac{L^2}{2GJ_p}\left(\frac{CS^2}{\phi^2}[\phi s+2c-2]\right) \quad (3.17)$$

$$f_{22} = \frac{L^3}{12EI}\left(\frac{1}{\phi^3}\{6C^4[\phi-3sc+2\phi c^2]+6C^2S^2[\phi+3sc-4\phi c] + S^4[-3\phi+2\phi^3+3sc]+S^2[3\phi+2\phi^3-3sc]\}\right) - \frac{L^3}{24GJ_p}\left(\frac{C^2S^2}{\phi^3}[-9\phi-2\phi^3-24\phi c+12\phi s^2+33sc]\right) - \frac{L}{2EA}\left(\frac{C^2}{\phi}[\phi+sc]\right) + \frac{L}{4GA}\left(\frac{C^2}{\phi}[\phi-sc]+2S^2\right) \quad (3.18)$$

$$f_{23} = \frac{L^3}{4EI}\left(\frac{1}{\phi^3}\{CS[\phi c - s - \phi^2 s] + 2C^3S[s + 2sc - 3\phi c] + CS^3[-3s - \phi c - \phi^2 s + 4\phi]\}\right) - \frac{L^3}{8GJ_p}\left(\frac{C^3S}{\phi^3}[5s - 5\phi c + 4sc + \phi^2 s - 4\phi]\right) + \frac{L}{EA}\left(\frac{CS}{\phi}[s]\right) - \frac{L}{2GA}\left(\frac{CS}{\phi}[s]\right) \quad (3.19)$$

$$f_{24} = \frac{L^2}{4EI}\left(\frac{1}{\phi^2}\{S[-s^2 - \phi^2] + 2C^2S[-c^2 + 2c - 1] + S^3[s^2 - \phi^2]\}\right) - \frac{L^2}{8GJ_p}\left(\frac{C^2S}{\phi^2}[-4 + 4c + s^2 + \phi^2]\right) \quad (3.20)$$

$$f_{25} = \frac{L^2}{4EI}\left(\frac{1}{\phi^2}\{S[sc - \phi] + 2C^2S[\phi - sc] + S^3[\phi - sc]\}\right) - \frac{L^2}{8GJ_p}\left(\frac{C^2S}{\phi^2}[\phi - sc]\right) \quad (3.21)$$

$$f_{26} = \frac{L^2}{EI}\left(\frac{1}{\phi^2}\{C^3[\phi c - s] + CS^2[s - \phi]\}\right) - \frac{L^2}{2GJ_p}\left(\frac{CS^2}{\phi^2}[-\phi c - \phi + 2s]\right) \quad (3.22)$$

$$f_{33} = \frac{L^3}{2EI}\left(\frac{1}{\phi^3}\{C^2[\phi - sc] + C^2S^2[3\phi + sc - 4s]\}\right) - \frac{L^3}{4GJ_p}\left(\frac{C^4}{\phi^3}[4s - 3\phi - sc]\right) + \frac{L}{EA}[S^2] + \frac{L}{2GA}[C^2] \quad (3.23)$$

$$f_{34} = \frac{L^2}{2EI}\left(\frac{1}{\phi^2}\{\, C[\phi s] + CS^2[2c-2+\phi s]\,\}\right) - \frac{L^2}{4GJ_p}\left(\frac{C^3}{\phi^2}[-2c+2-\phi s]\right) \tag{3.24}$$

$$f_{35} = \frac{L^2}{2EI}\left(\frac{1}{\phi^2}\{\, C[s-\phi c] + CS^2[s-\phi c]\,\}\right) - \frac{L^2}{4GJ_p}\left(\frac{C^3}{\phi^2}[\phi c - s]\right) \tag{3.25}$$

$$f_{36} = \frac{L^2}{EI}\left(\frac{C^2 S}{\phi^2}[s-\phi]\right) - \frac{L^2}{2GJ_p}\left(\frac{C^2 S}{\phi^2}[s-\phi]\right) \tag{3.26}$$

$$f_{44} = \frac{L}{2EI}\left(\frac{C^2}{\phi}[-\phi+sc]+2\right) + \frac{L}{4GJ}\left(\frac{C^2}{\phi}[-\phi+sc]\right) \tag{3.27}$$

$$f_{45} = \left(\frac{L}{2EI}-\frac{L}{4GJ}\right)\left(\frac{C^2}{\phi}[s^2]\right) \tag{3.28}$$

$$f_{46} = \left(\frac{L}{EI}-\frac{L}{2GJ}\right)\left(\frac{CS}{\phi}[1-c]\right) \tag{3.29}$$

$$f_{55} = \frac{L}{2EI}\left([1+S^2]-\frac{C^2}{\phi}[sc]\right) + \frac{L}{4GJ}\left(\frac{C^2}{\phi}[\phi+sc]\right) \tag{3.30}$$

$$f_{56} = \left(\frac{L}{2GJ}-\frac{L}{EI}\right)\left(\frac{CS}{\phi}[s]\right) \tag{3.31}$$

$$f_{66} = \frac{L}{EI}[C^2] + \frac{L}{2GJ}[S^2] \tag{3.32}$$

Equations (3.11) represent the scalar displacements and rotations of the end of the helical rod, in terms of the XYZ components of the applied force and moment, and the geometrical parameters defining the helix, namely, a and ϕ. By making suitable substitutions, it is possible to reduce them to those of a cantilevered straight beam. This is demonstrated in the following subsection.

3.2.1 Reduction of the General Equations to the Straight Beam Case

The equations for the helical arc may be reduced to those for the straight beam in two equivalent ways: by setting $a = 0$, which forces ϕ to be zero, and alternatively by letting ϕ approach zero. This is illustrated in Figure 3.1. It is important to realize that we cannot simply substitute $\phi = 0$ into the general equations, but must express $\sin\phi$ and $\cos\phi$ as Taylor series about $\phi = 0$ and then neglect the higher order terms. Both the methods yield identical results, which are exactly the same as the strength-of-materials deflections for the straight cantilevered beam. We present below the reduced equations that result from applying the first method:

$$\triangle X = \frac{F_X L^3}{3EI} + \frac{F_X L}{2GA} \tag{3.33}$$

$$\triangle Y = \frac{F_Y L^3}{3EI} + \frac{F_Y L}{2GA} \tag{3.34}$$

$$\triangle Z = \frac{F_Z L}{EA} \tag{3.35}$$

$$\triangle\theta_X = -\frac{F_Y L^2}{2EI} \tag{3.36}$$

$$\triangle\theta_Y = \frac{F_X L^2}{2EI} \tag{3.37}$$

$$\triangle\theta_Z = 0 \tag{3.38}$$

3.2.2 Reduction to a Circular Arc of Small Curvature in the XY Plane

The reduction of the general equations to the case of a circular arc in the XY plane is accomplished by setting $b = 0$ or $a = L$, and expressing $\sin\phi$ and $\cos\phi$ as Taylor series about $\phi = 0$ and retaining terms upto the order of ϕ^2. We have, then, the following results:

$$\Delta X = F_X \left(\frac{L^3}{60EI}[20 - 9\phi^2] + \frac{L}{3EA}[\phi^2] + \frac{L}{6GA}[3 - \phi^2] \right) - F_Y \left(\frac{5L^3}{24EI}[\phi] + \frac{L}{4GA}[\phi] - \frac{L}{2EA}[\phi] \right) \tag{3.39}$$

$$\Delta Y = F_X \left(\frac{5L^3}{24EI}[\phi] + \frac{L}{4GA}[\phi] - \frac{L}{2EA}[\phi] \right) - F_Y \left(\frac{2L^3}{15EI}[\phi^2] + \frac{L}{6GA}[\phi^2] + \frac{L}{3EA}[3 - \phi^2] \right) \tag{3.40}$$

$$\Delta Z = F_Z \left(\frac{L^3}{15EI}[5 - \phi^2] + \frac{L^3}{40GJ_p}[\phi^2] + \frac{L}{2GA} \right) \tag{3.41}$$

$$\Delta\theta_X = F_Z \left(\frac{L^2}{12EI}[6 - \phi^2] - \frac{L^2}{48GJ_p}[\phi^2] \right) \tag{3.42}$$

$$\Delta\theta_Y = F_Z \left(\frac{L^2}{6EI}[\phi] - \frac{L^2}{12GJ_p}[\phi] \right) \tag{3.43}$$

$$\Delta\theta_Z = F_X \left(\frac{L^2}{8EI}[-4 + \phi^2] \right) + F_Y \left(-\frac{L^2}{3EI}[\phi] \right) \tag{3.44}$$

Note that if we now set ϕ to zero in the above equations, we obtain the displacements of a straight cantilever beam in the XY plane, analogous to those presented for the case in which $a = 0$, presented in Section 3.2.1. In the next chapter, we impose two different conditions of compatibility of displacements of the muzzle ends of the gun tube and the shroud. We thus obtain the force exerted on the gun tube by the thermal shroud

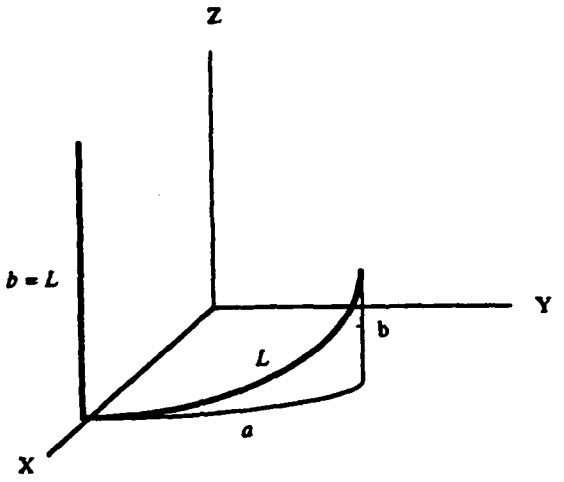

(i) Reduction to Straight Beam by Setting a = 0

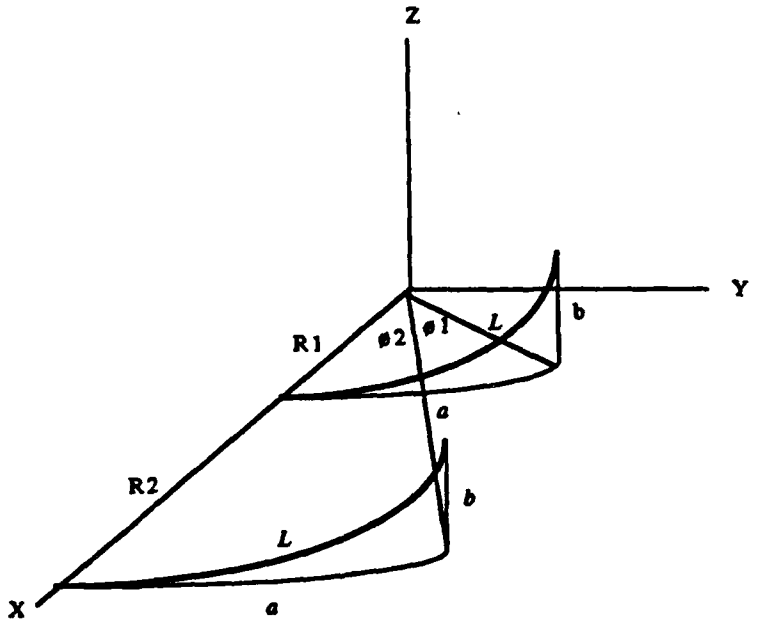

(ii) Reduction to Straight Beam by Letting ϕ Approach Zero

Figure 3-1: Reduction of the Helical Arc to a Straight Beam

due to its expansion, and thereby, the displacement of the end of the gun tube.

CHAPTER 4

IMPOSITION OF COMPATIBILITY CONSTRAINTS

4.1 A Convenient Coordinate System

In chapters 2 and 3, we developed an analytical solution for the displacement at the end of a helical rod of constant circular cross-section in terms of an applied force and moment. However, in the actual problem, we do not know, a priori, what the value of the force exerted on the gun tube by the shroud is. The problem is statically indeterminate. Hence we must rely on the imposition of compatibility of the displacements of the ends of the gun tube and the thermal shroud to resolve this indeterminacy.

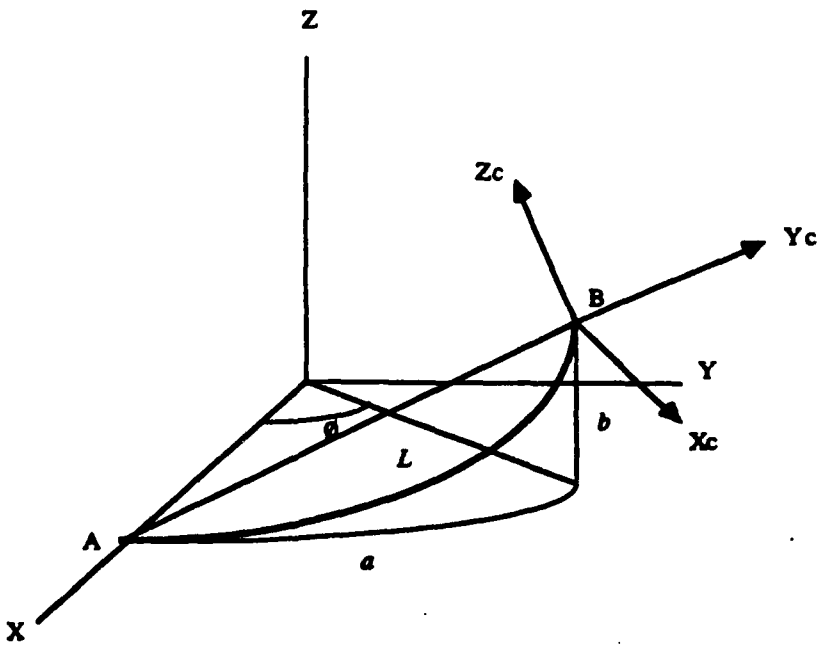

Figure 4-1: The Chord System

Note that by varying the parameters a and ϕ, we can vary the curvature and torsion of the helical rod. In order to perform a parametric study of the displacement, we must vary the curvature κ and torsion λ of the helical rod, and solve the compatibility conditions that we impose for each such case to obtain the force acting on the rod, and then compute the six displacements of the muzzle end. For this purpose, we make the reasonable assumption that the centroidal axis of the thermal shroud passes through the two end points A and B of the helical rod, which define a chord between them. This is shown in Figure 4.1. We therefore define a coordinate system whose Y axis is in the direction of the vector $\overrightarrow{AB}$, and whose X axis lies in a plane parallel to the XY plane, so that if we set $b = 0$ and let ϕ approach zero, the coordinate system becomes identical to the global coordinate system. This coordinate system is called the *chord* system.

The chord system is the coordinate system that we shall use in Chapter 5 for the parametric studies that compare displacements for different initial curvatures and torsions of the gun tube, and different axial and bending stiffnesses of the shroud.

4.2 Unit Vectors in the Chord System

Let $X_c Y_c Z_c$ denote the chord system shown in Figure 4.1. The position vectors of points A and B are:

$$\vec{p}(A) = \frac{a}{\phi}\,\mathbf{i}$$

$$\vec{p}(B) = \frac{a}{\phi}\cos\phi\,\mathbf{i} + \frac{a}{\phi}\sin\phi\,\mathbf{j} + b\,\mathbf{k} \tag{4.1}$$

Therefore, the vector $\overrightarrow{AB}$ is given by:

$$\vec{AB} = \frac{a}{\phi}(\cos\phi - 1)\,\mathbf{i} + \frac{a}{\phi}\sin\phi\,\mathbf{j} + b\,\mathbf{k} \tag{4.2}$$

From Equation (4.2), we may write the unit vector along the Y_c axis as:

$$\mathbf{j}_c = \frac{\vec{AB}}{\vec{AB}} = \frac{(\cos\phi - 1)\,\mathbf{i} + \sin\phi\,\mathbf{j} + (\phi b/a)\,\mathbf{k}}{\sqrt{2(1-\cos\phi) + (\phi b/a)^2}} \tag{4.3}$$

Having obtained $\mathbf{j}_c$ in terms of $\mathbf{i}$, $\mathbf{j}$ and $\mathbf{k}$, the unit vectors in the global coordinate system, we now proceed to obtain $\mathbf{i}_c$ and $\mathbf{k}_c$. As mentioned in Section 4.1, the X_c axis is parallel to the global XY plane. Thus $\mathbf{i}_c$ may be written as:

$$\mathbf{i}_c = p\,\mathbf{i} - q\,\mathbf{j} + 0\,\mathbf{k} \tag{4.4}$$

Since $\mathbf{i}_c$ and $\mathbf{j}_c$ are mutually perpendicular, their scalar product must be zero, i.e.,

$$\mathbf{i}_c \cdot \mathbf{j}_c = 0 \tag{4.5}$$

That is,

$$p(\cos\phi - 1) - q\sin\phi = 0. \tag{4.6}$$

Since $\mathbf{i}_c$ is a unit vector, we have:

$$p^2 + q^2 = 1 \tag{4.7}$$

Solving equations (4.6) and (4.7) for p and q, we get

$$\mathbf{i}_c = \frac{\sin\phi\,\mathbf{i} + (1-\cos\phi)\,\mathbf{j}}{\sqrt{2(1-\cos\phi)}} \tag{4.8}$$

Having obtained $\mathbf{i}_c$ and $\mathbf{j}_c$, we may simply write $\mathbf{k}_c$ as:

$$\mathbf{k}_c = \mathbf{i}_c \times \mathbf{j}_c = \frac{(\phi b/a)(1-\cos\phi)\,\mathbf{i} - (\phi b/a)\sin\phi\,\mathbf{j} + 2(1-\cos\phi)\,\mathbf{k}}{\sqrt{4(1-\cos\phi)^2 + 2(\phi b/a)^2(1-\cos\phi)}} \tag{4.9}$$

Equations (4.3), (4.8) and (4.9) give us the desired unit vectors in the chord system in terms of the unit vectors in the global XYZ system. From these three equations, we now derive the chord-to-global transformation matrix, **CG**, that relates the components of displacement and force in the chord system to their equivalents in the global system.

4.3 CG: The Chord-to-Global Transformation Matrix

Consider a generic vector, $\vec{u}_c$, that is to be transformed from the chord coordinate system into the global coordinate system. Let **s** be the matrix whose rows consist of the coefficients of i, j and k unit vectors in equations (4.3), (4.8) and (4.9) respectively. If $\vec{u}_c$ is written as $\vec{u}_c = u_{Xc}\mathbf{i}_c + u_{Yc}\mathbf{j}_c + u_{Zc}\mathbf{k}_c$, then substituting for $\mathbf{i}_c$, $\mathbf{j}_c$ and $\mathbf{k}_c$ from the above-mentioned equations, we get

$$\begin{aligned}\vec{u}_c = & \; u_{Xc}\left[s_{11}\,\mathbf{i} + s_{12}\,\mathbf{j} + s_{13}\,\mathbf{k} \right] \\ & - u_{Yc}\left[s_{21}\,\mathbf{i} + s_{22}\,\mathbf{j} + s_{23}\,\mathbf{k} \right] \\ & - u_{Zc}\left[s_{31}\,\mathbf{i} + s_{32}\,\mathbf{j} + s_{33}\,\mathbf{k} \right] \end{aligned} \tag{4.10}$$

Rearranging terms, we get the following:

$$\begin{aligned}\vec{u}_c = & \left[s_{11}\,u_{Xc} - s_{21}\,u_{Yc} + s_{31}\,u_{Zc} \right]\mathbf{i} \\ & - \left[s_{12}\,u_{Xc} - s_{22}\,u_{Yc} + s_{32}\,u_{Zc} \right]\mathbf{j} \\ & - \left[s_{13}\,u_{Xc} - s_{23}\,u_{Yc} + s_{33}\,u_{Zc} \right]\mathbf{k} \end{aligned} \tag{4.11}$$

Clearly, from Equation (4.11), we see that **CG**, the chord-to-global transformation matrix is the transpose of **s**:

$$\mathbf{CG} = \mathbf{s}^T \tag{4.12}$$

Thus, to convert the components of a vector $\mathbf{u} = \left[u_{Xc}\; u_{Yc}\; u_{Zc} \right]^T$ from the chord system to the global system, we pre-multiply **u** with **CG**. The global-to-chord transformation is achieved by inverting **CG**. But since the transformation is orthogonal, $\mathbf{GC} = \mathbf{CG}^{-1} = \mathbf{CG}^T = \mathbf{s}$. In Section 2.1, we presented the expressions for the tangent, binormal and principal normal to a helix, at a generic point along its length, in terms of the global unit vectors **i**, **j** and **k**. The matrix formed by the coefficients of these unit vectors in equations (2.7), (2.8) and (2.9) similarly represent the elements of the global-to-tangent transformation matrix at any point along the helix.

4.4 Flexibility Matrix in the Chord System

Since the position of the thermal shroud in the chord system is always fixed while it varies in the global coordinate system with changing curvature and torsion, it is clear that compatibility of the displacements of the ends of the gun tube and the shroud must be imposed in the chord system. This means that we must transform the flexibility matrix of Equation (3.11), which yields displacements in the global system, to one that gives displacements directly in the chord system.

An important point to note here is the assumption that the angular displacements $\triangle\theta_X$, $\triangle\theta_Y$, and $\triangle\theta_Z$ may be decomposed into components along the coordinate axes and transformed between different coordinate systems in exactly the manner the translational displacements are. This is acceptable for small angular displacements as in our case.

Consider a 6×6 chord-to-global transformation matrix $\mathbf{T}$, which is block diagonal, both the 3×3 diagonal blocks being equal to $\mathbf{CG}$. Let $\mathbf{f}$ and $\mathbf{f}_c$ denote the 6×6 flexibility matrices in the global and chord coordinate systems. Further, let $\triangle$, $\mathbf{F}$ and $\triangle_c$, $\mathbf{F}_c$ represent the 6×1 displacement and force vectors in the global and chord systems respectively. Then we have the following:

$$\triangle = \mathbf{f}\mathbf{F} \tag{4.13}$$

$$\triangle_c = \mathbf{f}_c\mathbf{F}_c \tag{4.14}$$

$$\triangle = \mathbf{T}\triangle_c \tag{4.15}$$

$$\mathbf{f} = \mathbf{T}\mathbf{f}_c \tag{4.16}$$

Substituting equations (4.15) and (4.16) into Equation (4.13), and pre-multiplying both sides by $\mathbf{T}^{-1} = \mathbf{T}^T$, we get:

$$\triangle_c = [\mathbf{T}^T\mathbf{f}\mathbf{T}]\mathbf{F}_c \tag{4.17}$$

Comparing equations (4.14) and (4.17), we get $\mathbf{f}_c$ as:

$$\mathbf{f}_c = \mathbf{T}^T \mathbf{f} \mathbf{T} \tag{4.18}$$

4.5 Compatibility 1: Shroud with Zero Transverse Stiffness

We assume a condition of compatibility of displacements of the thermal shroud and gun tube ends wherein the shroud has stiffness only in its axial direction. That is, the shroud has no transverse or rotational stiffness. Thus translational movement is permitted to the gun tube end freely in the transverse direction, perpendicular to the centroidal axis of the shroud. As a result, there is no opposing force exerted by the shroud in the transverse direction. In fact, the only force exerted by the shroud on the gun tube acts along the Y_c axis of the chord system. Rotations of the gun tube end are also permitted about all three axes in the chord system, and similarly, there are no moments exerted at the gun tube end.

If F_{Yc} is the force exerted on the end of the gun tube, then its displacement in the direction of the force is given as

$$\triangle Y_c(gun\ tube) = f_{c22} F_{Yc} \tag{4.19}$$

where f_{c22} is the element belonging to the 2^{nd} row and 2^{nd} column of the *chord* flexibility matrix. The gun tube, by Newton's Third Law, must in its turn exert an equal but opposite force on the end of the shroud. Let L_s, α, E_s, A_s and $\triangle T$ be the length, coefficient of thermal expansion, modulus of elasticity, cross-sectional area and rise in temperature of the shroud respectively. The displacement of the end of the shroud is composed of two contributions, namely, the thermal expansion and the contraction due to the opposing axial force exerted by the gun tube. Thus we have

$$\triangle Y_c(shroud) = L_s \alpha \triangle T - \frac{F_{Yc} L_s}{E_s A_s} \tag{4.20}$$

Compatibility asserts that the displacements in equations (4.19) and (4.20) be equal. Thus we find the force acting on the end of the gun tube to be

$$F_{Yc} = \frac{L_s \alpha \triangle T}{f_{c22} + L_s/(E_s A_s)}, \tag{4.21}$$

where L_s, the length of the shroud, may be easily seen from Figure 2.1 to be

$$L_s = \left(\left[\frac{a}{\phi} (\cos\phi - 1) \right]^2 + \left[\frac{a}{\phi} \sin\phi \right]^2 + b^2 \right)^{\frac{1}{2}}. \tag{4.22}$$

The six displacements of the end of the gun tube may. now be found by substituting F_{Yc} into equations (3.11) rewritten with elements of the flexibility matrix in the chord system.

4.6 Compatibility 2: Shroud with Finite Non-Zero Transverse Stiffness

In this section, we consider a different kind of compatibility condition in which we assume the shroud to have a finite non-zero transverse stiffness. The gun tube end is permitted both transverse displacements as well as rotations relative to the shroud. However, since the shroud now has stiffness in the transverse direction, it will exert a resistance to the transverse displacement of the gun tube end. An equivalent way of representing such a compatibility relationship is to consider the gun tube end as being attached to the shroud end through a ball and socket joint.

Since the shroud now offers resistance to the transverse motion of the gun tube end, F_{Xc} and F_{Zc} are non-zero. The compatibility of all three components of displacement of the ends of the gun tube and the shroud must be enforced in order to determine the forces on the gun tube. Thus, the imposition of compatibility results in a set of three simultaneous equations in F_{Xc}, F_{Yc} and F_{Zc}, which are presented below:

$$-\frac{F_{Xc} L_s^3}{3 E_s I_s} = f_{c11} F_{Xc} + f_{c12} F_{Yc} + f_{c13} F_{Zc}$$

$$L_s \alpha \triangle T - \frac{F_{Yc} L_s}{E_s A_s} = f_{c21} F_{Xc} + f_{c22} F_{Yc} + f_{c23} F_{Zc}$$

$$-\frac{F_{Zc} L_s^3}{3 E_s I_s} = f_{c31} F_{Xc} + f_{c32} F_{Yc} + f_{c33} F_{Zc} \qquad (4.23)$$

Here, I_s represents the moment of inertia of the cross-section of the shroud. It is worth noting that if the inertia, I_s, of the shroud were to approach zero (which would, in physical terms, amount to the shroud becoming infinitely flexible), F_{Xc} and F_{Zc}, which represent the opposition of the shroud to bending, would also tend to zero, and the above compatibility conditions would reduce to those of the first case. The next chapter contains parametric plots showing the variation of the forces and displacements experienced by the end of the gun tube for different initial curvatures and torsions, for both of the above compatibility conditions.

CHAPTER 5

A PARAMETRIC STUDY OF DISPLACEMENT

5.1 Introduction

Having obtained a closed-form solution for the end displacement of the gun tube in Chapter 3, and developed equations of compatibility of gun tube and shroud displacements in Chapter 4, we proceed to perform a parametric study of the force and displacement experienced by the end of gun tube. The parameters in this study are the initial curvature and torsion of the gun tube, the kind of compatibility condition imposed, namely, one of the two kinds discussed in sections 4.5 and 4.6, and the axial and flexural rigidity of the thermal shroud.

Several plots of force and displacement components in the chord system are included in this chapter, usually accompanied by discussions regarding their physical interpretation. These are calculated for a fixed rise in temperature of 100 ° C of the thermal shroud. The variation of the components of force and displacement with temperature would, of course, be linear. The gun tube and shroud data assumed in the computations follow.

Gun Tube:

Length = 5.25 m
Inner radius = 0.06 m
Outer radius = 0.10 m
Elasticity modulus = 4.35097×10^9 N/m^2
Shear modulus = 1.67345×10^9 N/m^2

Thermal Shroud:

Inner radius = 0.11 m
Outer radius = 0.145 m
Elasticity modulus = 4.35097×10^{9} N/m^{2}
Coefficient of thermal expansion = 1.206×10^{-5} / °C

Each parametric plot is a surface depicting the variation of the particular force or displacement component, taken in the chord system, for different values of initial curvature and torsion of the gun tube. It is assumed that the length of the gun tube is a constant. The length of the thermal shroud is the distance between the two ends of the gun tube, and therefore varies with the gun tube geometry as given by Equation (4.22). The force and displacement components are plotted for the normal values of axial rigidity, EA, and flexural rigidity, EI, of the thermal shroud, and also for high and low EA and EI, the values being increased and decreased respectively by a factor of a thousand. In the following section, we define the geometrical parameters employed in the study, namely, the initial curvature and torsion of the gun tube, in terms of the corresponding geometrical parameters that define the shape of the helix of Figure 2.1, namely, a and ϕ.

5.2 The Definition of Curvature and Torsion

Every space curve of constant curvature and torsion is uniquely and completely specified by these two quantities, apart from its position in space. While it would be possible to consider a and ϕ, which define the shape of the helix of Figure 2.1, as a legitimate choice of geometrical parameters for this study, we have chosen to employ the initial curvature, κ, and torsion, λ, of the centroidal axis of the gun tube as parameters to represent its initial shape on account of their generality. We now derive relationships between these two sets of geometrical parameters.

The curvature and torsion of a space curve are defined by the following two Frenet-Serret formulae,

$$\frac{d\vec{\tau}}{ds} = \kappa \vec{\nu}, \quad \kappa > 0 \tag{5.1}$$

$$\frac{d\vec{\beta}}{ds} = \lambda \vec{\nu} \tag{5.2}$$

where $\vec{\tau}, \vec{\beta}$ and $\vec{\nu}$ are the vector tangent, binormal and principal normal to the curve, and s is the arc length. By definition, κ and λ are zero for a straight line. The cross product $\vec{\tau} \times \vec{\nu}$ defines the binormal vector, $\vec{\beta}$, which is the outward normal to the osculating plane. The torsion, λ, measures the rate at which the direction of $\vec{\beta}$ changes along the curve. From equations (2.7), (2.8), (2.9), (5.1) and (5.2), the curvature and torsion of the helix are found to be:

$$\kappa = \frac{\phi a}{L^2} = \frac{a^2}{RL^2} \tag{5.3}$$

$$\lambda = -\frac{\phi b}{L^2} = -\frac{ab}{RL^2} \tag{5.4}$$

The parameters a, b, R and L in equations (5.3) and (5.4) are exactly as shown in Figure 2.1. Note that R represents the radius of the cylindrical surface that contains the helix. Note also that the length of the gun tube, L, is fixed, and b is given as $\sqrt{L^2 - a^2}$.

Since we are only concerned with the magnitude of torsion, for the purposes of this analysis, we rewrite Equation (5.4) as

$$\lambda = \frac{\phi b}{L^2} = \frac{ab}{RL^2}. \tag{5.5}$$

From equations (5.3) and (5.5), we get

$$\frac{\kappa}{\lambda} = \frac{a}{b}, \tag{5.6}$$

and thus, we have the following two expressions for a and b in terms of κ and λ:

$$a = \frac{\kappa L}{\sqrt{\kappa^2 - \lambda^2}} \tag{5.7}$$

$$b = \frac{\lambda L}{\sqrt{\kappa^2 - \lambda^2}} \tag{5.8}$$

From equations (5.3) and (5.7), we also obtain the following expressions for ϕ and R in terms of κ and λ:

$$\phi = L\sqrt{\kappa^2 - \lambda^2} \tag{5.9}$$

$$R = \frac{\kappa}{\kappa^2 + \lambda^2} \tag{5.10}$$

Having obtained the curvature, κ, and torsion, λ, in terms of a, ϕ and constant L, and also developed reciprocal relationships for a, b, ϕ and R in terms of κ, λ and L, we are equipped to compute the force and displacement components that we seek to plot, given the values of initial curvature and torsion of the gun tube. This may be done by first computing a, b, ϕ and R from equations (5.7), (5.8), (5.9) and (5.10) respectively, and L_s from Equation (4.22), then solving the particular compatibility equations, equations (4.21) or (4.23) as the case may be, to obtain the applied force components, and lastly, substituting these scalar forces into equations (3.11) to get the required displacements and rotations of the gun tube end.

5.3 Compatibility 1: Physical Interpretation

In Compatibility 1, we assume that the shroud has stiffness only in its axial direction. The shroud is assumed to have *zero* transverse or rotational stiffness. Since the gun tube end is free to move in the transverse direction, the only force that acts on it is directed along the centroidal axis of the shroud.

5.3.1 "In-Plane" Force and Displacements: An Anomaly Explained

Each point on the curve has an associated osculating plane which is normal to the binormal vector at that point. The variation of the osculating plane along the curve for the values of curvature and torsion considered is very small. In other words, the helical arc described by the centroidal axis of the gun tube, and the chord along which the shroud is aligned, form a surface that is almost planar. The non-planarity of this surface is measured in terms of the rate of change of the binormal vector along the arc, $\lambda = |d\vec{\beta}/ds|$, and is at a maximum when the curvature and torsion are equal. This is illustrated in Figure 5.1, for a fixed radius, R. It can be proven mathematically that this characteristic is unchanged even if the radius is allowed to vary along a constant curvature contour.

This surface is almost identical to the $X_c Y_c$ plane in the chord system of Figure 4.1. The forces and displacements in the $X_c Y_c$ plane, namely, F_{Xc}, F_{Yc}, M_{Zc}, and U_c, V_c, and θ_{Zc}, may be regarded as being in the plane of the curve and will be referred to in the following discussion as the "in-plane" forces and displacements. Since all the forces and displacements we refer to are in the chord system, we will drop the "chord" subscript for convenience.

F_X and F_Z are identically zero due to the fact that the shroud offers no resistance to the motion of the gun tube end in the transverse direction. Figure 5.2 shows a plot of F_Y. Note that F_Y decreases as the curvature increases, whereas it is virtually unaffected by torsion. The decrease of F_Y with increase in curvature is consistent with experience with rods with plane curvature. The apparent independence of F_Y on torsion is somewhat surprising at first sight, since both curvature and torsion may be thought of as representing deviations from straightness. At a physical level, this may be rationalized by saying that the helical arc representing the centroidal curve of the gun tube is an almost circular arc in the $X_c Y_c$ plane whose curvature is held fixed (along a constant curvature contour). Thus increasing torsion only increases the deviation of the curve from the $X_c Y_c$ plane upto a maximum at $\kappa = \lambda$. As λ grows greater than κ, the curve approaches a straight line, since b becomes much greater than a. This leads us to expect an increase in F_Y with increasing

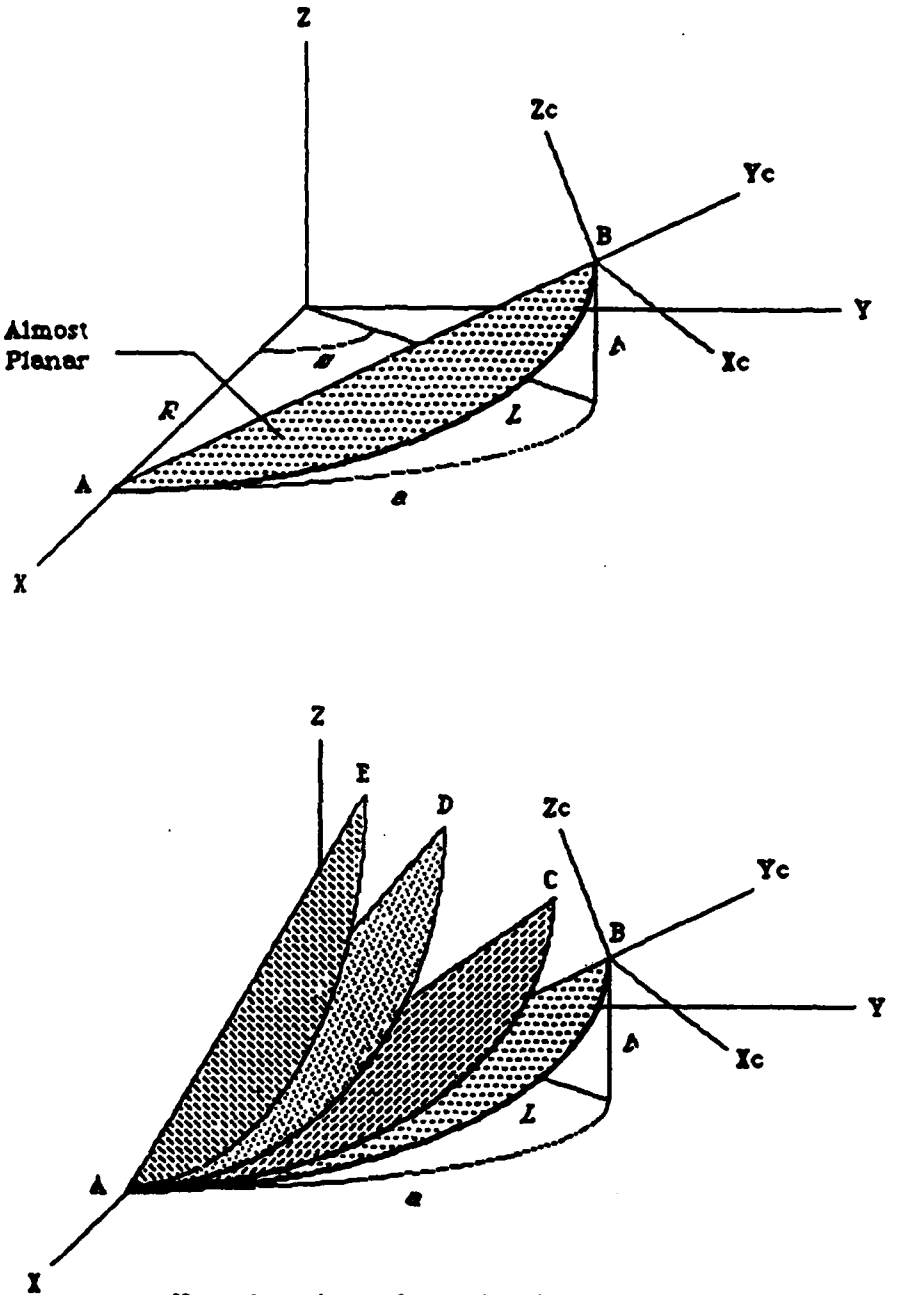

Figure 5-1: The "Plane" Containing the Helical Arc

torsion. This is borne out by the numbers generated for the plot of Figure 5.2. The increase in F_Y is more apparent for low values of curvature than for high values, because when the curvature is small, F_Y is very close to the limiting value for a straight rod.

The behavior observed for F_Y also occurs in the plots of U, V and θ_Z (figures 5.3 - 5.5), namely, they do not show an appreciable variation with torsion along lines of constant curvature. The same argument holds, namely, the torsion changes the deviation of the helical arc from the $X_c Y_c$ plane but the curve is essentially circular, has the same curvature and is almost contained in the $X_c Y_c$ plane, so that the displacements are virtually unaffected by a variation of torsion. Note that θ_Z is always negative; this demonstrates that the helical rod "unwinds" as it is stretched.

The U and θ_Z displacements show a maximum along lines of constant torsion. This is a result of the imposition of compatibility and may be explained as follows: Initially, the curvature lends the rod an added flexibility as a result of which the displacements increase. However, as curvature increases, the force developed due to the interaction between the shroud and the gun tube, F_Y, decreases monotonically. A point is reached when the decrease in the force overtakes the increase in flexibility.

5.3.2 Out-of-Plane Displacements

The W, θ_X and θ_Y displacements of figures 5.6 - 5.7 (θ_X is negligibly small and has not been shown), on the other hand, represent motions of the end of the gun tube in a direction perpendicular to the $X_c Y_c$ plane. These are therefore termed as the "out-of-plane" displacements. θ_X remains essentially zero for all values of the applied force. Since the applied force is in the $X_c Y_c$ plane, and the helical arc is also essentially confined to this plane, we naturally expect that the out-of-plane displacements will be smaller in magnitude. This is seen to be the case. These displacements show peaks in the region defined by $\kappa = \lambda$. This is because when $\kappa = \lambda$, the rod departs from the plane the most. In the plot of W however, the peak is off the $\kappa = \lambda$ line of symmetry. This may be attributed to the imposition of compatibility as explained in Section 5.2.1.

AXIS	SCALE	RANGE
X (Curvature)	1 unit = Cur x 10.0 (Log)	1.0E-4 /m to 1.0E-1 /m
Y (Torsion)	1 unit = Tor x 10.0 (Log)	0, 1.0E-4 /m to 1.0E-1 /m
Z (Dependent Variable plotted for a temp. rise of 100 deg. C)	1 unit = 13440.0000 N	5190.7310 N to 61442.1406 N

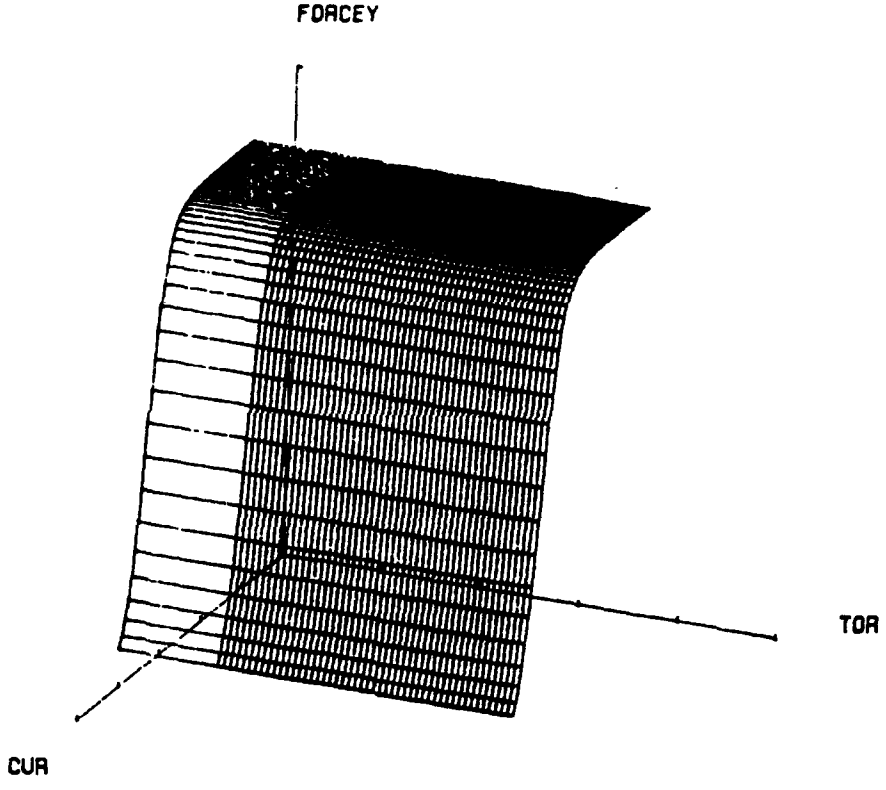

Compatibility 1: Fy (Chord) vs Cur vs Tor

Figure 5-2: Compatibility 1: F_Y versus Curvature versus Torsion

AXIS	SCALE	RANGE
X (Curvature)	1 unit = Cur x 10.0 (Log)	1.0E-4 /m to 1.0E-1 /m
Y (Torsion)	1 unit = Tor x 10.0 (Log)	0. 1.0E-4 /m to 1.0E-1 /m
Z (Dependent Variable plotted for a temp. rise of 100 deg. C)	1 unit = 0.0420 m	0.0006 m to 0.0990 m

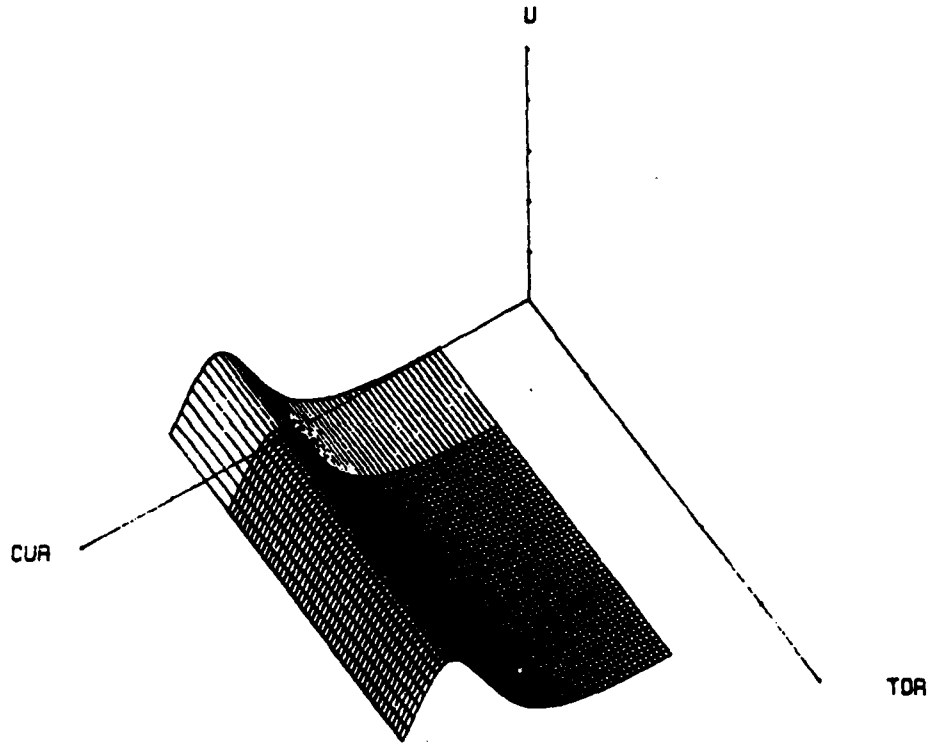

Compatibility 1: U vs Cur vs Tor

Figure 5-3: Compatibility 1: *U* versus Curvature versus Torsion

AXIS	SCALE	RANGE
X (Curvature)	1 unit = Cur x 10.0 (Log)	1.0E-4 /m to 1.0E-1 /m
Y (Torsion)	1 unit = Tor x 10.0 (Log)	0. 1.0E-4 /m to 1.0E-1 /m
Z (Dependent Variable plotted for a temp. rise of 100 deg. C)	1 unit = 0.0024 m	0.0037 m to 0.0060 m

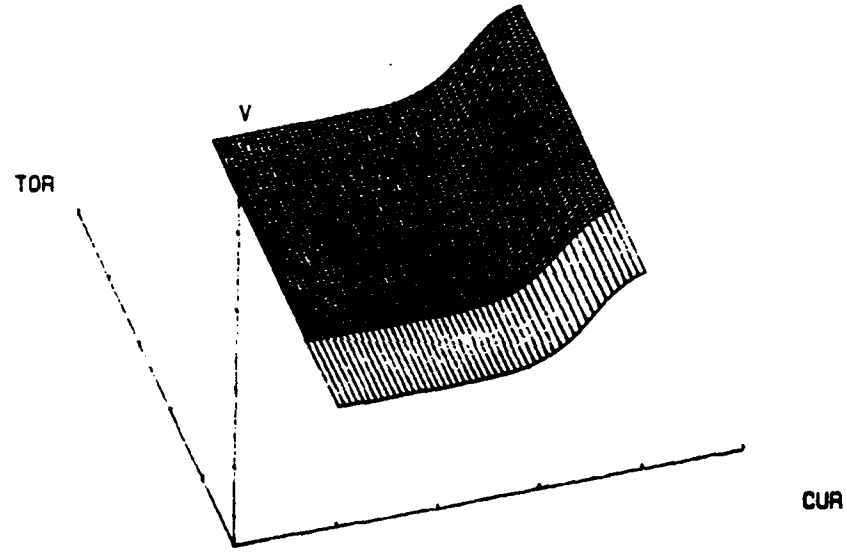

Compatibility 1: V vs Cur vs Tor

Figure 5-4: Compatibility 1: *V* versus Curvature versus Torsion

AXIS	SCALE	RANGE
X (Curvature)	1 unit = Cur x 10.0 (Log)	1.0E-4 /m to 1.0E-1 /m
Y (Torsion)	1 unit = Tor x 10.0 (Log)	0. 1.0E-4 /m to 1.0E-1 /m
Z (Dependent Variable plotted for a temp. rise of 100 deg. C)	1 unit = 0.4800 deg	-2.1629 deg to -0.0142 deg

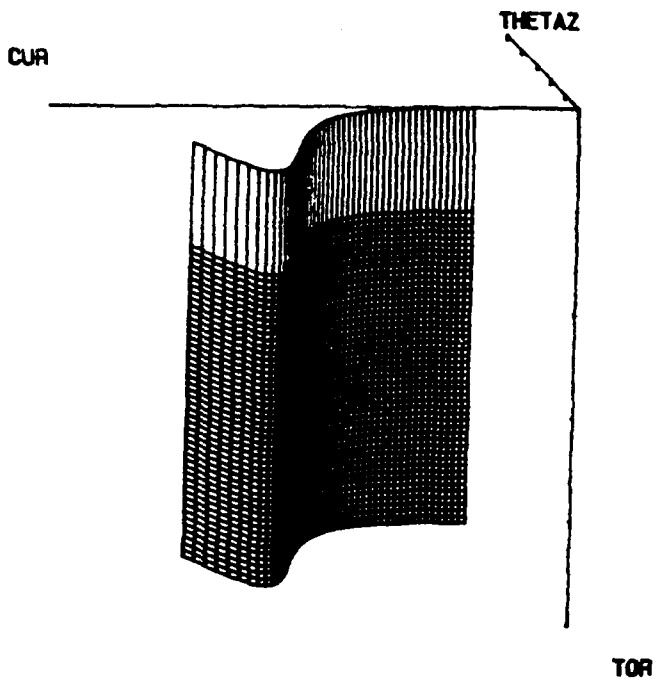

Compatibility 1: Thetaz vs Cur vs Tor

Figure 5-5: Compatibility 1: θ_Z versus Curvature versus Torsion

Note that in Compatibility 1, the displacement is dominated by U, that is, the U component of displacement is of the largest magnitude. This is because V is constrained due to the axial rigidity of the shroud, and W is small because it is an out-of-plane displacement.

Note also that the anomalous behavior with respect to torsion is largely due to the fact that the displacement components plotted are in the chord system. In other words, if the XY plane of the system, in which the displacements are described, were not to almost contain the helical curve, there would no longer be any sense in which a displacement could be considered to be in-plane or out-of-plane, and the effects of these two kinds of motions would be fused.

5.4 Compatibility 2 and its Variations

In Compatibility 1, we assumed that the shroud is infinitely flexible in the transverse direction. Compatibility 2, on the other hand, is a condition wherein the shroud is assumed to have a finite non-zero transverse stiffness. This gives rise to two additional components of force exerted on the gun tube at its end, namely, F_X and F_Z.

5.4.1 Compatibility 2

The shape of the plots of the different force and displacement quantities against curvature and torsion is unchanged by the change of the compatibility condition. In other words, the in-plane forces and displacements, F_X, F_Y and U, V, θ_Z of figures 5.8, 5.9 and 5.11, 5.12, 5.16 respectively show the same lack of variation with torsion along lines of constant curvature. In addition, U (and the corresponding force of resistance F_X) and θ_Z show the same maxima along constant torsion contours. As explained earlier, these are due to the imposition of compatibility. The out-of-plane displacements W, θ_X, and θ_Y also

AXIS	SCALE	RANGE
X (Curvature)	1 unit = Cur x 10.0 (Log)	1.0E-4 /m to 1.0E-1 /m
Y (Torsion)	1 unit = Tor x 10.0 (Log)	0. 1.0E-4 /m to 1.0E-1 /m
Z (Dependent Variable plotted for a temp. rise of 100 deg. C)	1 unit = 0.0020 m	0.0000 m to 0.0017 m

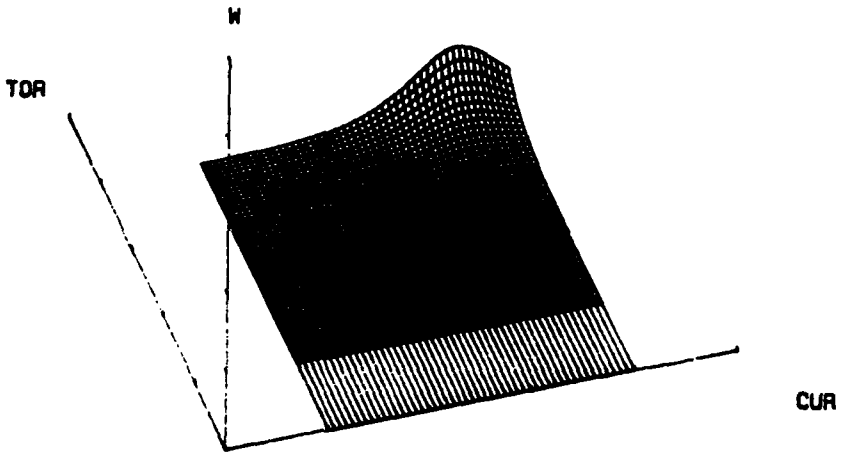

Compatibility 1: W vs Cur vs Tor

Figure 5-6: Compatibility 1: *W* versus Curvature versus Torsion

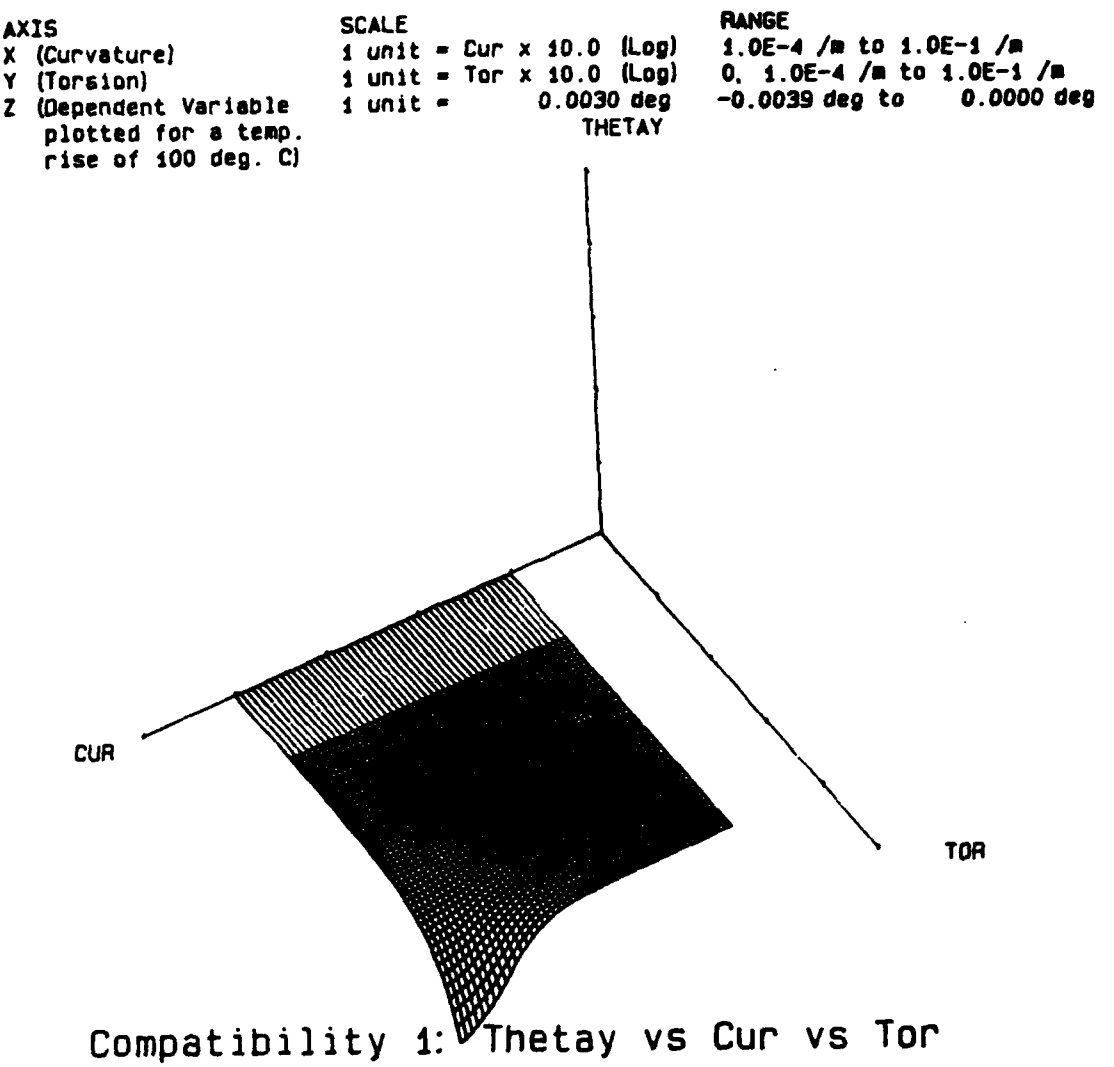

Figure 5-7: Compatibility 1: θ_y versus Curvature versus Torsion

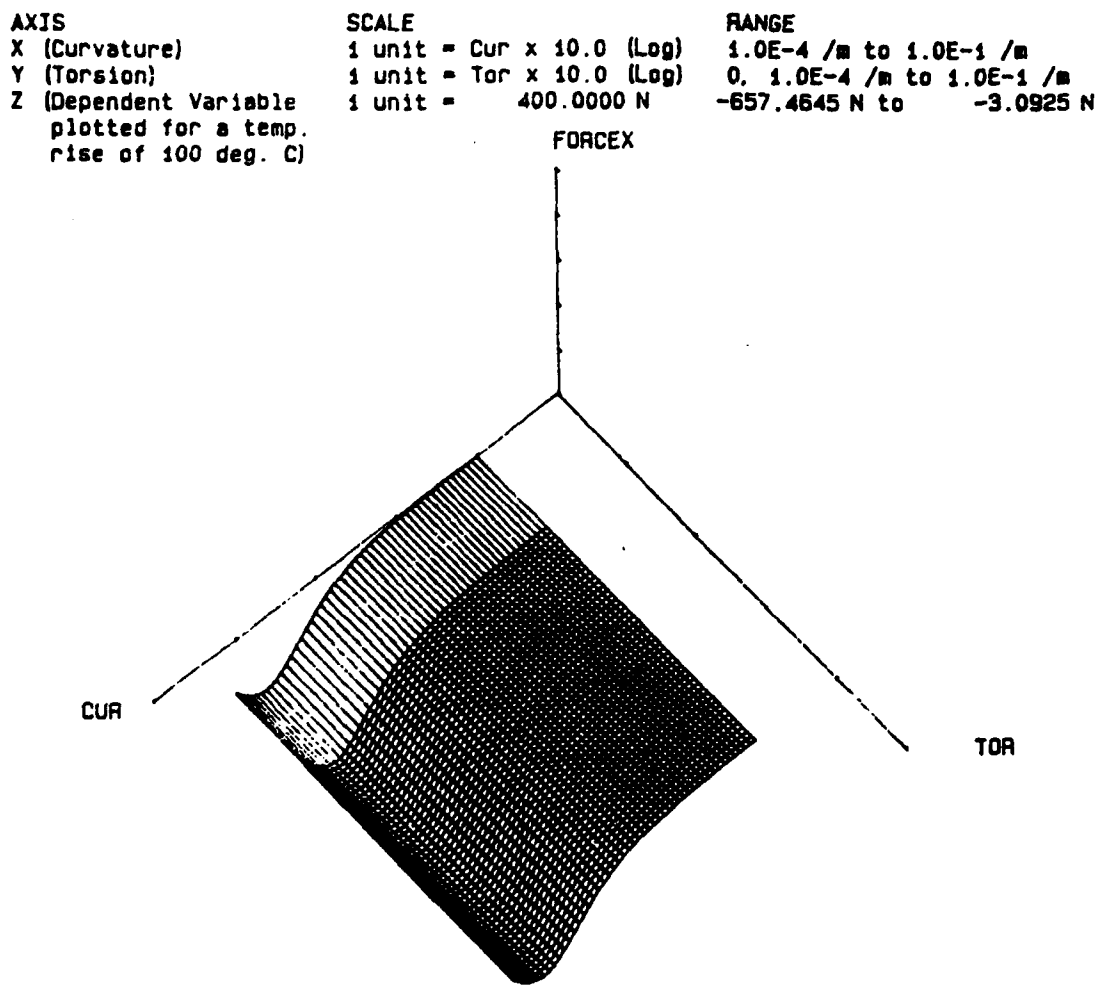

Compatibility 2: Fx vs Cur vs Tor

Figure 5-8: Compatibility 2: F_X versus Curvature versus Torsion

AXIS	SCALE	RANGE
X (Curvature)	1 unit = Cur x 10.0 (Log)	1.0E-4 /m to 1.0E-1 /m
Y (Torsion)	1 unit = Tor x 10.0 (Log)	0, 1.0E-4 /m to 1.0E-1 /m
Z (Dependent Variable plotted for a temp. rise of 100 deg. C)	1 unit = 13440.0000 N	9294.3164 N to 61442.4570 N

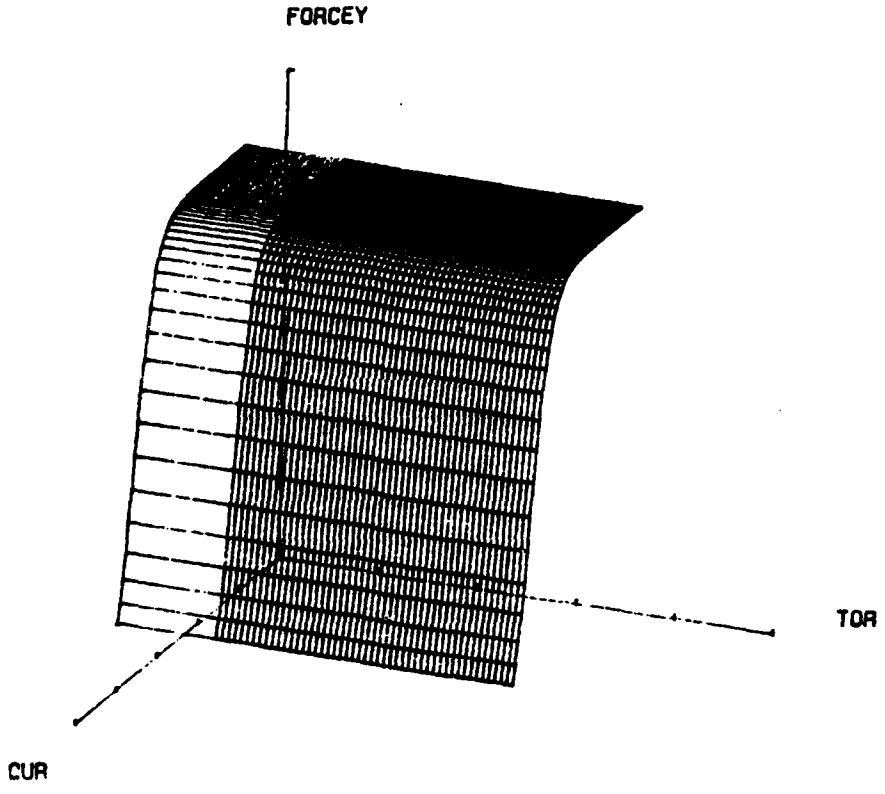

Compatibility 2: Fy vs Cur vs Tor

Figure 5-9: Compatibility 2: F_Y versus Curvature versus Torsion

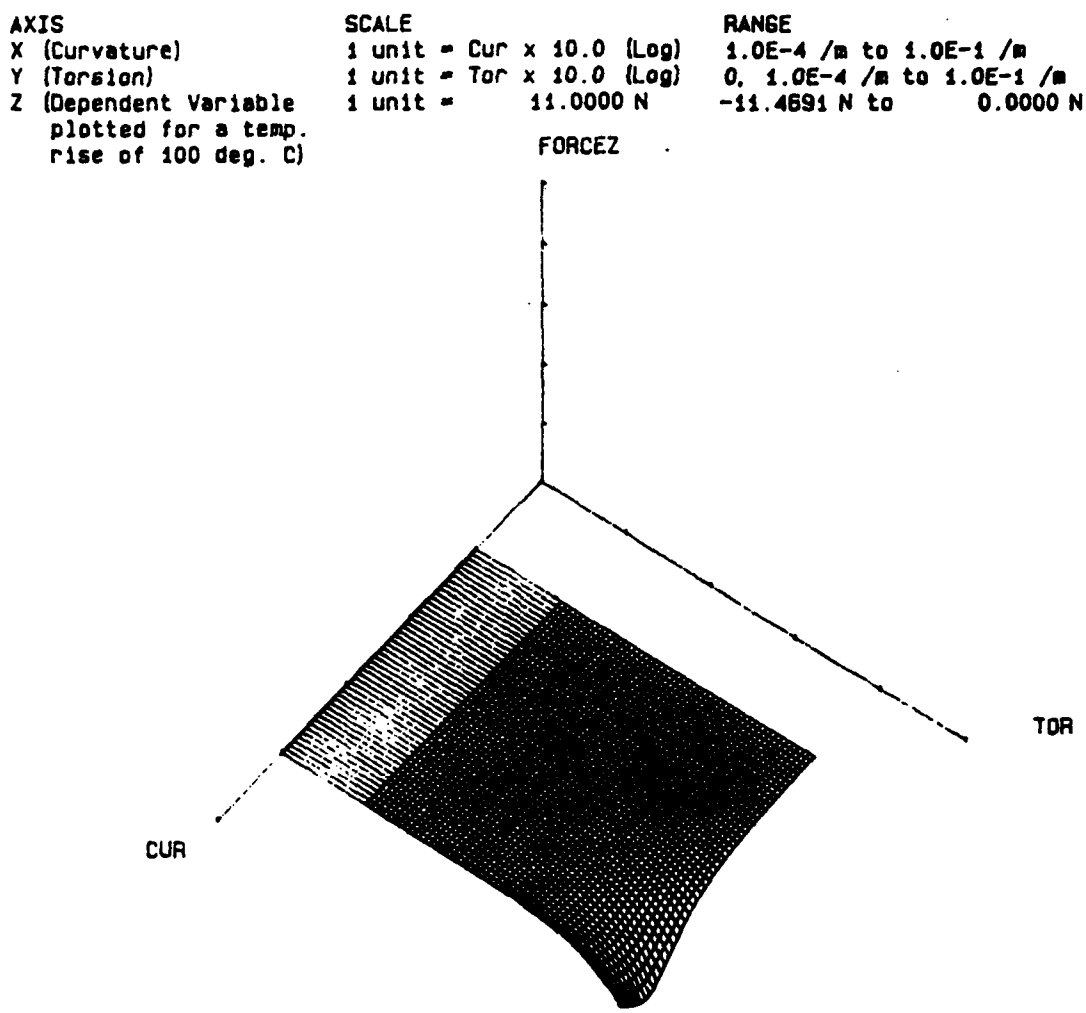

Compatibility 2: Fz vs Cur vs Tor

Figure 5-10: Compatibility 2: F_Z versus Curvature versus Torsion

AXIS	SCALE	RANGE
X (Curvature)	1 unit = Cur x 10.0 (Log)	1.0E-4 /m to 1.0E-1 /m
Y (Torsion)	1 unit = Tor x 10.0 (Log)	0. 1.0E-4 /m to 1.0E-1 /m
Z (Dependent Variable plotted for a temp. rise of 100 deg. C)	1 unit = 0.0200 m	0.0001 m to 0.0312 m

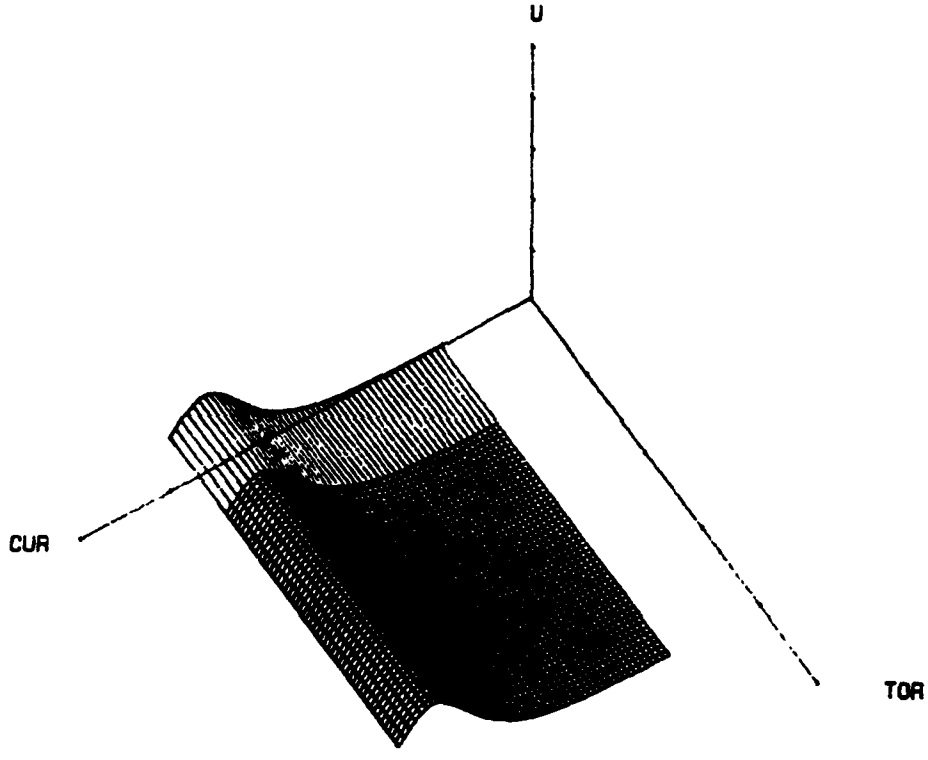

Compatibility 2: U vs Cur vs Tor

Figure 5-11: Compatibility 2: U versus Curvature versus Torsion

AXIS	SCALE	RANGE
X (Curvature)	1 unit = Cur x 10.0 (Log)	1.0E-4 /m to 1.0E-1 /m
Y (Torsion)	1 unit = Tor x 10.0 (Log)	0. 1.0E-4 /m to 1.0E-1 /m
Z (Dependent Variable plotted for a temp. rise of 100 deg. C)	1 unit = 0.0024 m	0.0037 m to 0.0059 m

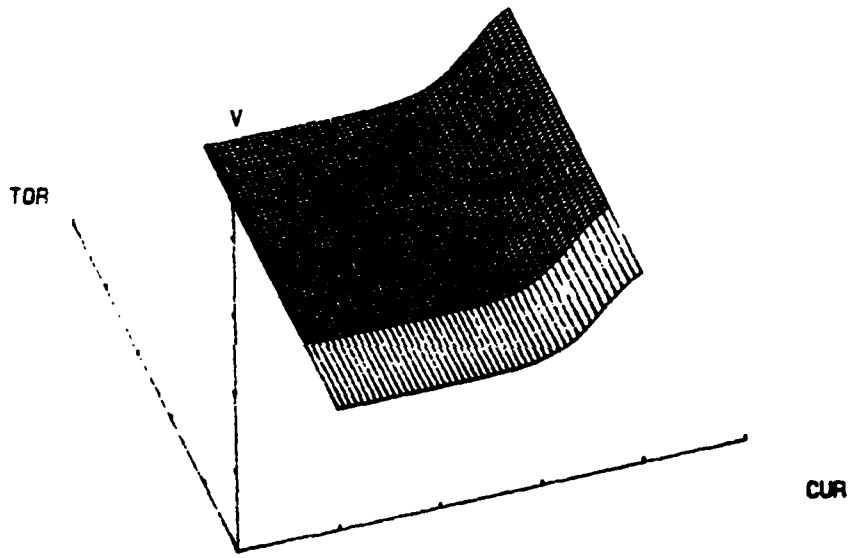

Compatibility 2: V vs Cur vs Tor

Figure 5-12: Compatibility 2: *V* versus Curvature versus Torsion

AXIS	SCALE	RANGE
X (Curvature)	1 unit = Cur x 10.0 (Log)	1.0E-4 /m to 1.0E-1 /m
Y (Torsion)	1 unit = Tor x 10.0 (Log)	0. 1.0E-4 /m to 1.0E-1 /m
Z (Dependent Variable plotted for a temp. rise of 100 deg. C)	1 unit = 0.0005 m	0.0000 m to 0.0005 m

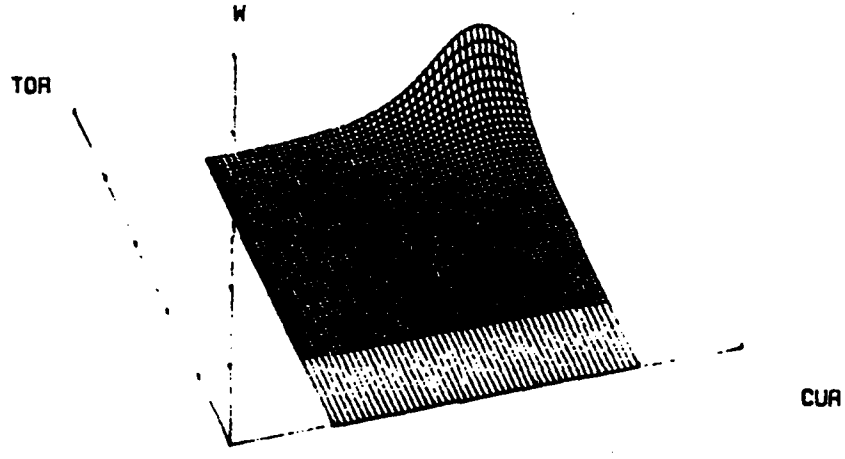

Compatibility 2: W vs Cur vs Tor

Figure 5-13: Compatibility 2: *W* versus Curvature versus Torsion

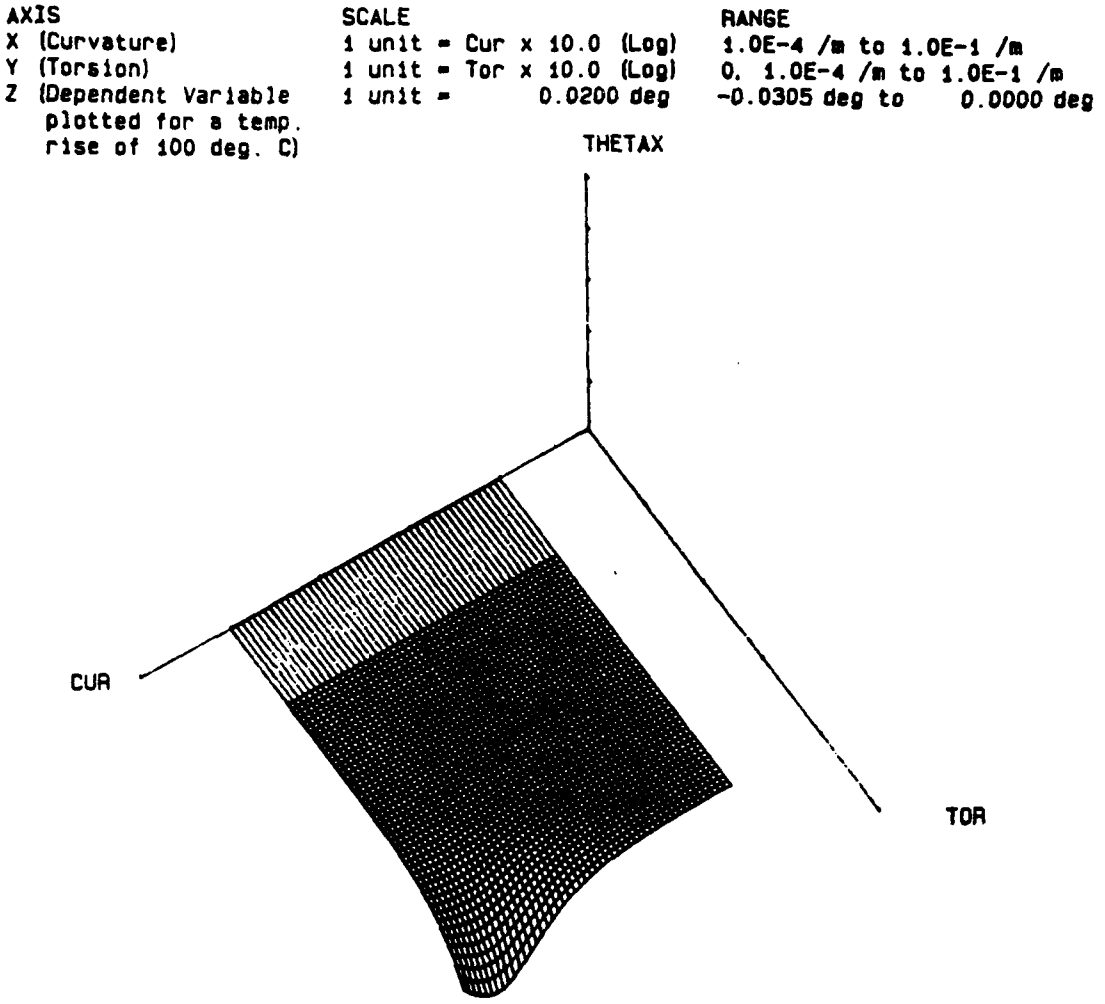

Figure 5-14: Compatibility 2: θ_X versus Curvature versus Torsion

AXIS	SCALE	RANGE
X (Curvature)	1 unit = Cur x 10.0 (Log)	1.0E-4 /m to 1.0E-1 /m
Y (Torsion)	1 unit = Tor x 10.0 (Log)	0, 1.0E-4 /m to 1.0E-1 /m
Z (Dependent Variable plotted for a temp. rise of 100 deg. C)	1 unit = 0.0100 deg	-0.0075 deg to 0.0000 deg

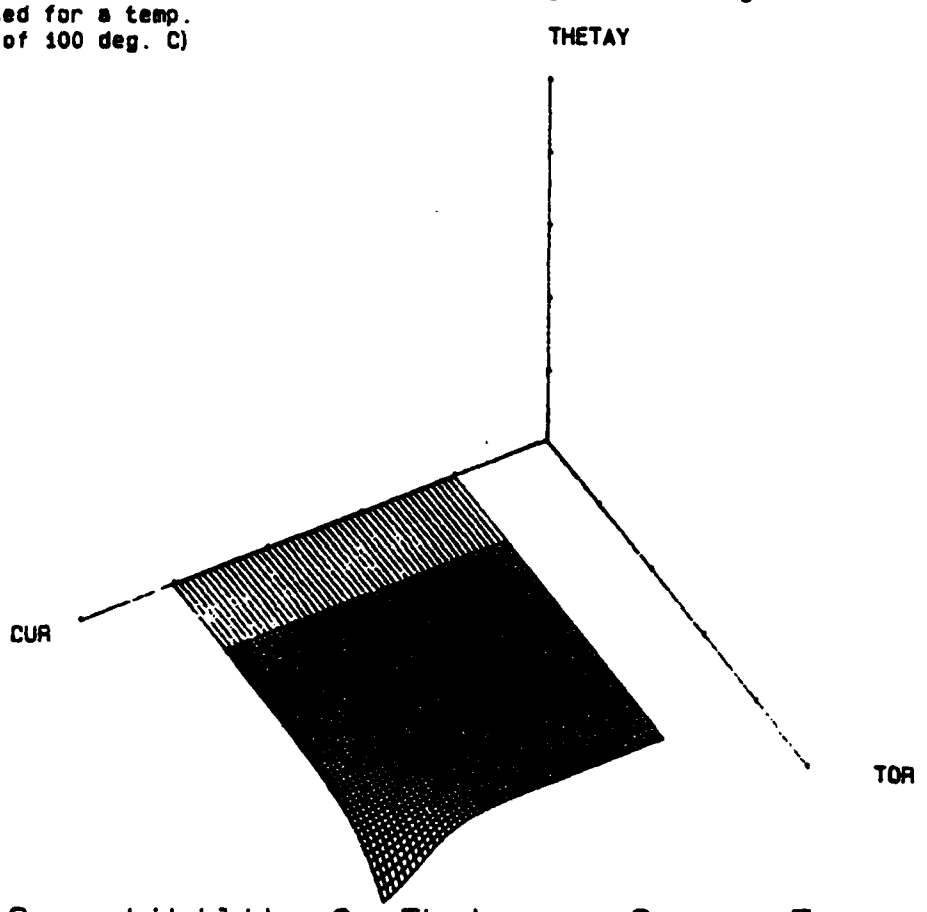

Compatibility 2: Thetay vs Cur vs Tor

Figure 5-15: Compatibility 2: θ_Y versus Curvature versus Torsion

AXIS	SCALE	RANGE
X (Curvature)	1 unit = Cur x 10.0 (Log)	1.0E-4 /m to 1.0E-1 /m
Y (Torsion)	1 unit = Tor x 10.0 (Log)	0. 1.0E-4 /m to 1.0E-1 /m
Z (Dependent Variable plotted for a temp. rise of 100 deg. C)	1 unit = 0.4800 deg	-1.2650 deg to -0.0060 deg

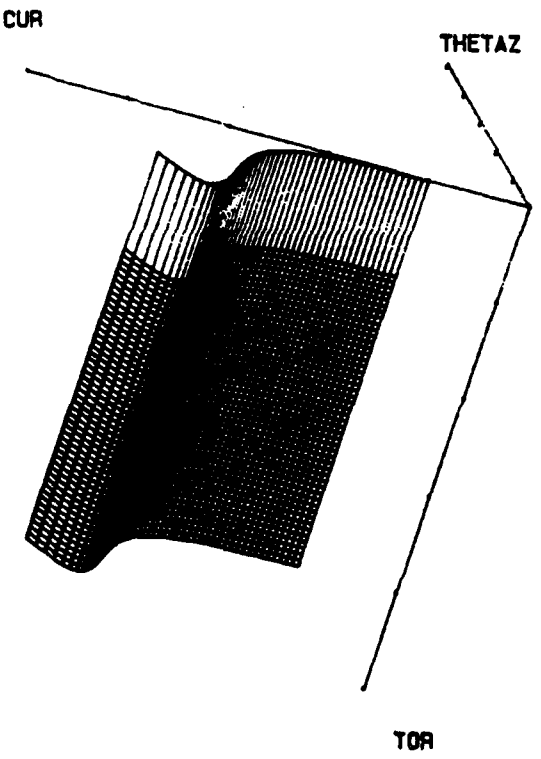

Compatibility 2: Thetaz vs Cur vs Tor

Figure 5-16: Compatibility 2: θ_Z versus Curvature versus Torsion

imitate those of Compatibility 1; they show peaks in the region where $\kappa = \lambda$.

The forces F_X and F_Z arise out of the resistance of the thermal shroud to the U and W displacements of the gun tube. Thus, their plots imitate those of U and W, with a reversal of sign. Note that F_Z is much smaller than F_X in magnitude. This is because the out-of-plane W displacement component is correspondingly smaller in magnitude than the in-plane U displacement, and as a result, the resistance offered by the shroud to W is also lesser. The U and W displacements decrease significantly in magnitude in comparison with those of Compatibility 1, as expected, due to the restraining forces F_X and F_Z respectively. Thus, we find that in Compatibility 2, V is the dominating displacement component. The behavior of the θ_X rotation represents the straightening of the helical arc of Figure 5.1 and the consequent reduction of its deviation from the $X_c Y_c$ plane. Thus θ_X remains always negative.

5.4.2 Variations on Compatibility 2

We now study the effect of variations of the axial and flexural rigidity of the shroud on the forces and displacements that the gun tube experiences. If either of the axial (EA) or transverse (EI) stiffnesses of the thermal shroud is increased, as expected, the force acting on the gun tube increases. If the shroud is made more axially stiff, that is, if EA is increased, the F_Y component of force increases more significantly than the F_X and F_Z components. The reverse is true of the case in which the shroud is stiffened laterally by increasing EI. This is evident from figures 5.17, 5.18, 5.20, 5.21, 5.23 and 5.24.

Comparing figures 5.9 and 5.20, we see that the increase in F_Y due to lateral stiffening is more significant for the larger values of curvature. For small values of curvature, this increase is insignificant. This is because when the curvature is small, the displacement of the gun tube end is primarily along the Y_c direction so that the increased EI has no bearing on the resistance offered by the shroud to the motion of the gun tube end. Thus F_Y is unaffected by increased EI for small curvature. On the other hand, for

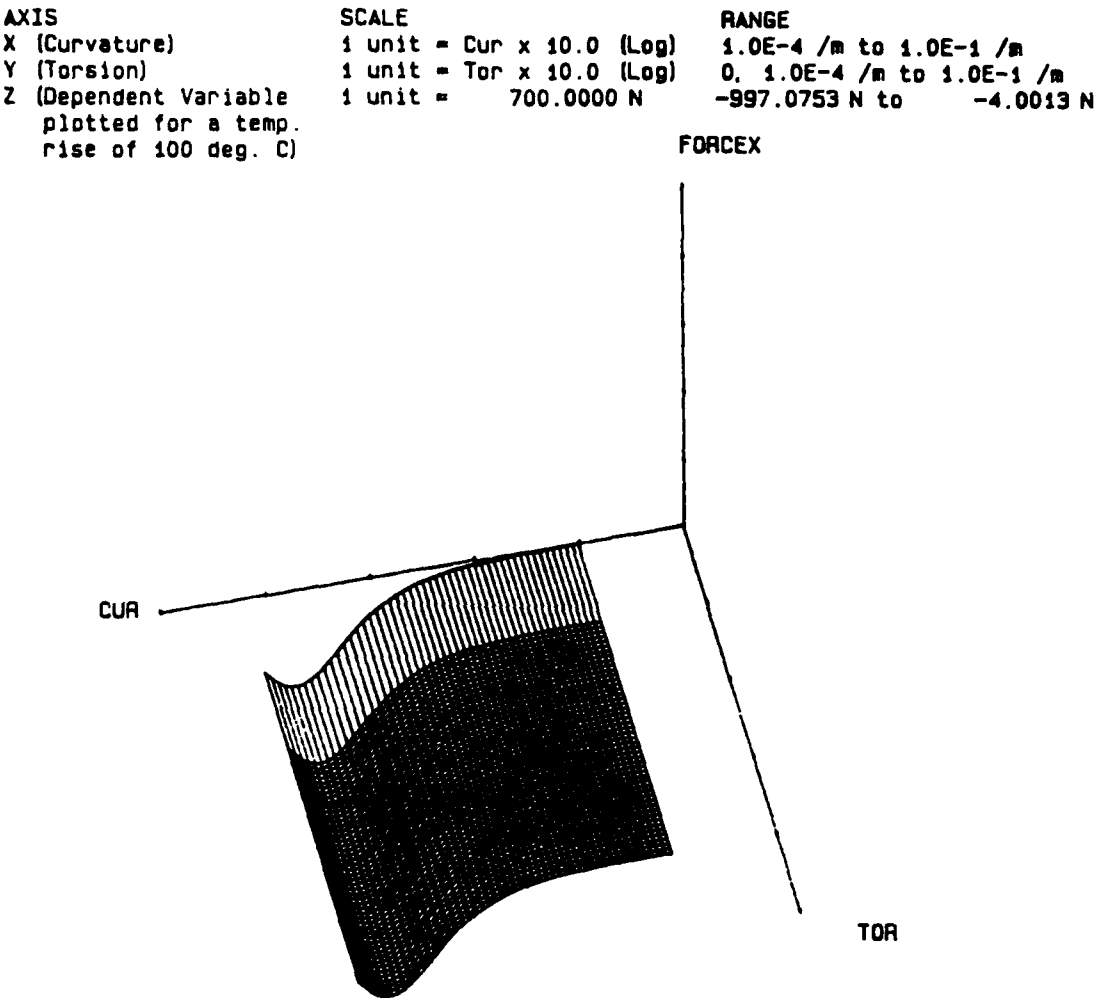

Compatibility 2, EI high: Fx vs Cur vs Tor

Figure 5-17: Compatibility 2, *EI* high: F_X versus Curvature versus Torsion

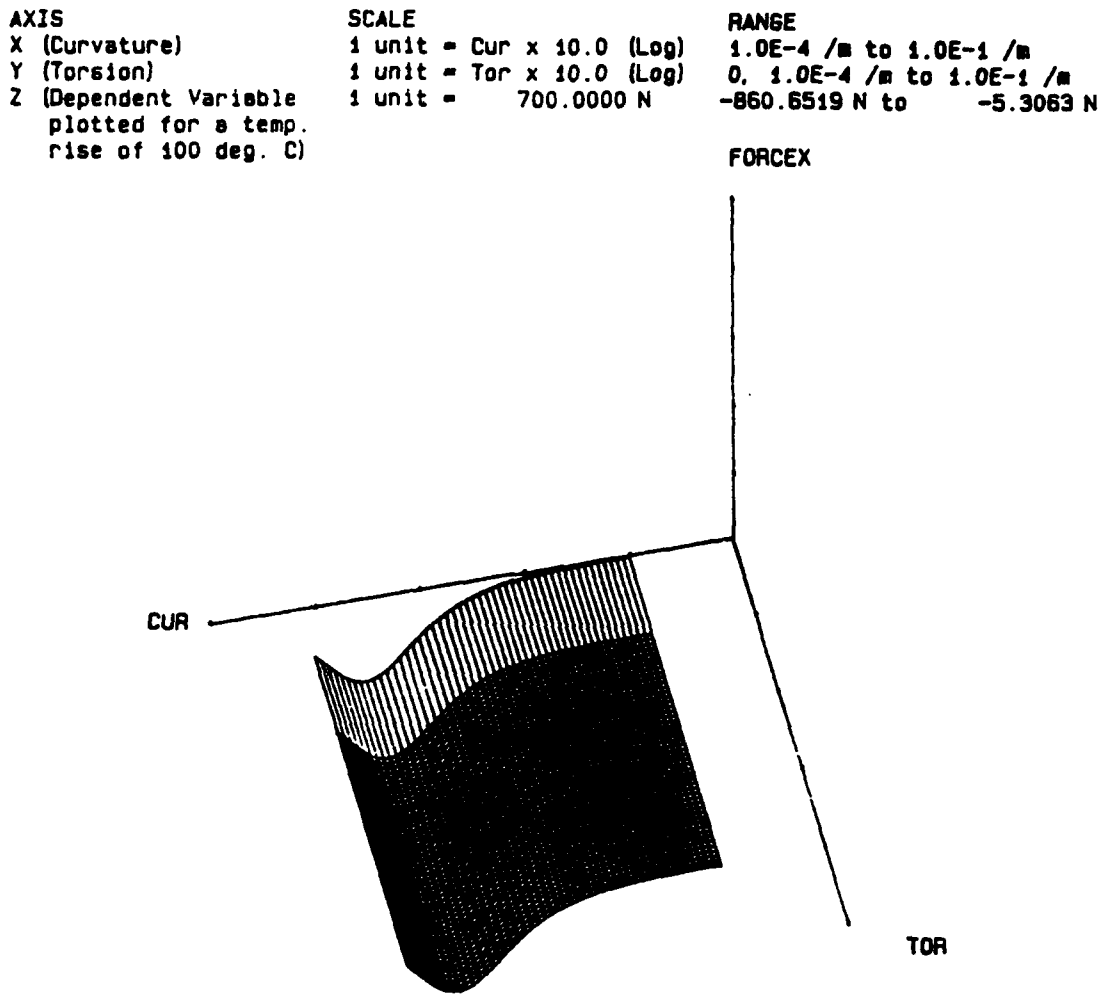

Compatibility 2, EA high: Fx vs Cur vs Tor

Figure 5-18: Compatibility 2, EA high: F_X versus Curvature versus Torsion

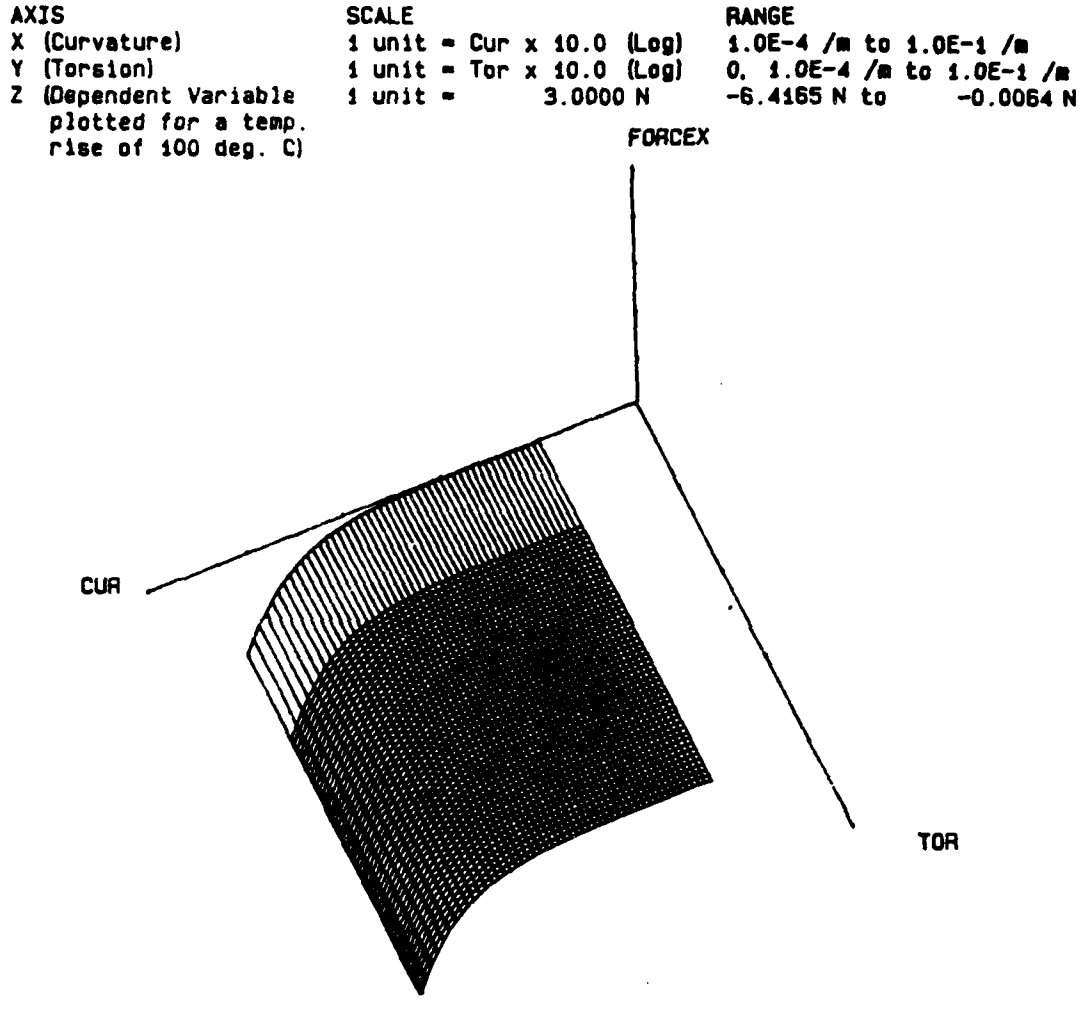

Compatibility 2, EA low: Fx vs Cur vs Tor

Figure 5-19: Compatibility 2, EA low: F_X versus Curvature versus Torsion

AXIS	SCALE	RANGE
X (Curvature)	1 unit = Cur x 10.0 (Log)	1.0E-4 /m to 1.0E-1 /m
Y (Torsion)	1 unit = Tor x 10.0 (Log)	0, 1.0E-4 /m to 1.0E-1 /m
Z (Dependent Variable plotted for a temp. rise of 100 deg. C)	1 unit = 13440.0000 N	12057.1631 N to 61442.5508 N

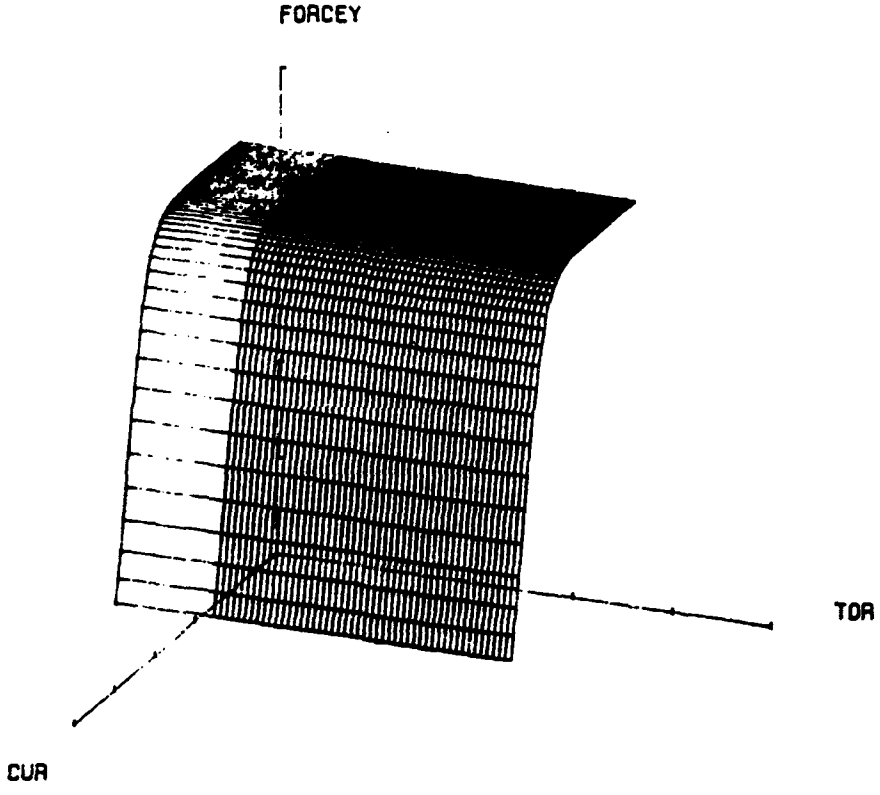

Compatibility 2, EI high: Fy vs Cur vs Tor

Figure 5-20: Compatibility 2, *EI* high: F_Y versus Curvature versus Torsion

AXIS	SCALE	RANGE
X (Curvature)	1 unit = Cur x 10.0 (Log)	1.0E-4 /m to 1.0E-1 /m
Y (Torsion)	1 unit = Tor x 10.0 (Log)	0. 1.0E-4 /m to 1.0E-1 /m
Z (Dependent Variable plotted for a temp. rise of 100 deg. C)	1 unit = 21000.0000 N	9920.3818 N to 105426.0156 N

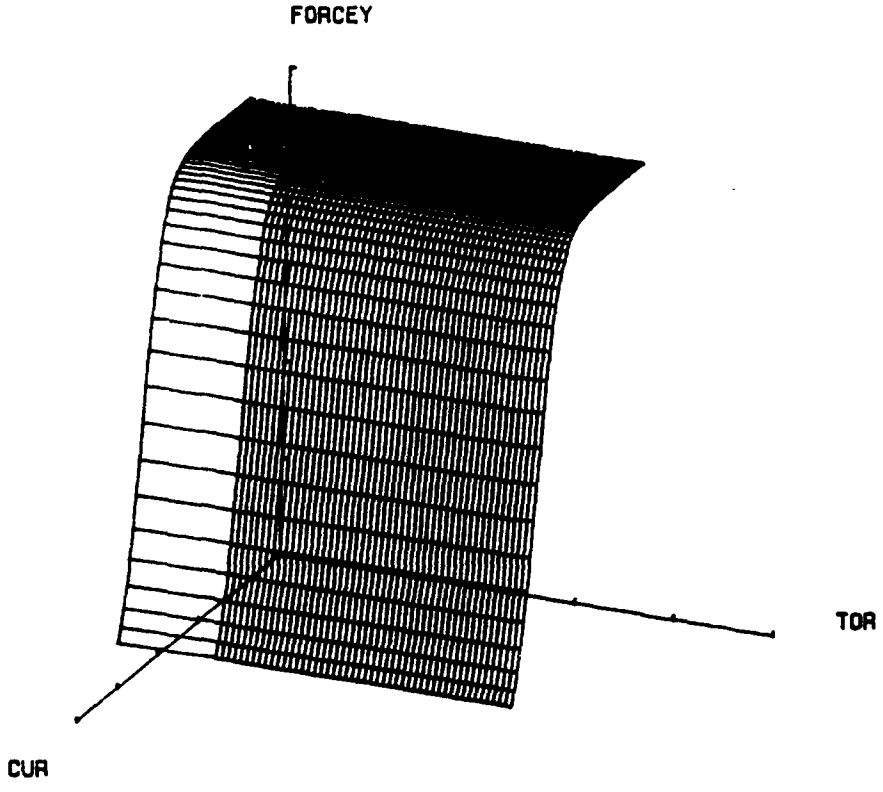

Compatibility 2, EA high: Fy vs Cur vs Tor

Figure 5-21: Compatibility 2, EA high: F_Y versus Curvature versus Torsion

AXIS	SCALE	RANGE
X (Curvature)	1 unit = Cur x 10.0 (Log)	1.0E-4 /m to 1.0E-1 /m
Y (Torsion)	1 unit = Tor x 10.0 (Log)	0, 1.0E-4 /m to 1.0E-1 /m
Z (Dependent Variable plotted for a temp. rise of 100 deg. C)	1 unit = 30.0000 N	133.6712 N to 135.4133 N

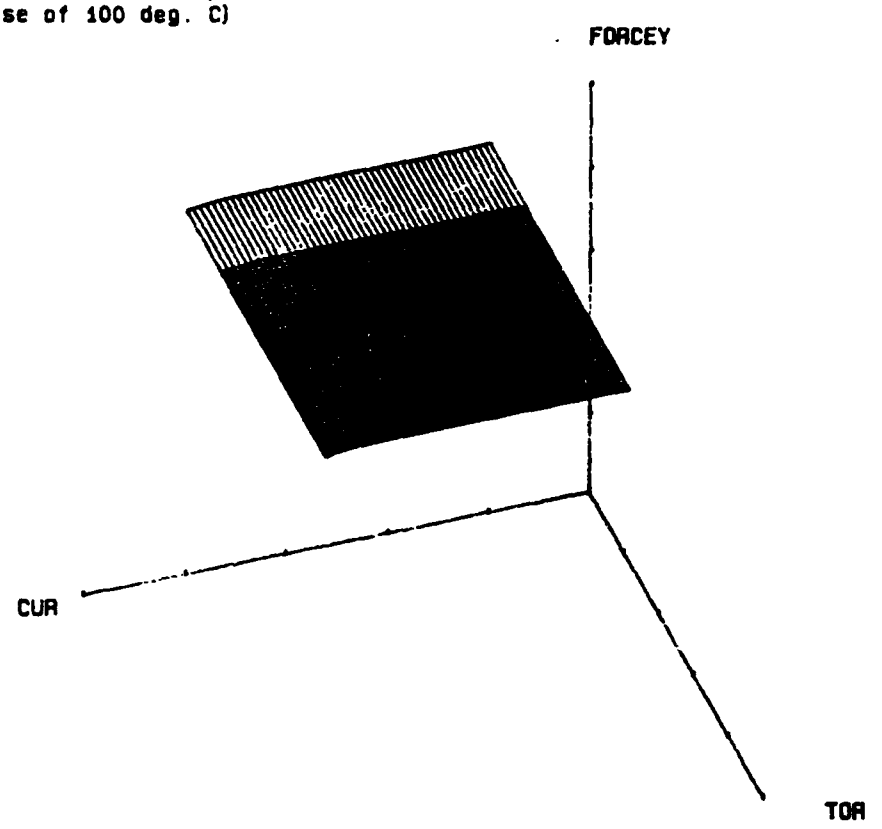

Compatibility 2, EA low: Fy vs Cur vs Tor

Figure 5-22: Compatibility 2, *EA* low: F_Y versus Curvature versus Torsion

AXIS	SCALE	RANGE
X (Curvature)	1 unit = Cur x 10.0 (Log)	1.0E-4 /m to 1.0E-1 /m
Y (Torsion)	1 unit = Tor x 10.0 (Log)	0, 1.0E-4 /m to 1.0E-1 /m
Z (Dependent Variable plotted for a temp. rise of 100 deg. C)	1 unit = 12.0000 N	-17.3472 N to 0.0000 N

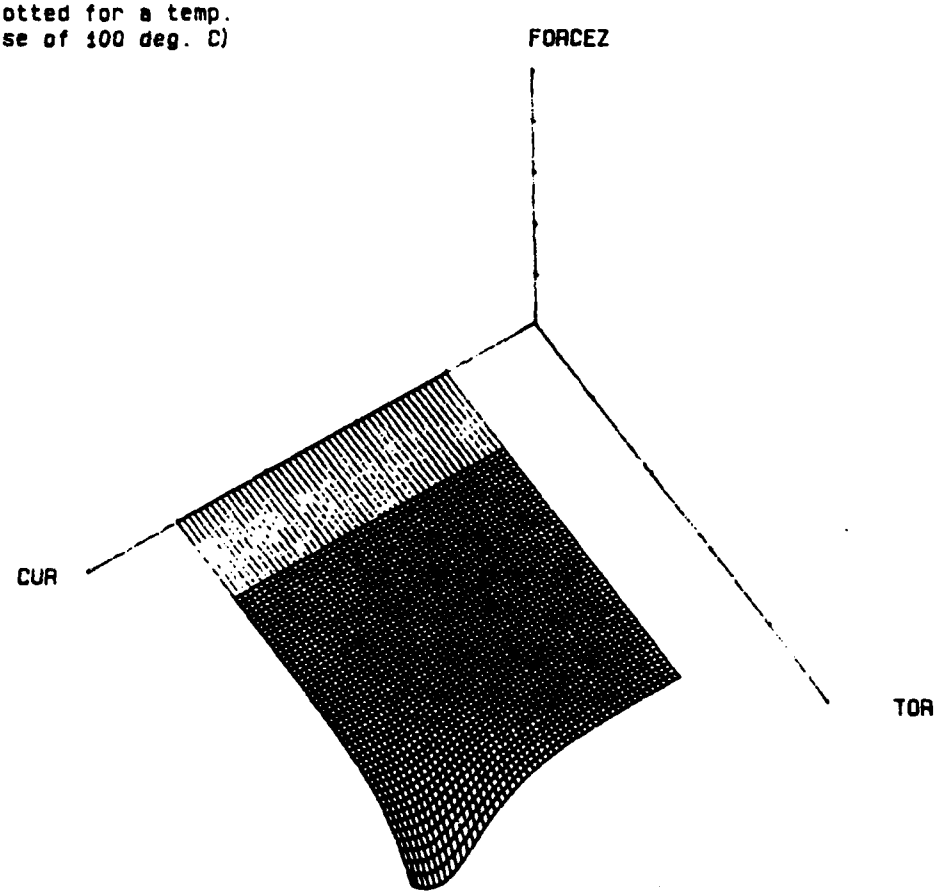

Compatibility 2, EI high: Fz vs Cur vs Tor

Figure 5-23: Compatibility 2, *EI* high: F_Z versus Curvature versus Torsion

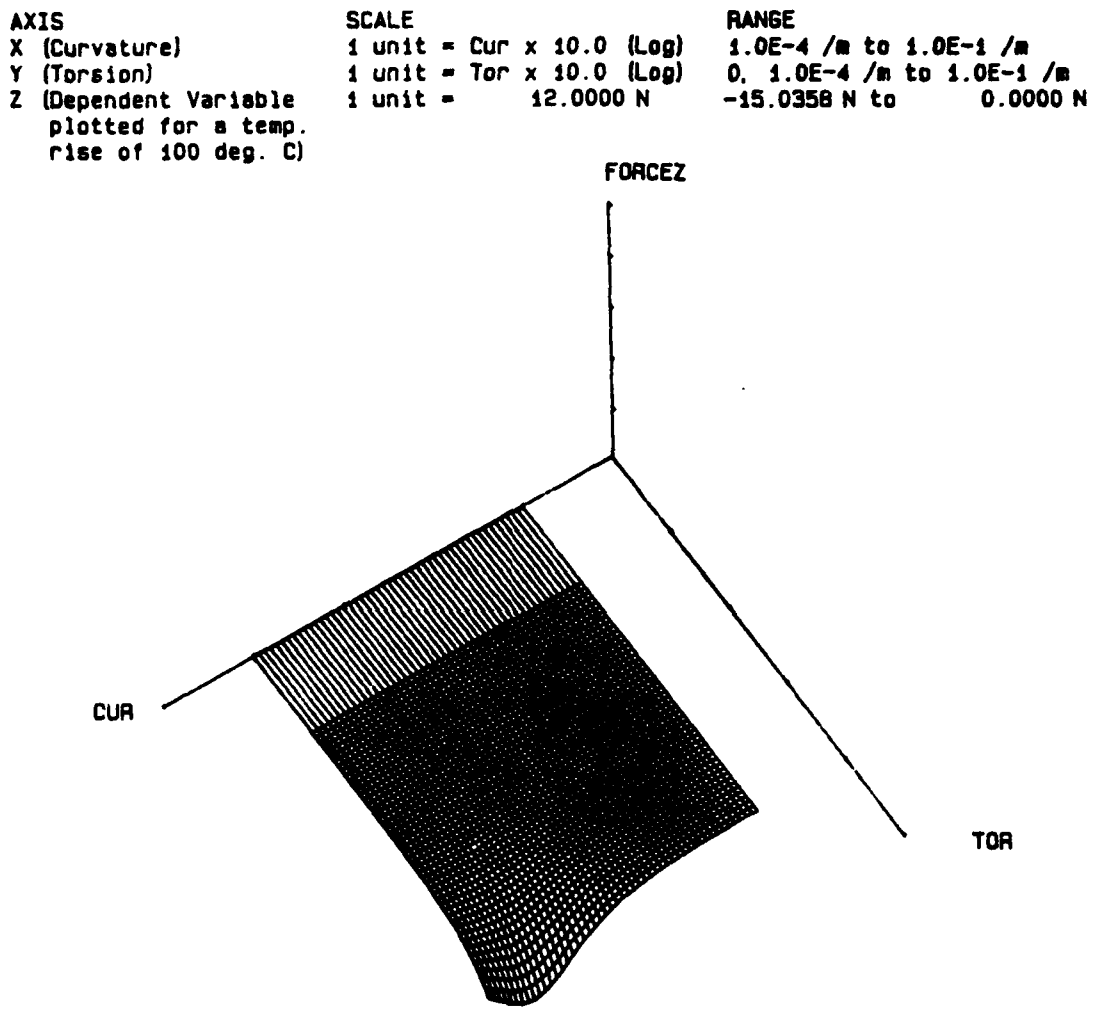

Figure 5-24: Compatibility 2, *EA* high: F_Z versus Curvature versus Torsion

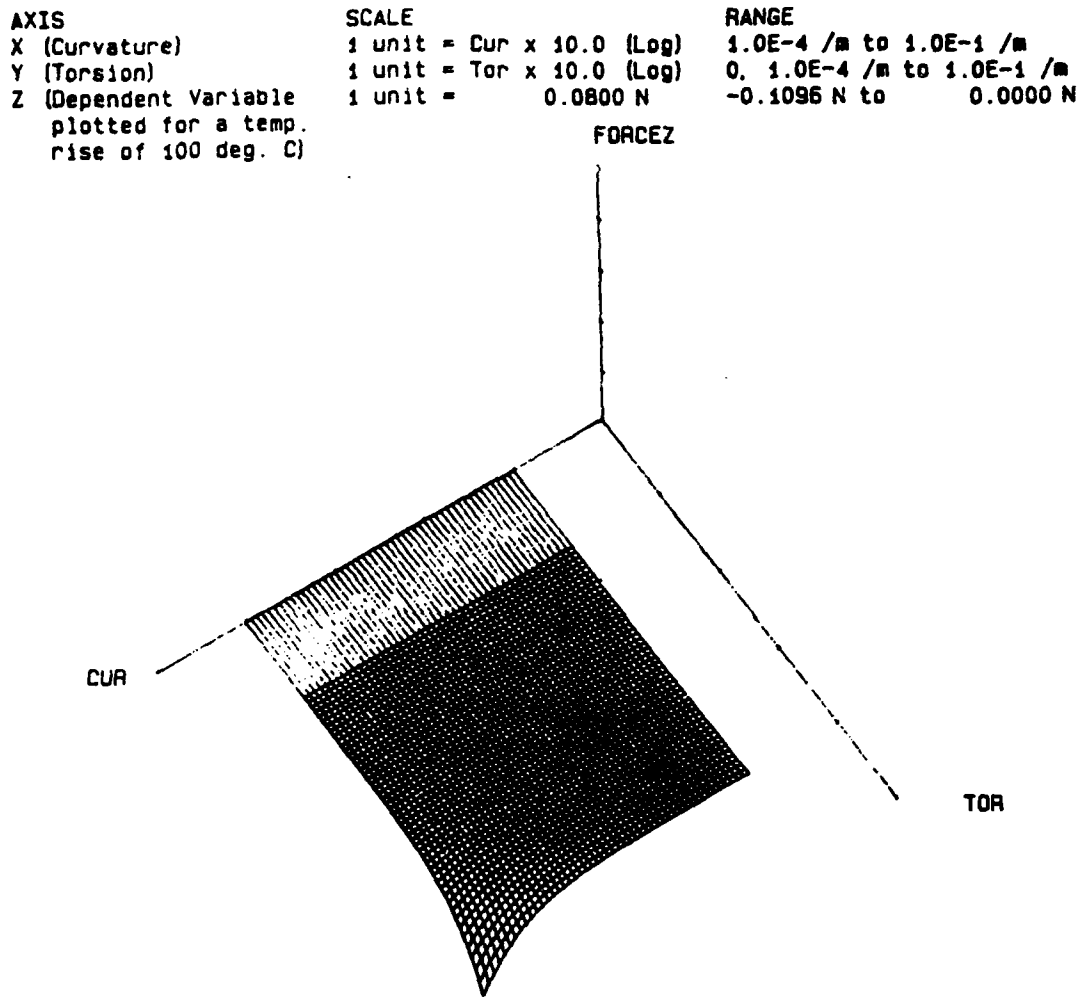

Compatibility 2, EA low: Fz vs Cur vs Tor

Figure 5-25: Compatibility 2, EA low: F_Z versus Curvature versus Torsion

large curvatures, the gun tube end experiences lateral motion to which the shroud, due to its increased EI, offers increased resistance. Thus the overall resistance increases and so does F_Y. Referring to Figure 5.21, we see that the increase in F_Y due to axial stiffening is felt most for small values of curvature. A converse reasoning may be used to explain this situation.

If the EA of the shroud is decreased, which amounts to making it more easily extensible, F_Y becomes almost constant at approximately 135.0 N. This is explained in terms of equations (4.23) as follows: As the EA of the shroud is decreased, we expect that the force F_Y decreases. This means that the displacements also decrease, resulting in lower values of F_X and F_Z. For the purpose of this argument, therefore, we replace the compatibility equations (4.23) with Equation (4.21). Now, if EA is decreased, it is clear from Equation (4.21) that the $L_s/(E_sA_s)$ term dominates the denominator, so that F_Y is approximately constant and equal to $E_sA_s\alpha\triangle T$, which for the assumed data, evaluates to 147.1 N. The difference, of course, is due to the fact that we cannot reduce equations (4.23) to Equation (4.21), since F_X and F_Z are non-zero in reality. Note from figures 5.19 and 5.25 that F_X and F_Z are indeed greatly reduced in magnitude as supposed in the above argument.

Another point worth noting is that the graphs of F_X and F_Z do not show the maxima along constant torsion contours as for previous compatibility conditions. Recall that in Compatibility 1, we explained the maxima in the U and θ_Z plots as representing the meeting point of two conflicting tendencies, the increase in flexibility of the rod with increasing curvature, and the decrease in force resulting from the solution of Equation (4.21). Here, however, the force F_Y is almost constant, so that these maxima are obviously out of the question.

If, on the other hand, we decrease the EI of the shroud, Compatibility 2 reduces, in the limit, to Compatibility 1, since the shroud becomes more flexible and offers negligible resistance to the lateral motion of the end of the gun tube. The plots for low EI have not been included for precisely this reason.

AXIS	SCALE	RANGE
X (Curvature)	1 unit = Cur x 10.0 (Log)	1.0E-4 /m to 1.0E-1 /m
Y (Torsion)	1 unit = Tor x 10.0 (Log)	0, 1.0E-4 /m to 1.0E-1 /m
Z (Dependent Variable plotted for a temp. rise of 100 deg. C)	1 unit = 0.0000 m	0.0000 m to 0.0000 m

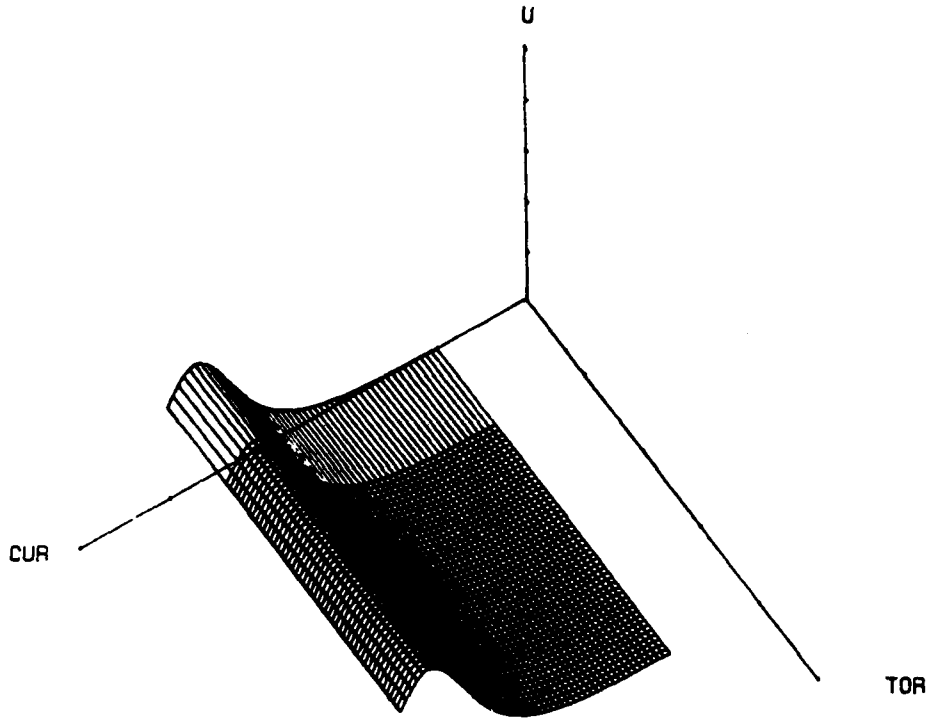

Compatibility 2, EI high: U vs Cur vs Tor

Figure 5-26: Compatibility 2, *EI* high: *U* versus Curvature versus Torsion

AXIS	SCALE	RANGE
X (Curvature)	1 unit = Cur x 10.0 (Log)	1.0E-4 /m to 1.0E-1 /m
Y (Torsion)	1 unit = Tor x 10.0 (Log)	0, 1.0E-4 /m to 1.0E-1 /m
Z (Dependent Variable plotted for a temp. rise of 100 deg. C)	1 unit = 0.0200 m	0.0003 m to 0.0409 m

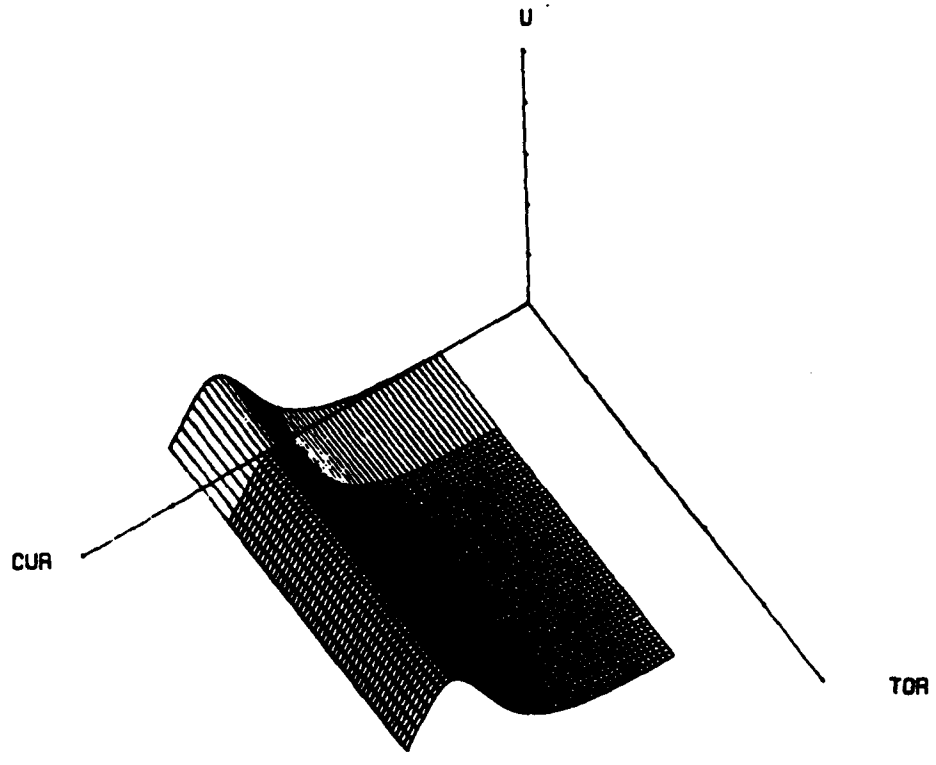

Compatibility 2, EA high: U vs Cur vs Tor

Figure 5-27: Compatibility 2, *EA* high: *U* versus Curvature versus Torsion

AXIS	SCALE	RANGE
X (Curvature)	1 unit = Cur x 10.0 (Log)	1.0E-4 /m to 1.0E-1 /m
Y (Torsion)	1 unit = Tor x 10.0 (Log)	0. 1.0E-4 /m to 1.0E-1 /m
Z (Dependent Variable plotted for a temp. rise of 100 deg. C)	1 unit = 0.0001 m	0.0000 m to 0.0004 m

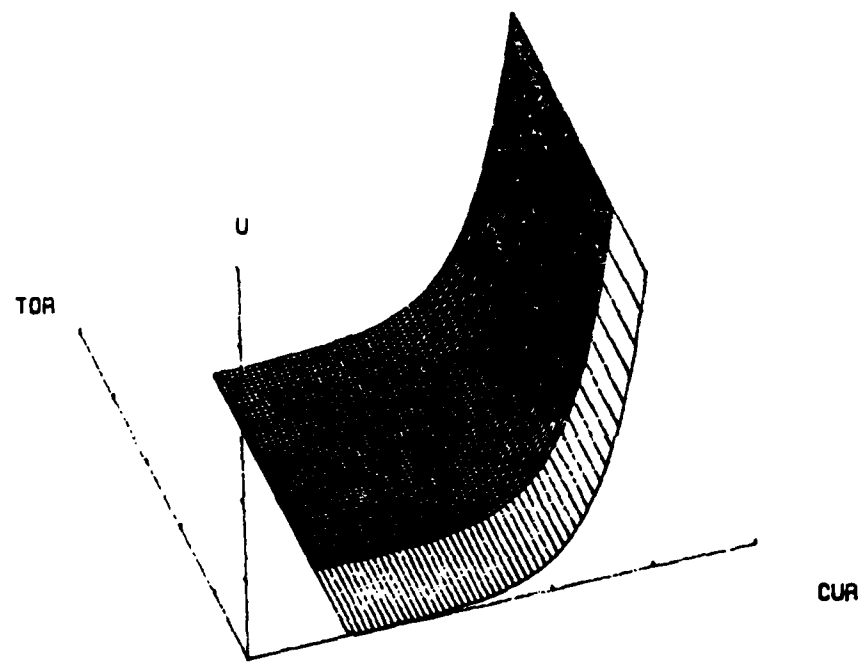

Compatibility 2, EA low: U vs Cur vs Tor

Figure 5-28: Compatibility 2, *EA* low: *U* versus Curvature versus Torsion

AXIS	SCALE	RANGE
X (Curvature)	1 unit = Cur x 10.0 (Log)	1.0E-4 /m to 1.0E-1 /m
Y (Torsion)	1 unit = Tor x 10.0 (Log)	0. 1.0E-4 /m to 1.0E-1 /m
Z (Dependent Variable plotted for a temp. rise of 100 deg. C)	1 unit = 0.0024 m	0.0037 m to 0.0057 m

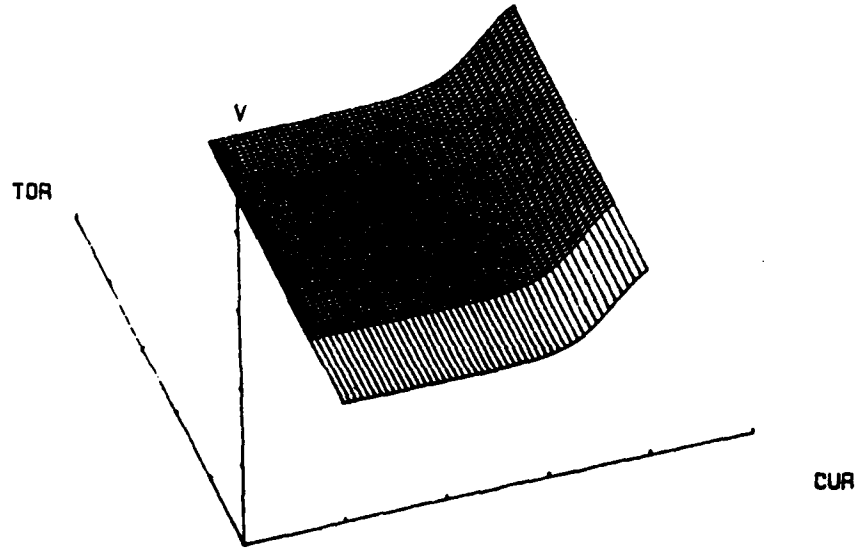

Compatibility 2, EI high: V vs Cur vs Tor

Figure 5-29: Compatibility 2, *EI* high: *V* versus Curvature versus Torsion

AXIS	SCALE	RANGE
X (Curvature)	1 unit = Cur x 10.0 (Log)	1.0E-4 /m to 1.0E-1 /m
Y (Torsion)	1 unit = Tor x 10.0 (Log)	0, 1.0E-4 /m to 1.0E-1 /m
Z (Dependent Variable plotted for a temp. rise of 100 deg. C)	1 unit = 0.0024 m	0.0063 m to 0.0063 m

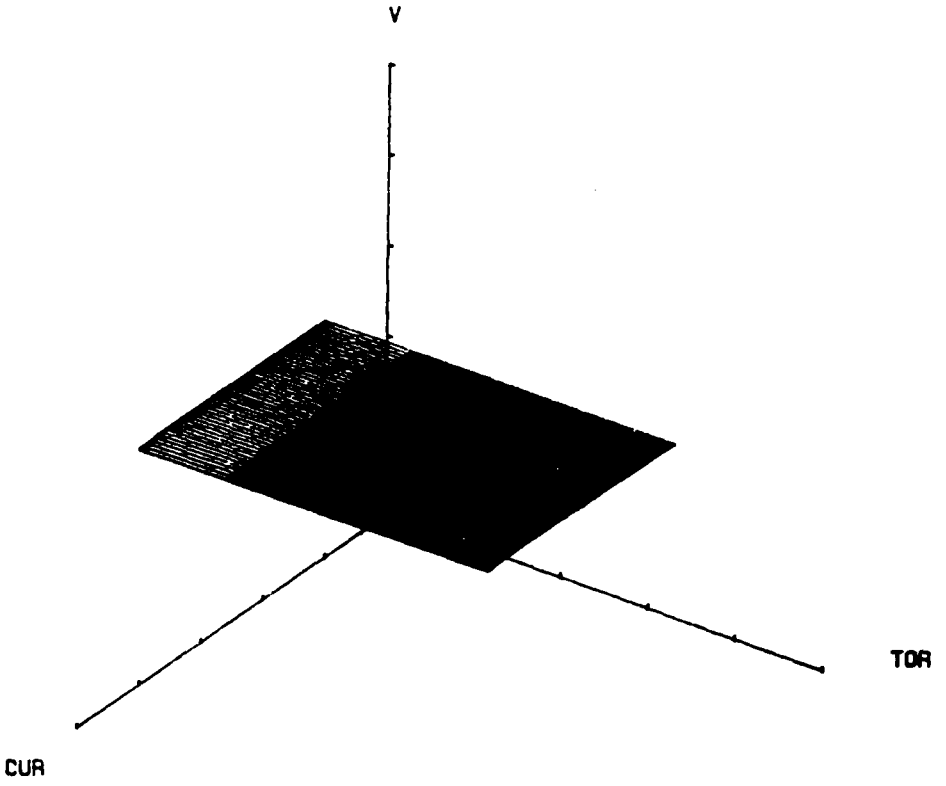

Compatibility 2, EA high: V vs Cur vs Tor

Figure 5-30: Compatibility 2, *EA* high: *V* versus Curvature versus Torsion

AXIS	SCALE	RANGE
X (Curvature)	1 unit = Cur x 10.0 (Log)	1.0E-4 /m to 1.0E-1 /m
Y (Torsion)	1 unit = Tor x 10.0 (Log)	0, 1.0E-4 /m to 1.0E-1 /m
Z (Dependent Variable plotted for a temp. rise of 100 deg. C)	1 unit = 0.0000 m	0.0000 m to 0.0001 m

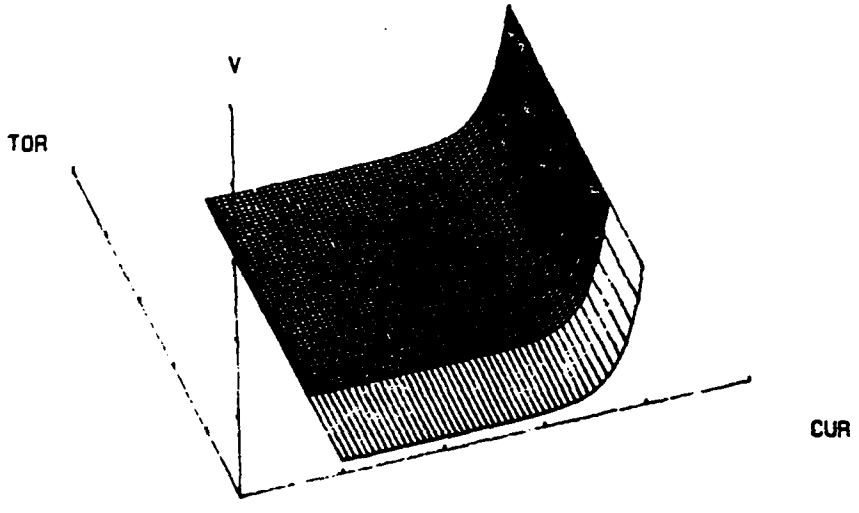

Compatibility 2, EA low: V vs Cur vs Tor

Figure 5-31: Compatibility 2, *EA* low: *V* versus Curvature versus Torsion

AXIS	SCALE	RANGE
X (Curvature)	1 unit = Cur x 10.0 (Log)	1.0E-4 /m to 1.0E-1 /m
Y (Torsion)	1 unit = Tor x 10.0 (Log)	0. 1.0E-4 /m to 1.0E-1 /m
Z (Dependent Variable plotted for a temp. rise of 100 deg. C)	1 unit = 0.0000 m	0.0000 m to 0.0000 m

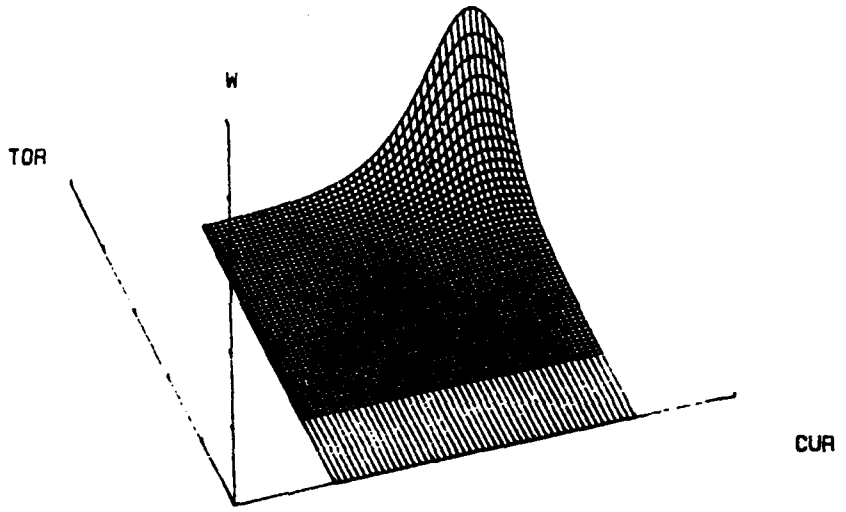

Compatibility 2, EI high: W vs Cur vs Tor

Figure 5-32: Compatibility 2, *EI* high: *W* versus Curvature versus Torsion

AXIS	SCALE	RANGE
X (Curvature)	1 unit = Cur x 10.0 (Log)	1.0E-4 /m to 1.0E-1 /m
Y (Torsion)	1 unit = Tor x 10.0 (Log)	0, 1.0E-4 /m to 1.0E-1 /m
Z (Dependent Variable plotted for a temp. rise of 100 deg. C)	1 unit = 0.0005 m	0.0000 m to 0.0007 m

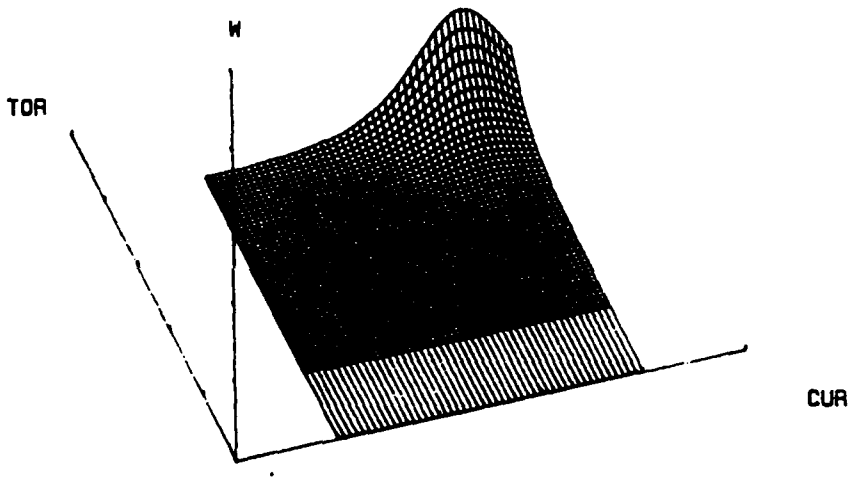

Compatibility 2, EA high: W vs Cur vs Tor

Figure 5-33: Compatibility 2, *EA* high: *W* versus Curvature versus Torsion

AXIS	SCALE	RANGE
X (Curvature)	1 unit = Cur x 10.0 (Log)	1.0E-4 /m to 1.0E-1 /m
Y (Torsion)	1 unit = Tor x 10.0 (Log)	0. 1.0E-4 /m to 1.0E-1 /m
Z (Dependent Variable plotted for a temp. rise of 100 deg. C)	1 unit = 0.0000 m	0.0000 m to 0.0000 m

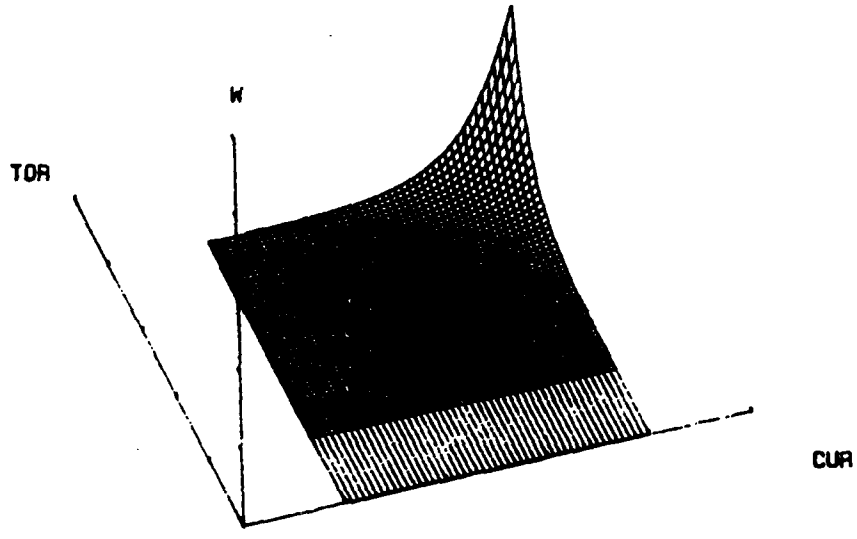

Compatibility 2, EA low: W vs Cur vs Tor

Figure 5-34: Compatibility 2, *EA* low: *W* versus Curvature versus Torsion

We observe from figure 5.26 and 5.32 that when the EI of the shroud is increased, the transverse displacements, U and W, decrease considerably, although there is no change in the shape of the plots as compared to those of Compatibility 2. The V displacement shown in Figure 5.29 decreases, for increased EI, noticeably for higher values of curvature, from 0.0059 m in Compatibility 2 (Figure 5.12), to 0.0057 m in the present case, since F_Y increases for higher values of curvature as explained earlier.

If EA of the shroud is increased, the V displacement attains an almost constant value of 0.0063 m. This is shown in Figure 5.30. This is because the shroud has now become almost infinitely rigid as compared to the gun tube. Thus the curvature and torsion of the gun tube are irrelevant. The magnitude of V is, in the limit, simply equal to the expansion of the thermal shroud, that is, $L_s \alpha \triangle T$. The transverse displacements U and W *increase* from their values in Compatibility 2. This may be attributed to the enormous increase in the force exerted by the shroud on the gun tube.

If the EA of the shroud is decreased, we find that the maxima along lines of constant torsion seen in the plots of U and W, and the inflexion point in the plots of V disappear. This is due to the fact that the force exerted by the shroud on the gun tube is almost a constant, as can be seen from Figure 5.22. All of the above displacements decrease considerably in magnitude, mainly due to the fact that the force exerted by the shroud on the gun tube is very small.

The rotations θ_X, θ_Y, and θ_Z are the angular displacements of the tangent to the centroidal axis of the gun tube. These therefore represent the straightening of the helical arc as it is extended. The plots of θ_X, θ_Y, and θ_Z of figures 5.35 - 5.43 are generally similar to those of Compatibility 2. If either of the EI or EA of the shroud is increased, all of the rotations increase since the gun tube tends to straighten to a greater extent, on account of the shroud's increased stiffness. If the EA of the shroud decreases, then the maxima of the plots of θ_X and θ_Z that occur in the region $\kappa = \lambda$, disappear. This is because the force exerted on the gun tube by the shroud approaches a constant value.

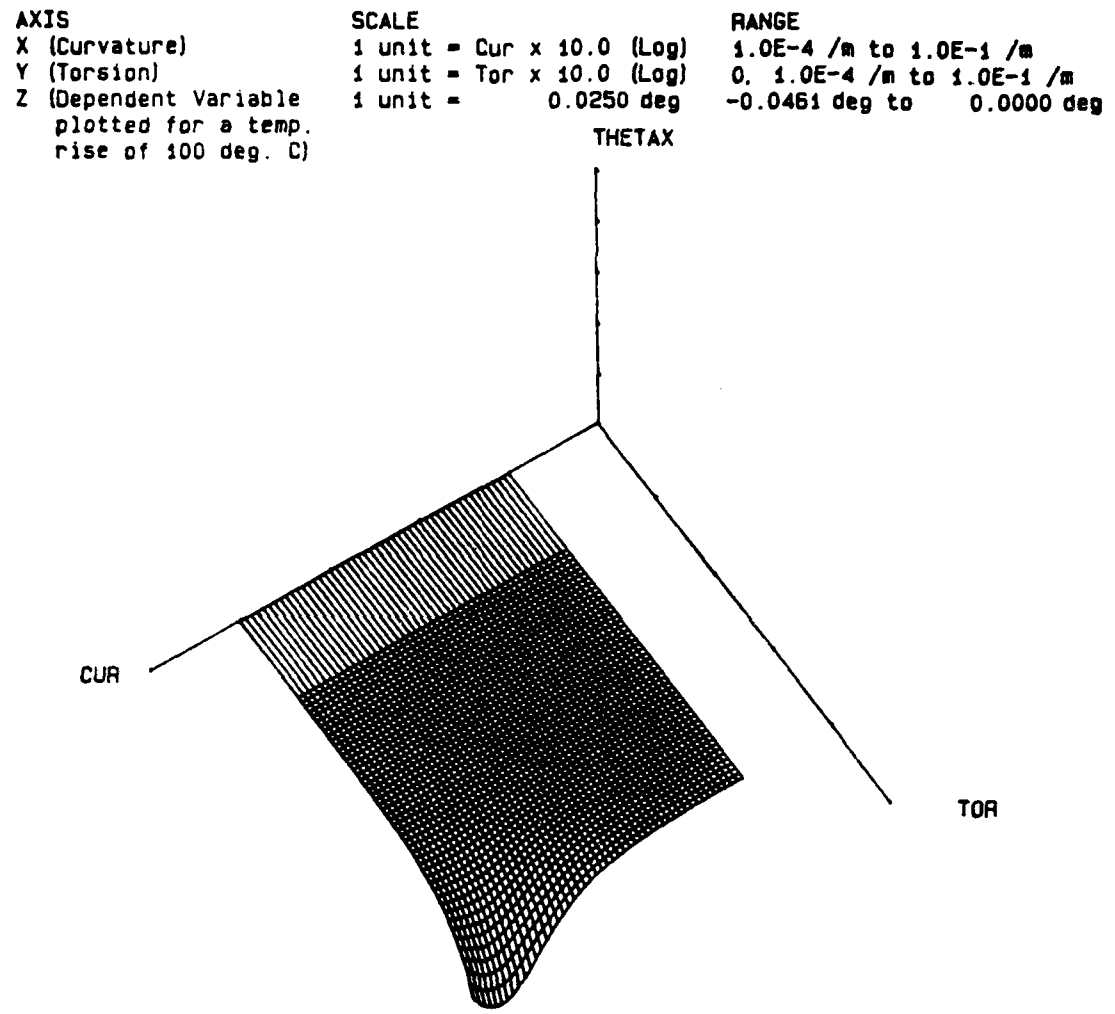

Compatibility 2, EI high: Thetax vs Cur vs Tor

Figure 5-35: Compatibility 2, *EI* high: θ_X versus Curvature versus Torsion

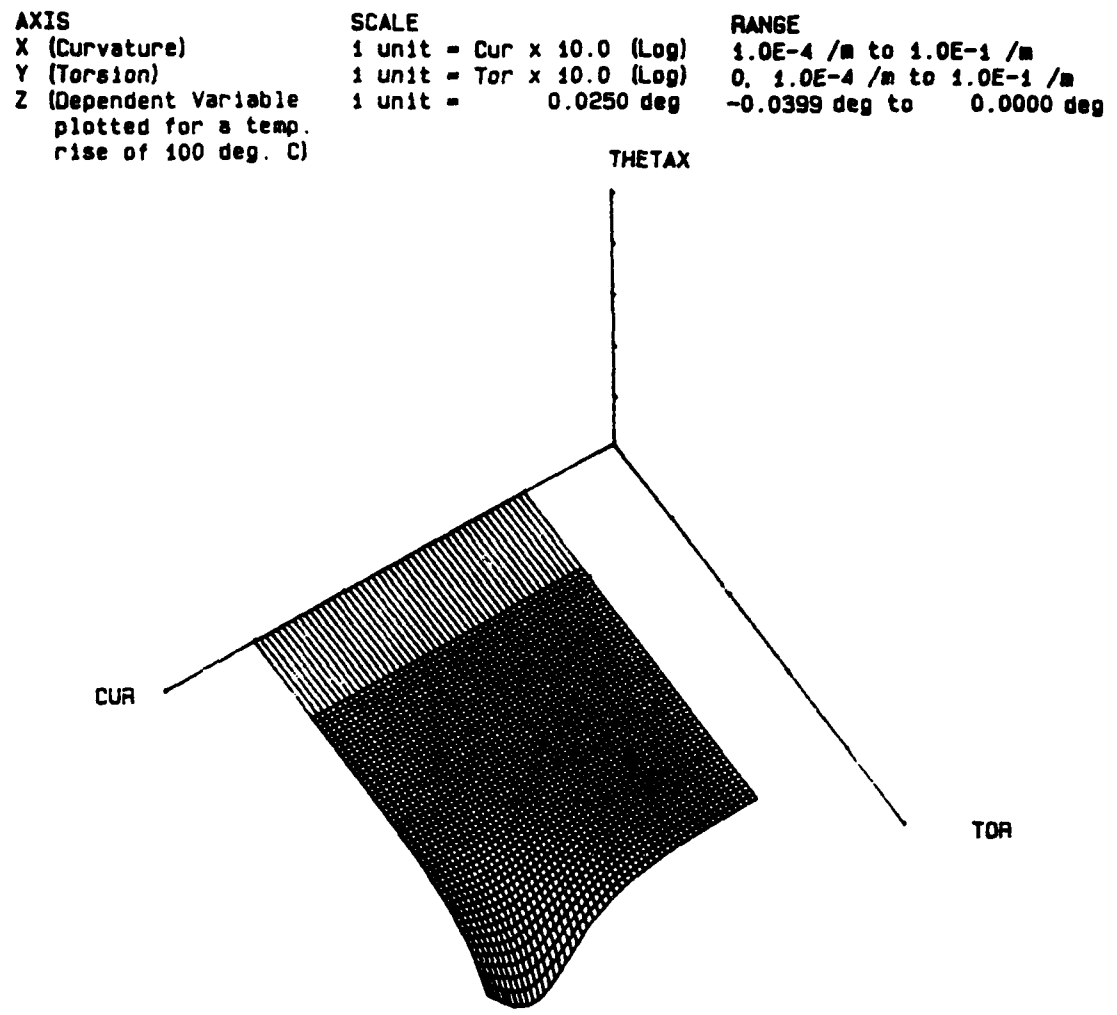

Compatibility 2, EA high: Thetax vs Cur vs Tor

Figure 5-36: Compatibility 2, *EA* high: θ_X versus Curvature versus Torsion

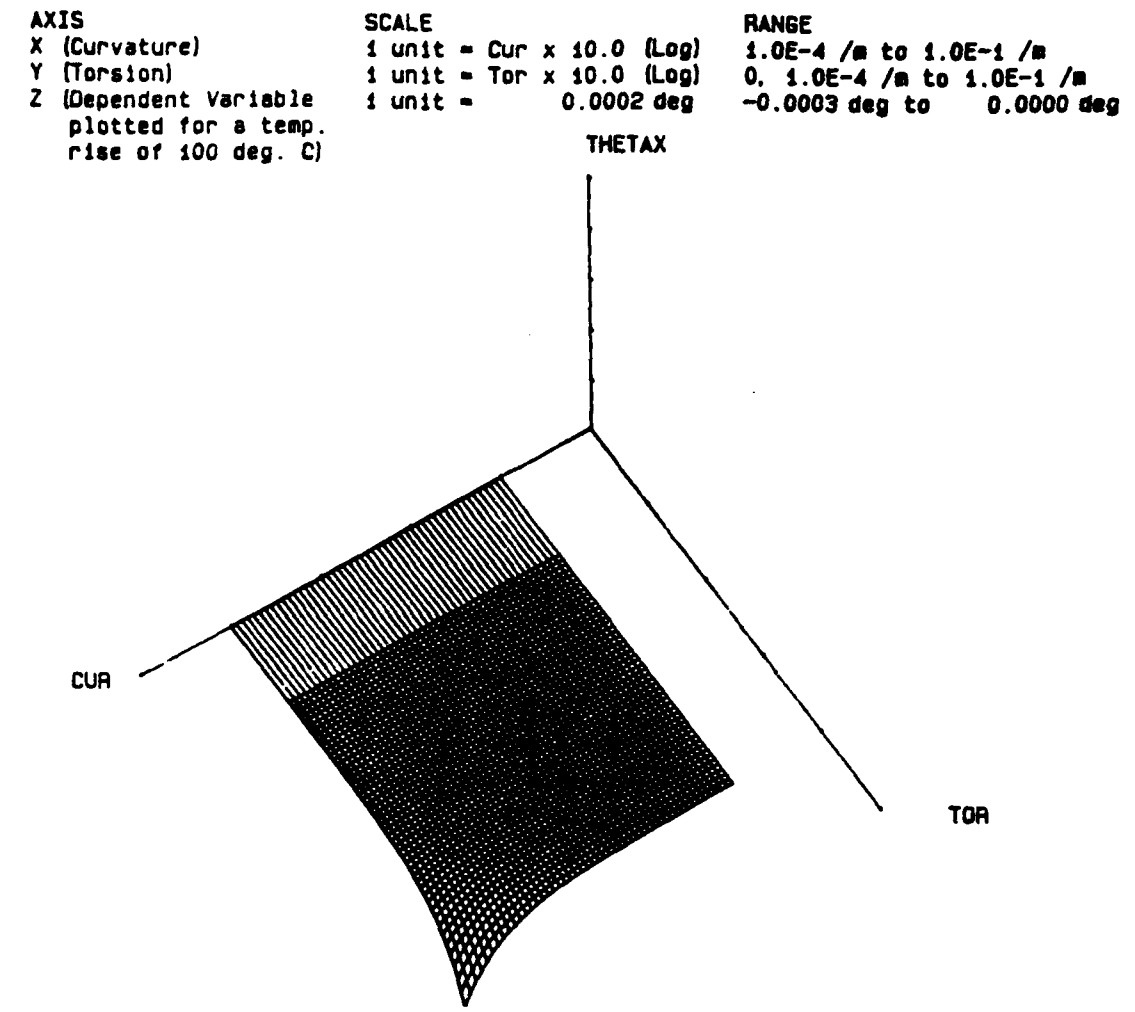

Compatibility 2, EA low: Thetax vs Cur vs Tor

Figure 5-37: Compatibility 2. *EA* low: θ_X versus Curvature versus Torsion

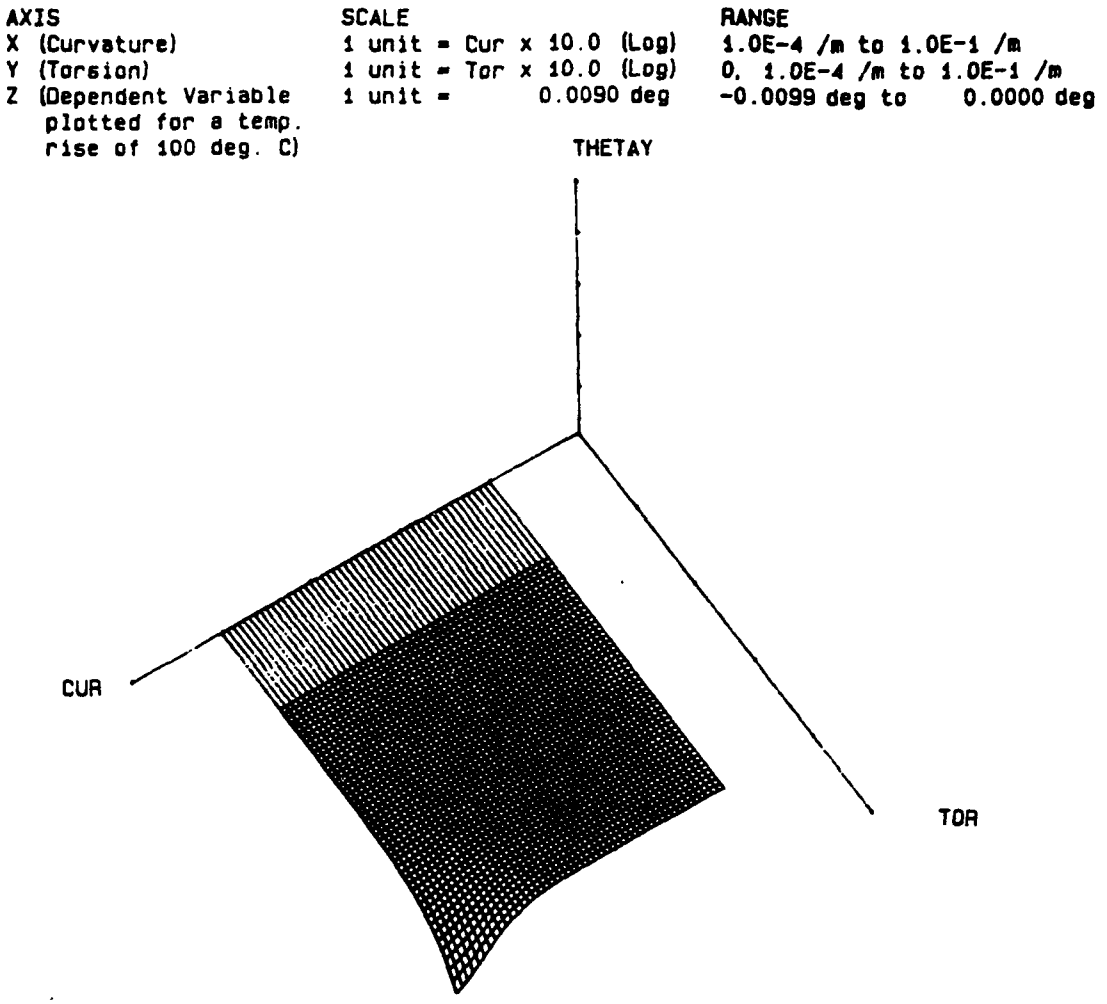

Compatibility 2, EI high: Thetay vs Cur vs Tor

Figure 5-38: Compatibility 2, *EI* high: θ_Y versus Curvature versus Torsion

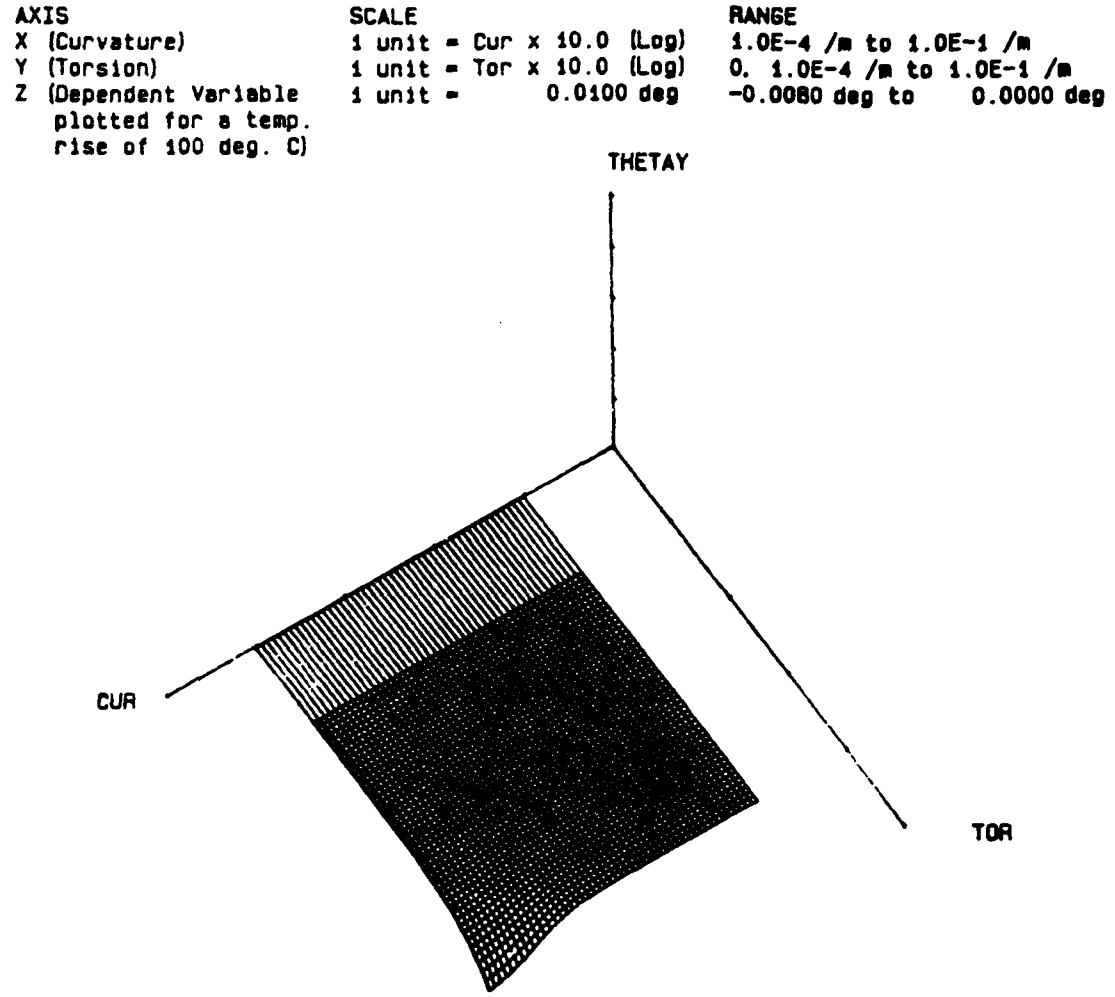

Compatibility 2, EA high: Thetay vs Cur vs Tor

Figure 5-39: Compatibility 2, *EA* high: θ_Y versus Curvature versus Torsion

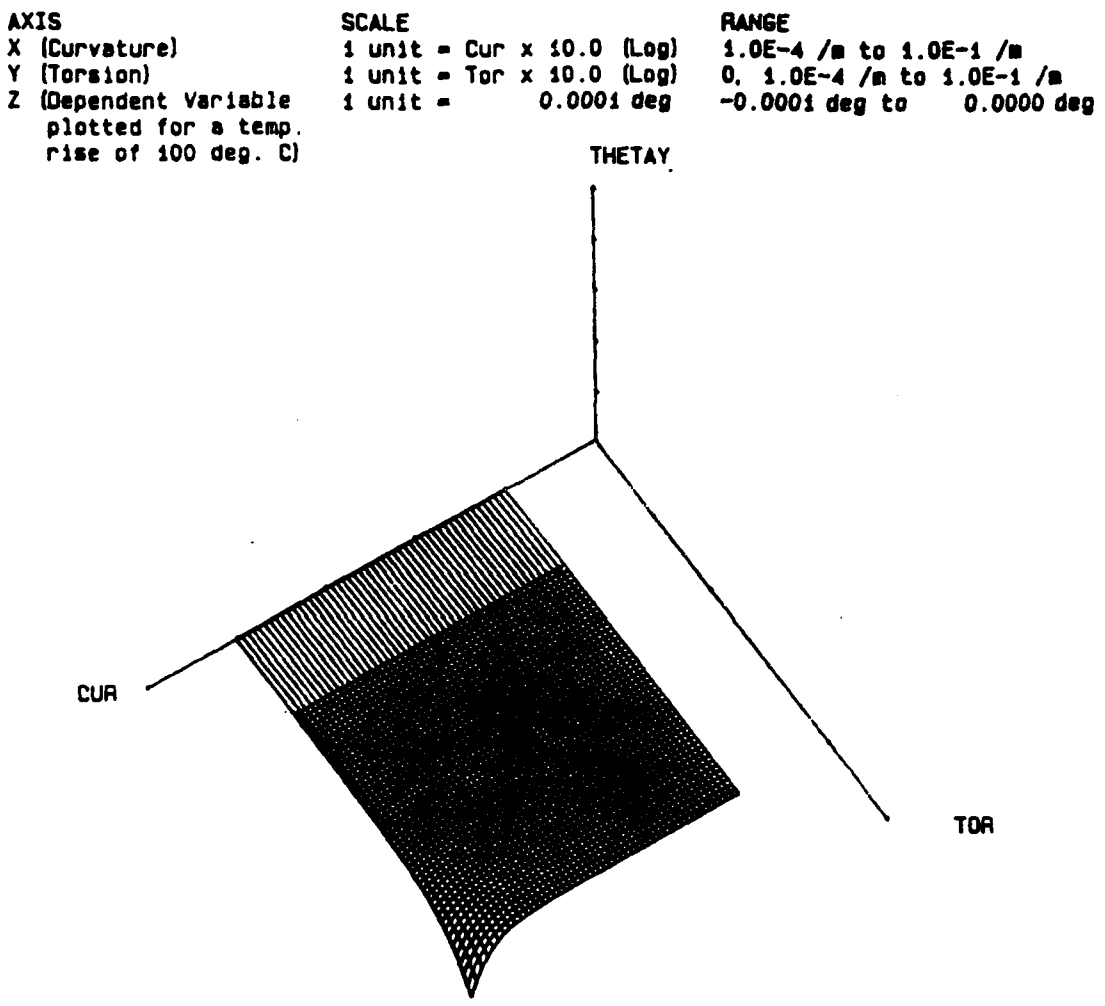

Compatibility 2, EA low: Thetay vs Cur vs Tor

Figure 5-40: Compatibility 2, EA low: θ_Y versus Curvature versus Torsion

AXIS	SCALE	RANGE
X (Curvature)	1 unit = Cur x 10.0 (Log)	1.0E-4 /m to 1.0E-1 /m
Y (Torsion)	1 unit = Tor x 10.0 (Log)	0, 1.0E-4 /m to 1.0E-1 /m
Z (Dependent Variable plotted for a temp. rise of 100 deg. C)	1 unit = 0.4800 deg	-0.8846 deg to -0.0036 deg

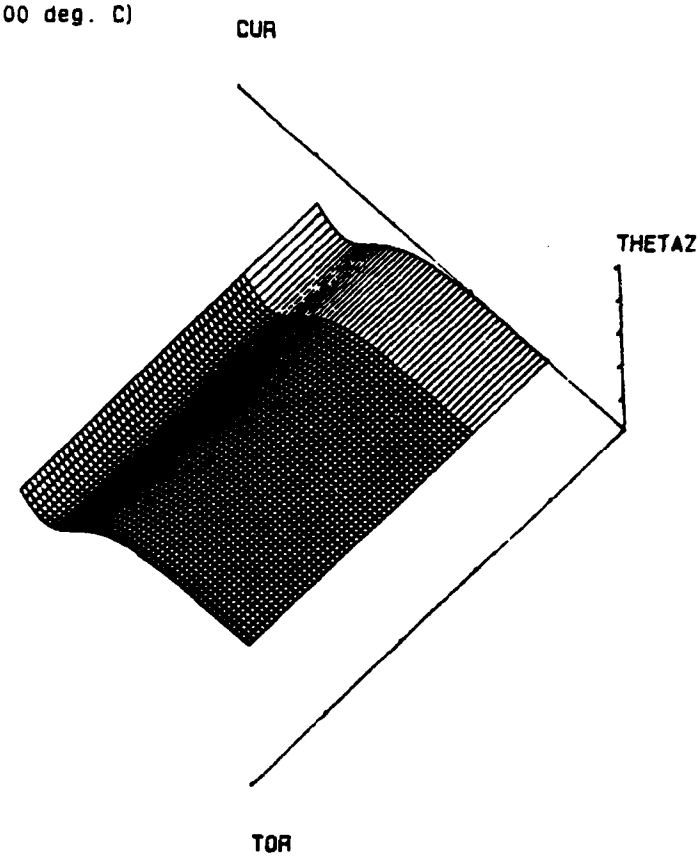

Compatibility 2, EI high: Thetaz vs Cur vs Tor

Figure 5-41: Compatibility 2, *EI* high: θ_Z versus Curvature versus Torsion

AXIS	SCALE	RANGE
X (Curvature)	1 unit = Cur x 10.0 (Log)	1.0E-4 /m to 1.0E-1 /m
Y (Torsion)	1 unit = Tor x 10.0 (Log)	0. 1.0E-4 /m to 1.0E-1 /m
Z (Dependent Variable plotted for a temp. rise of 100 deg. C)	1 unit = 0.4800 deg	-1.6577 deg to -0.0102 deg

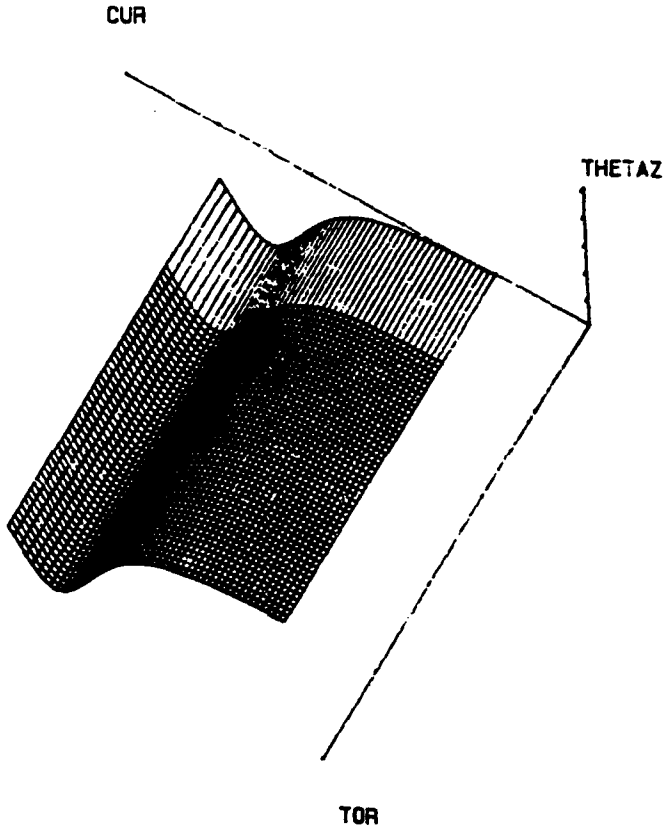

Compatibility 2, EA high: Thetaz vs Cur vs Tor

Figure 5-42: Compatibility 2, EA high: θ_Z versus Curvature versus Torsion

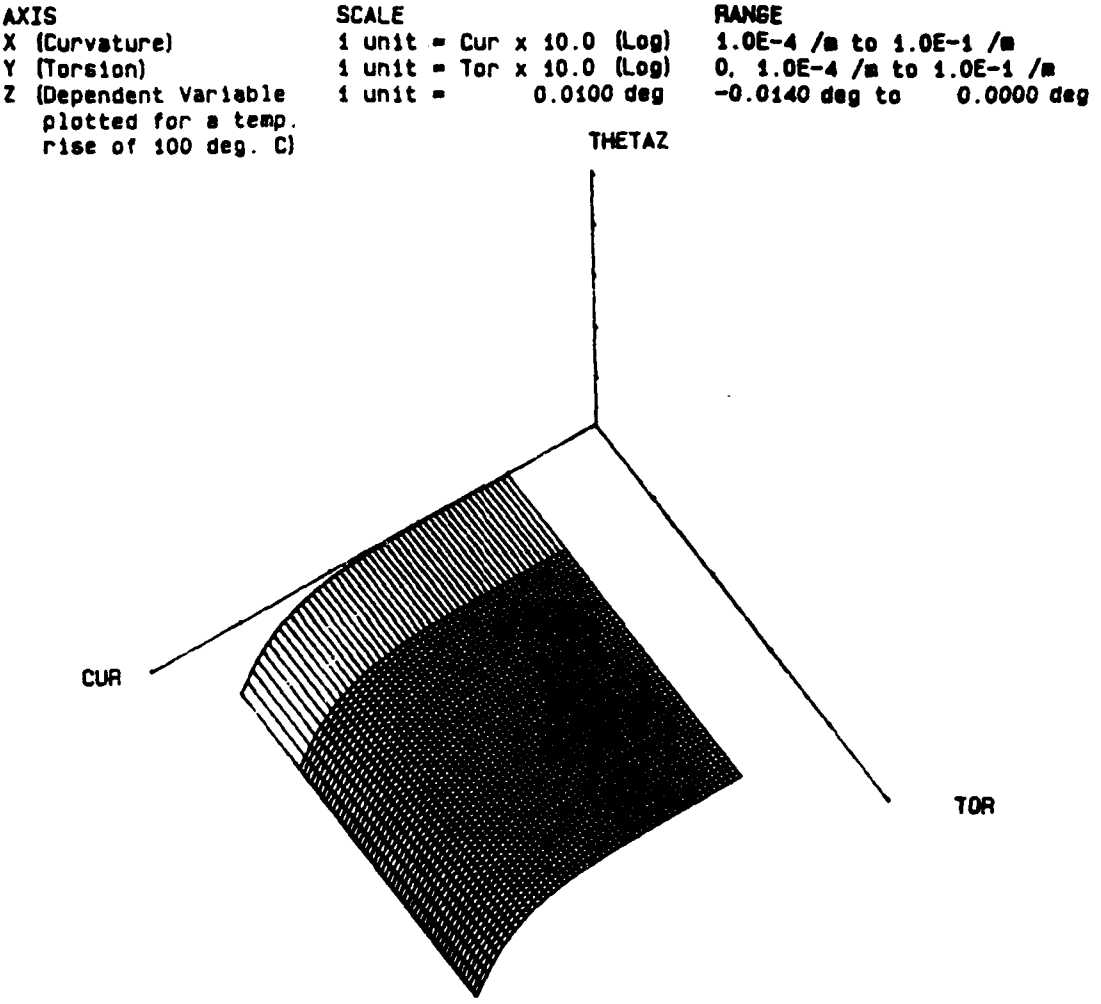

Compability 2, EA low: Thetaz vs Cur vs Tor

Figure 5-43: Compatibility 2, *EA* low: θ_Z versus Curvature versus Torsion

The following chapter contains the formulation of a general space-curved finite element which is later used to independently confirm the values of the more exact displacements found from the first method of solution.

CHAPTER 6

A GENERAL SPACE-CURVED FINITE BEAM ELEMENT

6.1 Introduction

In the previous chapters, we formulated and performed a parametric study of an exact solution to the problem of finding the displacements of the end of the gun tube. In the present chapter, we present an alternative approach: the development of a general space-curved finite beam element within which variable curvature and torsion are permitted. By the use of an assemblage of such elements, we may model a rod of arbitrarily varying cross-section. and curvature and torsion.

The element is derived by employing the variational method. The formulation assumes the expression for the deformation strain energy density of a curved beam, whose centroidal axis is an arbitrary space curve of variable torsion and curvature, obtained by Tsay and Kingsbury. [Tsay 86] This expression is derived from the linearized strain-displacement relations due to Kingsbury [Kingsbury 84], which assume that cross-sections remain plane and normal to the centroidal curve under deformation.

The most important feature of this element is its generality. The element stiffness matrix obtained is valid for any beam element whose centroidal axis is a curve with a constant rate of change of curvature and torsion throughout its length and also a constant shape of cross-section. In the following chapter, we shall present a comparison between the exact and the finite element solutions.

6.2 The Displacement Field

6.2.1 Assumptions of the Formulation

The differential equations describing the motion of space-curved beams have been formulated by Kingsbury in terms of the displacement components u, v, w and ϕ which represent four of the six unknown displacements or degrees of freedom permitted to any point on the beam. Exact solution of these four differential equations is made difficult by the fact that they are involve coupling in the above four variables due to the introduction of torsion. u, v and w are translational displacements of the centroid of a generic cross-section in the directions of the local principal normal, binormal and tangent respectively, and φ represents the angular displacement of any point of the cross-section about the local tangent. These four displacement quantities vary along the length of the beam; this may be expressed as

$$\begin{aligned} u &= u(z) \\ v &= v(z) \\ w &= w(z) \\ \phi &= \varphi(z) \end{aligned} \tag{6.1}$$

where z is the arc length measured along the space-curved beam. The remaining two angular displacements are derived [Kingsbury 84] from $u(z)$, $v(z)$ and $w(z)$, according to the equations below, which follow from the neglect of transverse shear deformation:

$$\alpha_z = -\frac{\partial v}{\partial z} - \lambda u \tag{6.2}$$

$$\alpha_y = \frac{\partial u}{\partial z} - \lambda v + \kappa w \tag{6.3}$$

The second assumption made is that angular displacements are small and hence may be transformed from one coordinate system to another the same way as translational displacements are.

6.2.2 The Displacement Field: A Polynomial Representation

Consider the finite element shown in Figure 6.1. Each node of the element has six degrees of freedom, three translational and three rotational. The element, therefore, has twelve degrees of freedom in all. As stated in the foregoing section, the four displacements in terms of which the differential equations are formulated are functions of the independent variable z, the arc length along the beam.

Noting that the highest orders of derivatives of these displacements, u, v, w and ϕ appearing in the four coupled differential equations of Kingsbury are four, four, two and two respectively, we adopt the following polynomial representation of the displacement field:

$$u(z) = a_1 - a_2 z - a_3 z^2 - a_4 z^3$$

$$v(z) = b_1 - b_2 z - b_3 z^2 - b_4 z^3$$

$$w(z) = c_1 - c_2 z$$

$$\phi(z) = d_1 - d_2 z \tag{6.4}$$

The reader may note that the total number of undetermined constants in the above equations is the same as the number of element degrees of freedom to be specified, that is, twelve. It may be mentioned here that the above displacement field satisfies the differential equations of Kingsbury *exactly* in the case that curvature κ and torsion λ (and their derivatives) are identically zero, in other words, in the straight beam case. It does not, however, satisfy the differential equations for the space-curved beam. However, in consideration of the fact that we are dealing with small curvatures and torsions representing the imperfections in the straightness of gun tubes, this assumption appears to be reasonable.

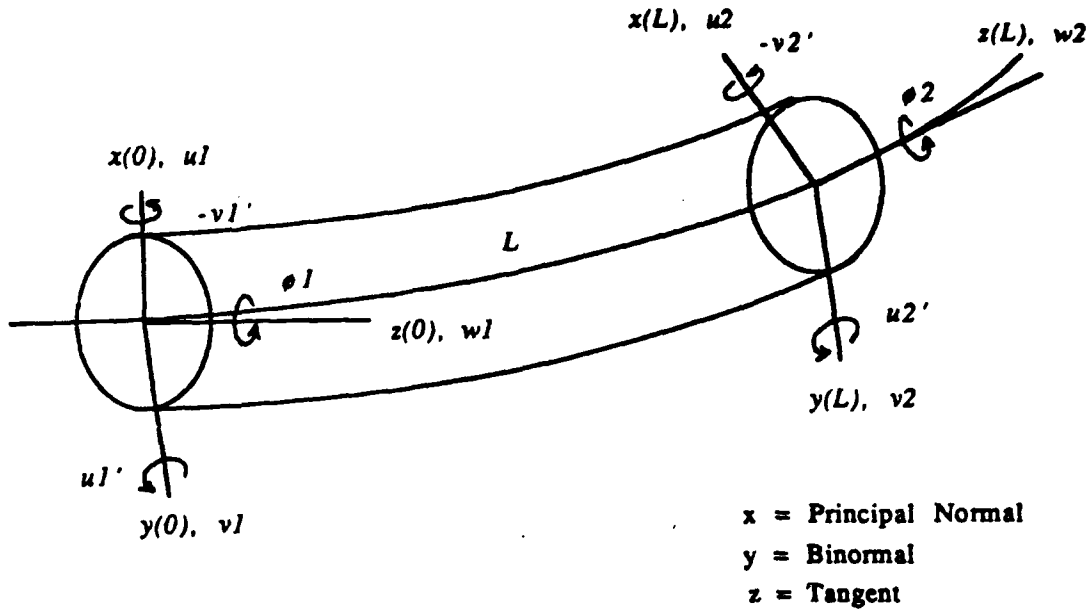

Figure 6-1: Degrees of Freedom of the Finite Element

Having chosen polynomials to describe the displacements, we now seek to obtain the shape functions for the displacement field. To achieve this, we must first determine the unknown constants introduced in equations (6.4). These constants are expressed in terms of the values of the element d.o.f. (degrees of freedom), which are specified. Differentiating equations (6.4)a and (6.4)b, we have:

$$u'(z) = \frac{du}{dz} = a_2 + 2a_3 z + 3a_4 z^2$$

$$v'(z) = \frac{dv}{dz} = b_2 + 2b_3 z + 3b_4 z^2 \qquad (6.5)$$

Let u_1, v_1, w_1, u_1', v_1', ϕ_1, and u_2, v_2, w_2, u_2', v_2', ϕ_2 be the values of the element d.o.f. at the two nodes given by $z = 0$ and $z = l$ respectively. Evaluating equations (6.4) and (6.5) at the two nodes, setting them equal to the known values of the d.o.f. and inverting the relationships, we arrive at the following expressions for the constants:

$$a_1 = u_1$$

$$a_2 = u_1'$$

$$a_3 = \frac{3(u_2 - u_1)}{l^2} - \frac{(2u_1' + u_2')}{l}$$

$$a_4 = \frac{2(u_1 - u_2)}{l^3} - \frac{(u_1' - u_2')}{l^2}$$

$$b_1 = v_1$$

$$b_2 = v_1'$$

$$b_3 = \frac{3(v_2 - v_1)}{l^2} - \frac{(2v_1' - v_2')}{l}$$

$$b_4 = \frac{2(v_1 - v_2)}{l^3} + \frac{(v_1' + v_2')}{l^2}$$

$$c_1 = w_1$$

$$c_2 = \frac{(w_2 - w_1)}{l}$$

$$d_1 = \phi_1$$

$$d_2 = \frac{(\phi_2 - \phi_1)}{l} \qquad \textbf{(6.6)}$$

6.2.3 The Shape Function Representation

Having determined the unknown constants in terms of the known nodal values of the displacements, we may now write the shape functions for the assumed displacement field. Substituting equations (6.6) into equations (6.4) and rearranging the terms, we obtain the shape functions for the displacements u and v to be the following cubic polynomials in z:

$$L_1(z) = 1 - \frac{3z^2}{l^2} + \frac{2z^3}{l^3}$$

$$L_2(z) = z - \frac{2z^2}{l} + \frac{z^3}{l^2}$$

$$L_3(z) = \frac{3z^2}{l^2} - \frac{2z^3}{l^3}$$

$$L_4(z) = -\frac{z^2}{l} + \frac{z^3}{l^2} \tag{6.7}$$

We also obtain the following linear shape functions for displacements w and ϕ:

$$N_1(z) = 1 - \frac{z}{l}$$

$$N_2(z) = \frac{z}{l} \tag{6.8}$$

Combining the shape functions of equations (6.7) and (6.8) with the nodal values of the displacements, we obtain the following expressions for the four displacements:

$$u(z) = \left(1 - \frac{3z^2}{l^2} + \frac{2z^3}{l^3}\right) u_1 + \left(z - \frac{2z^2}{l} + \frac{z^3}{l^2}\right) u_1'$$

$$+ \left(\frac{3z^2}{l^2} - \frac{2z^3}{l^3}\right) u_2 + \left(-\frac{z^2}{l} + \frac{z^3}{l^2}\right) u_2'$$

$$v(z) = (1-\frac{3z^2}{l^2}+\frac{2z^3}{l^3})\,v_1 + (z-\frac{2z^2}{l}+\frac{z^3}{l^2})\,v_1' - (\frac{3z^2}{l^2}-\frac{2z^3}{l^3})\,v_2 + (-\frac{z^2}{l}+\frac{z^3}{l^2})\,v_2'$$

$$w(z) = (1-\frac{z}{l})\,w_1 + (\frac{z}{l})\,w_2$$

$$\phi(z) = (1-\frac{z}{l})\,\phi_1 + (\frac{z}{l})\,\phi_2 \qquad (6.9)$$

Having obtained the displacements as interpolations of their nodal values in terms of the arc length z, we are now in a position to get an expression for the strain energy of deformation of the beam element in terms of the nodal values of the displacements. This is accomplished in the following section.

6.3 Strain Energy of the Beam Element

6.3.1 The Linear Strain Energy Density Function

The expression for the linear strain energy density (strain energy per unit arc length) of the deformed beam, as obtained by Tsay and Kingsbury [Tsay 86], is:

$$\begin{aligned} F = {} & I_{zz}\,\{E[\frac{(v'')^2}{2}+\frac{(u\lambda')^2}{2}+\frac{(u'\lambda)^2}{2}+uv''\lambda'+u'v''\lambda \\ & +uu'\lambda\lambda'-v''\kappa\phi-u\lambda'\kappa\phi-u'\lambda\kappa\phi]+G[\frac{(v'\kappa)^2}{2}+uv'\lambda\kappa^2 \\ & -v'\phi'\kappa-\frac{(u\lambda\kappa)^2}{2}+u\lambda\kappa\phi'+\frac{(\phi')^2}{2}+\frac{(\lambda\phi)^2}{2}+\frac{(\kappa\phi)^2}{2}]\} \\ & +I_{xy}\,\{E[v''w\kappa'+v''w'\kappa-vv''\lambda'-v'v''\lambda+u''v'' \\ & +uw\lambda'\kappa'+uw'\lambda'\kappa-uv(\lambda')^2-uv'\lambda\lambda'+uu''\lambda'+u'w\lambda\kappa' \\ & +u'w'\lambda\kappa-u'v\lambda\lambda'-u'v'\lambda^2+u'u''\lambda-w\kappa\kappa'\phi-w'\kappa^2\phi \end{aligned}$$

$$
\begin{aligned}
&- v\lambda'\kappa\phi - v'\lambda\kappa\phi - u''\kappa\phi \,] + G[\, v'w\kappa^3 + uw\lambda\kappa^3 + w\kappa^2\phi' \\
&- vv'\lambda\kappa^2 + u'v'\kappa^2 - v'\lambda\kappa\phi - uv(\lambda\kappa)^2 - v\lambda\kappa\phi' + uu'\lambda\kappa^2 \\
&- u'\kappa\phi' - u\kappa\lambda^2\phi \,]\} \\
&- I_{yy}\ \{ E[\, \frac{(u'')^2}{2} + \frac{(v'\lambda)^2}{2} + \frac{(v\lambda')^2}{2} + \frac{(w\kappa')^2}{2} + \frac{(w'\kappa)^2}{2} \\
&- u''v'\lambda - u''v\lambda' + u''w\kappa' - u''w'\kappa + vv'\lambda\lambda' - v'w\lambda\kappa' \\
&- v'w'\lambda\kappa - vw\lambda'\kappa' - vw'\lambda'\kappa + ww'\kappa\kappa' \,] + G[\, \frac{w^2\kappa^4}{2} - vw\lambda\kappa^3 \\
&- u'w\kappa^3 - w\lambda\kappa^2\phi + \frac{(v\lambda\kappa)^2}{2} - u'v\lambda\kappa^2 - v\lambda^2\kappa\phi + \frac{(u'\kappa)^2}{2} \\
&- u'\lambda\kappa\phi - \frac{(\phi')^2}{2} - \frac{(\lambda\phi)^2}{2} \,]\} \\
&- A\ \{ E[\, \frac{(w')^2}{2} - uw'\kappa + \frac{(u\kappa)^2}{2} \,]\}
\end{aligned}
\tag{6.10}
$$

6.3.2 Strain Energy of the Element

Substituting equations (6.9) into Equation (6.10), the strain energy density function, and integrating the result over the length of the element l, we arrive at the expression for its strain energy of deformation. This expression, however, is presented in Appendix B. owing to its length.

6.4 The Element Stiffness Matrix

Next, we apply Castigliano's First Theorem to the strain energy expression. The theorem states that if a linearly elastic structure is subjected to a displacement, the load in its direction that causes the displacement is equal to the partial derivative of the strain energy of deformation of the structure with respect to that displacement. We, therefore, differentiate the strain energy with respect to the nodal values of displacements which appear in the expression and thus obtain the components of the internal force and moment acting on the ends of the element in their respective local coordinate systems specified by the tangent, binormal and principal normal at those points.

The coefficients of the nodal values of displacements appearing in the expressions for nodal forces and moments obtained by differentiating the strain energy are in fact the elements of the element stiffness matrix **K**. The relationship between the nodal forces and the nodal displacements in terms of the element stiffness matrix **K** is:

$$\mathbf{F} = \mathbf{K}\triangle \tag{6.11}$$

where, **F** is the internal force vector given by

$$\mathbf{F} = \left[Vx_1\ Vy_1\ Vz_1\ Mx_1\ My_1\ Mz_1\ Vx_2\ Vy_2\ Vz_2\ Mx_2\ My_2\ Mz_2 \right]^T, \tag{6.12}$$

and $\triangle$ is the nodal displacement vector given by

$$\triangle = \left[u_1\ v_1\ w_1\ \alpha_{x1}\ \alpha_{y1}\ \phi_1\ u_2\ v_2\ w_2\ \alpha_{x2}\ \alpha_{y2}\ \phi_2 \right]^T. \tag{6.13}$$

The α_x and α_y values in the nodal displacement vector are as given by equations (6.2) and (6.3). Since we are interested in displacements occurring for small values of curvature κ and torsion λ, we drop the last term from Equation (6.2) and the last two terms from Equation (6.3). thereby getting the simpler results

$$\alpha_z = -\frac{\partial v}{\partial z} \qquad \text{and} \qquad \alpha_y = \frac{\partial u}{\partial z} \tag{6.14}$$

The above relationships hold *exactly* for the case of the straight beam, and are, therefore, consistent with the shape functions assumed for the element.

Note that this simplification results in an uncoupling of displacements, thereby rendering the problem more amenable to solution. We now have $\alpha_{z1} = -v_1'$, $\alpha_{y1} = u_1'$, $\alpha_{z2} = -v_2'$ and $\alpha_{y2} = u_2'$, as per Equation (6.14), so that the moments Mz_1, My_1, Mz_2 and My_2 are obtained by applying Castigliano's First Theorem as follows:

$$Mz_1 = -\frac{\partial U}{\partial v_1'}$$

$$My_1 = \frac{\partial U}{\partial u_1}$$

$$Mx_2 = -\frac{\partial U}{\partial v_2}$$

$$My_2 = \frac{\partial U}{\partial u_2} \tag{6.15}$$

The term U appearing in the above equations is the strain energy of deformation of the element.

The 12×12 element stiffness matrix is symmetric, as expected. The expressions for the elements of the stiffness matrix in terms of the geometrical parameters defining the element, κ, κ', λ, λ', l, cross-sectional properties I_{xx}, I_{xy}, I_{yy}, A, and material properties E and G, are provided in Appendix D, which contains a finite element program used to compare the displacements obtained by using the general space-curved beam element with those of the exact solution presented in previous chapters.

6.4.1 Reduction to the Straight Beam Case

In this subsection, we present a check on the element stiffness matrix obtained earlier for the case of the straight beam element. For the straight beam, we have zero torsion and curvature. Substituting these values into the expressions found for the elements of the stiffness matrix, we obtain the following results which agree with the standard straight beam element matrix [Zienkiewicz 77]. (Only the non-zero upper triangular elements are listed row-wise, since the matrix is symmetric.)

$$K(1,1) = -K(1,7) = \frac{12\,E\,I_{yy}}{l^3}$$

$$K(1,2) = -K(1,8) = \frac{12\,E\,I_{xy}}{l^3}$$

$$K(1,4) = K(1,10) = -\frac{6\,E\,I_{xy}}{l^2}$$

$$K(1,5) = K(1.11) = \frac{6\,E\,I_{yy}}{l^2}$$

$$K(2,2) = -\,K(2.8) = \frac{12\,E\,I_{zz}}{l^3}$$

$$K(2,4) = K(2.10) = -\,\frac{6\,E\,I_{zz}}{l^2}$$

$$K(2,5) = K(2.11) = \frac{6\,E\,I_{xy}}{l^2}$$

$$K(2,7) = -\,\frac{12\,E\,I_{xy}}{l^3}$$

$$K(3,3) = -\,K(3.9) = \frac{E\,A}{l}$$

$$K(4.4) = 2\,K(4.10) = \frac{4\,E\,I_{zz}}{l}$$

$$K(4,5) = 2\,K(4,11) = -\,\frac{4\,E\,I_{xy}}{l}$$

$$K(4,7) = -\,\frac{6\,E\,I_{yy}}{l^2}$$

$$K(4,8) = -\,\frac{6\,E\,I_{xy}}{l^2}$$

$$K(5,5) = 2\,K(5,11) = \frac{4\,E\,I_{yy}}{l}$$

$$K(5,7) = -\,\frac{6\,E\,I_{xy}}{l^2}$$

$$K(5,8) = -\,\frac{6\,E\,I_{zz}}{l^2}$$

$$K(5,10) = -\,\frac{2\,E\,I_{xy}}{l}$$

$$K(6,6) = -\,K(6,12) = \frac{G\,(I_{zz} + I_{yy})}{l}$$

$$K(7,7) = \frac{12\,E\,I_{yy}}{l^3}$$

$$K(7,8) = \frac{12\,E\,I_{xy}}{l^3}$$

$$K(7,10) = \frac{6\,E\,I_{xy}}{l^2}$$

$$K(7,11) = -\frac{6\,E\,I_{yy}}{l^2}$$

$$K(8,8) = \frac{12\,E\,I_{xx}}{l^3}$$

$$K(8,10) = \frac{6\,E\,I_{xx}}{l^2}$$

$$K(8,11) = -\frac{6\,E\,I_{xy}}{l^2}$$

$$K(9,9) = \frac{E\,A}{l}$$

$$K(10,10) = \frac{4\,E\,I_{xx}}{l}$$

$$K(10,11) = -\frac{4\,E\,I_{xy}}{l}$$

$$K(11,11) = \frac{4\,E\,I_{yy}}{l}$$

$$K(12,12) = \frac{G\,(I_{xx} - I_{yy})}{l} \qquad (6.16)$$

6.5 A Finite Element Example Solution

In this section. we present the results obtained by using the finite element program of Appendix D for the displacements of the end of the gun tube, whose model is shown in Figure 6.2. The gun tube is modeled as a cantilevered beam with three elements. Note that compatibility of displacements of the ends of the gun tube and the shroud is not enforced but we use as an approximation, the value of the force found for the exact solution. for the corresponding values of initial curvature and torsion. The shroud is removed. but the approximate shroud force is applied to the gun tube in a direction parallel to the chord joining the ends of the gun tube.

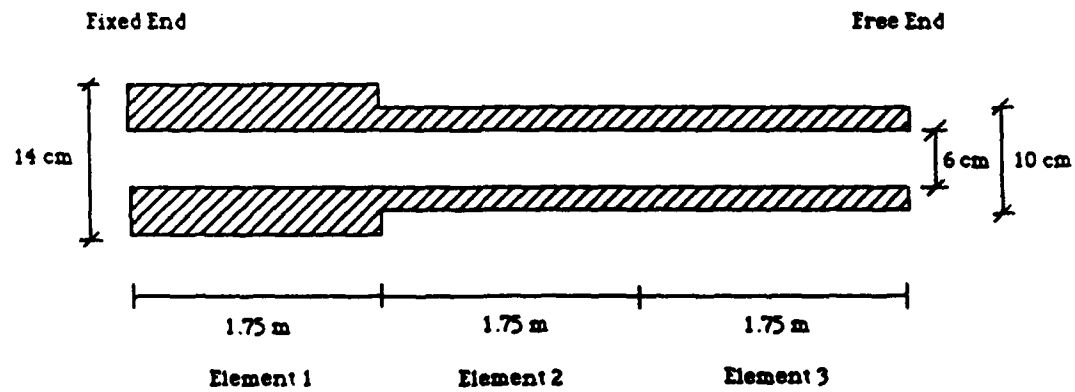

Figure 6-2: Model of a Gun Tube

It must be brought to attention that the global stiffness equation whose solution is implemented by the finite element program is formulated in the *chord* coordinate system. Since the element stiffness matrix is developed in the local tangent system, we make use of the transformations of Section 4.3 in obtaining the stiffness matrix in the chord system. This, although not a necessity, facilitates the comparison between the displacements found from the exact and the finite element solutions which is presented in the following chapter.

The solution of the global stiffness equation in the chord system, $\mathbf{F} = \mathbf{K}\triangle$, proceeds as follows: We first partition the global force and displacement vectors into blocks of known (denoted by the subscript α) and unknown (denoted by the subscript β) quantities, and rearrange the stiffness matrix accordingly. Thus the global equation may be written as:

$$\begin{pmatrix} \mathbf{F}_\beta \\ \mathbf{F}_\alpha \end{pmatrix} = \begin{pmatrix} \mathbf{K}_{\beta\beta} & \mathbf{K}_{\beta\alpha} \\ \mathbf{K}_{\alpha\beta} & \mathbf{K}_{\alpha\alpha} \end{pmatrix} \begin{pmatrix} \triangle_\alpha \\ \triangle_\beta \end{pmatrix} \tag{6.17}$$

Now, since one end of the gun tube is held fixed, the known displacements $\triangle_\alpha$ are zero. Thus the unknown displacements and forces (reactions) may be obtained from Equation (6.17) as:

$$\triangle_\beta = \mathbf{K}_{\alpha\alpha}{}^{-1}\, \mathbf{F}_\alpha$$

$$\mathbf{F}_\beta = \mathbf{K}_{\beta\alpha}\, \mathbf{K}_{\alpha\alpha}{}^{-1}\, \mathbf{F}_\alpha \tag{6.18}$$

The general finite element allows for variation of the curvature and torsion along its length. In the present example, however, this facility is not used. Data and results for this example follow.

Global Data:

Number of elements = 3
Length of gun tube = 5.25 m

Curvature κ = 1.0×10^{-4} per m
Torsion λ = 1.0×10^{-3} per m
Rate of change of curvature κ' = 0
Rate of change of torsion λ' = 0

Modulus of elasticity E = 4.35097×10^9 N/m^2
Shear modulus G = 1.67345×10^9 N/m^2

Force exerted by thermal shroud along the chord F_{Y_c} = 61441.952 N

Elemental Data:

Length of each element = 1.75 m

Cross-section of element 1:

Inner radius = 0.06 m = 6 cm
Outer radius = 0.14 m = 14 cm

Cross-sections of elements 2 and 3:

Inner radius = 0.06 m = 6 cm
Outer radius = 0.10 m = 10 cm

Results:

Computed Reactions at the Fixed End in the Chord System:

$$F_{Xc} = 7.409 \times 10^{-5} \text{ N}$$
$$F_{Yc} = -61441.952 \text{ N}$$
$$F_{Zc} = 1.964 \times 10^{-7} \text{ N}$$
$$M_{Xc} = -7.409 \times 10^{-2} \text{ N-m}$$
$$M_{Yc} = -1.954 \times 10^{-5} \text{ N-m}$$
$$M_{Zc} = -4.439 \times 10^{-4} \text{ N-m}$$

End Displacement of the Gun Tube in the Chord System:

$$\triangle X = 5.984 \times 10^{-4} \text{ m}$$
$$\triangle Y = 2.950 \times 10^{-3} \text{ m}$$
$$\triangle Z = 1.510 \times 10^{-6} \text{ m}$$
$$\triangle\theta_X = 3.712 \times 10^{-5} \text{ deg}$$
$$\triangle\theta_Y = 3.266 \times 10^{-8} \text{ deg}$$
$$\triangle\theta_Z = -1.146 \times 10^{-2} \text{ deg}$$

Note that the applied force acts along the chord and so passes through the point at which the gun tube is encastred. Thus the moments generated at the fixed end must be zero; so should the reactions in directions perpendicular to the chord. This is borne out by the computed reactions at the fixed end shown above, of course, with some error. In the next chapter, we shall present a comparison of the exact and finite element solutions.

CHAPTER 7

A COMPARISON OF THE EXACT AND FINITE ELEMENT ANALYSES

7.1 The Impact of Simplifying Assumptions

Recall that the displacement field that we assumed for the finite element formulation of Chapter 6 satisfied the differential equations of Kingsbury [Kingsbury 84] only in the case of the straight beam. In other words, if we were to substitute these displacements and their derivatives into the differential equations, we would expect a non-zero residual. This implies a certain inherent inaccuracy in the finite element, and we naturally expect that the element will show a greater accuracy for the smaller values of curvature and torsion.

It must also be noted that the simplification of Equation (6.14) would affect the accuracy of all the displacements, particularly w, α_x and α_y.

7.2 A Comparison of the Exact and Finite Element Methods

Presented, in this section, are some of the displacements obtained by the exact method under the first compatibility condition described in Section 4.5, and the corresponding displacements obtained using the general beam element of Chapter 6, for a few selected values of initial curvature and torsion of the gun tube. These displacements were computed using the programs given in appendices C and D respectively.

The applied forces used in the finite element program were supplied from the output of the program for generating the exact solutions, in which compatibility conditions

were enforced. The gun tube and shroud data assumed for the comparison were the same as those given in Chapter 5, and for ease of reference, they are presented below:

Gun Tube:

Length = 5.25 m
Inner radius = 0.06 m
Outer radius = 0.10 m
Elasticity modulus = 4.35097×10^9 N/m^2
Shear modulus = 1.67345×10^9 N/m^2

Thermal Shroud:

Inner radius = 0.11 m
Outer radius = 0.145 m
Temperature rise = 100 ° C
Elasticity modulus = 4.35097×10^9 N/m^2
Coefficient of thermal expansion = 1.206×10^{-5} / ° C

The finite element analysis of the gun tube was performed with a 3-element and a 10-element model to verify the expected increase in the accuracy of the solution against the exact solution. Five different cases of initial curvature and torsion are presented in this chapter with conclusions about the results inserted at suitable junctures. Note that the exact reactions at the fixed end of the gun tube consist of only one equal but opposite force $-F_{Y_c}$. Since the force due to the shroud acts along the chord itself, no reaction moments are produced at the fixed end.

CASE 1:

$\kappa = 1.0 \times 10^{-4}$ /m
$\lambda = 0.0$ /m

Applied force in the chord system, $F_{Y_c} = 61441.9292446$ N

Computed Reactions in the Chord System, in N and N-m:

	3 Elements	10 Elements
F_{X_c}	$-5.2988725 \times 10^{-12}$	$7.2120088 \times 10^{-13}$
F_{Y_c}	-61441.9292446	-61441.9292446

F_{Zc}	0.0	0.0
M_{Xc}	0.0	0.0
M_{Yc}	0.0	0.0
M_{Zc}	$-1.4694506 \times 10^{-4}$	$-1.3903836 \times 10^{-5}$

Displacements in the Chord System, in m and deg:

	Exact Solution	3 Elements	10 Elements
$\triangle X_c$	6.5259152×10^{-4}	6.5387099×10^{-4}	6.5387628×10^{-4}
$\triangle Y_c$	3.6873859×10^{-3}	3.6873662×10^{-3}	3.6873663×10^{-3}
$\triangle Z_c$	0.0	0.0	0.0
$\triangle\theta_{Xc}$	0.0	0.0	0.0
$\triangle\theta_{Yc}$	0.0	0.0	0.0
$\triangle\theta_{Zc}$	$-1.4272158 \times 10^{-2}$	$-1.4293170 \times 10^{-2}$	$-1.4293262 \times 10^{-2}$

CASE 2:

$\kappa = 1.0 \times 10^{-2}$ /m
$\lambda = 0.0$ /m

Applied force in the chord system, $F_{Yc} = 55426.4228976$ N

Computed Reactions in the Chord System, in N and N-m:

	3 Elements	10 Elements
F_{Xc}	$-4.4158832 \times 10^{-2}$	$-4.4949355 \times 10^{-3}$
F_{Yc}	-55426.4279317	-55426.4294723
F_{Zc}	0.0	0.0
M_{Xc}	0.0	0.0
M_{Yc}	0.0	0.0
M_{Zc}	-121.4720064	-12.4268252

Displacements in the Chord System, in m and deg:

	Exact Solution	3 Elements	10 Elements
$\triangle X_c$	5.8975078×10^{-2}	5.4112829×10^{-2}	5.8475782×10^{-2}
$\triangle Y_c$	3.9458062×10^{-3}	3.9069921×10^{-3}	3.9410363×10^{-3}
$\triangle Z_c$	0.0	0.0	0.0

$\triangle\theta_{Xc}$	0.0	0.0	0.0
$\triangle\theta_{Yc}$	0.0	0.0	0.0
$\triangle\theta_{Zc}$	−1.2873947	−1.2035964	−1.2799743

From the above figures for cases 1 and 2, we observe that the finite element method yields very accurate values of displacements, for zero torsion, when the curvature is small. As mentioned following the finite element example of the previous chapter, an indication of the accuracy of the solution is the accuracy of the computed reactions. We expect that the only non-zero reaction at the fixed end of the gun tube is an opposite force to that exerted by the thermal shroud.

With this in mind, it is easy to see that in the second case, the accuracy of the solutions is not as good as the first. However, the error in the moment M_{Zc}, whose value should be zero, is still not very large considering the enormous magnitude of the applied force. Note that in Case 1, the 10-element model produces slightly more accurate reactions than the 3-element model. There is also not much improvement in displacement values from the 3-element model to the 10-element model. This lack of improvement may be attributed to the inaccuracy of the element itself, inherent in the approximate displacement field assumed in its derivation. In Case 2, however, the improvement is much more visible.

CASE 3:

$\kappa = 1.0 \times 10^{-4}$ /m
$\lambda = 1.0 \times 10^{-4}$ /m

Applied force in the chord system, $F_{Yc} = 61441.9460865$ N

Computed Reactions in the Chord System, in N and N-m:

	3 Elements	10 Elements
F_{Xc}	7.4089804×10^{-7}	7.4090253×10^{-7}
F_{Yc}	−61441.9460865	−61441.9460865
F_{Zc}	$2.6942000 \times 10^{-10}$	$2.6942148 \times 10^{-10}$
M_{Xc}	$-7.4090486 \times 10^{-3}$	$-7.4090355 \times 10^{-3}$

M_{Yc}	$-7.4802397 \times 10^{-7}$	$-7.4802703 \times 10^{-7}$
M_{Zc}	$-1.4889072 \times 10^{-4}$	$-1.5849468 \times 10^{-5}$

Displacements in the Chord System, in m and deg:

	Exact Solution	3 Elements	10 Elements
$\triangle X_c$	6.5390314×10^{-4}	6.5387117×10^{-4}	6.5387646×10^{-4}
$\triangle Y_c$	3.6873852×10^{-3}	3.6873672×10^{-3}	3.6873674×10^{-3}
$\triangle Z_c$	1.1735696×10^{-8}	1.4904136×10^{-7}	1.4875948×10^{-7}
$\triangle\theta_{Xc}$	$8.6536987 \times 10^{-10}$	3.7464527×10^{-6}	3.7464405×10^{-6}
$\triangle\theta_{Yc}$	$-4.6529785 \times 10^{-11}$	2.3128574×10^{-9}	2.3147083×10^{-9}
$\triangle\theta_{Zc}$	$-1.4272162 \times 10^{-2}$	$-1.4293173 \times 10^{-2}$	$-1.4293266 \times 10^{-2}$

It is important to observe in Case 3 that even though the reactions have been computed very accurately (as compared to Case 2, for example), the displacements $\triangle Z_c$, $\triangle\theta_{Xc}$, $\triangle\theta_{Yc}$ which are "out-of-plane" in the sense of Section 5.2 show fairly large errors for both the 3-element and the 10-element models. This is because the introduction of torsion results in a coupling of displacements which is not accounted for in the finite element model. Thus the finite element solution is unresponsive, in terms of its accuracy with regard to these displacements, to an increase in the number of elements.

The assumptions that we made in Chapter 6 yield simplified forms of displacements as given by Equation (6.14). Clearly, in the original forms of equations (6.2) and (6.3), the displacements show coupling. However, without this simplification, it would be difficult to obtain the constant coefficients of the assumed displacement field in terms of the nodal values of displacement, since the differential equations of Kingsbury [Kingsbury 84] are set up in terms of four displacements, while the element has six degrees of freedom per node. In other words, in order to obtain a finite element that accounts for coupling, we would have to impose coupled nodal value conditions, which is clearly a non-trivial matter.

CASE 4:

$\kappa = 1.0 \times 10^{-2}$ /m
$\lambda = 1.0 \times 10^{-4}$ /m

Applied force in the chord system, $F_{Yc} = 55426.4229645$ N

Computed Reactions in the Chord System, in N and N-m:

	3 Elements	10 Elements
F_{Xc}	$-4.4092066 \times 10^{-2}$	$-4.4281777 \times 10^{-3}$
F_{Yc}	-55426.4280001	-55426.4295408
F_{Zc}	5.0363461×10^{-5}	6.5771379×10^{-5}
M_{Xc}	-0.6805012	-0.6694404
M_{Yc}	$-6.4613788 \times 10^{-3}$	$-6.7159999 \times 10^{-3}$
M_{Zc}	-121.4721685	-12.4269992

Displacements in the Chord System, in m and deg:

	Exact Solution	3 Elements	10 Elements
ΔX_c	5.8975078×10^{-2}	5.4112830×10^{-2}	5.8475781×10^{-2}
ΔY_c	3.9458062×10^{-3}	3.9069922×10^{-3}	3.9410363×10^{-3}
ΔZ_c	1.0319861×10^{-6}	1.4945806×10^{-5}	1.3573915×10^{-5}
$\Delta\theta_{Xc}$	$4.2030041 \times 10^{-17}$	3.4914457×10^{-4}	3.3897723×10^{-4}
$\Delta\theta_{Yc}$	$-4.1399281 \times 10^{-7}$	2.0471505×10^{-5}	2.0838240×10^{-5}
$\Delta\theta_{Zc}$	-1.2873947	-1.2035963	-1.2799743

CASE 5:

$\kappa = 1.0 \times 10^{-4}$ /m
$\lambda = 1.0 \times 10^{-2}$ /m

Applied force in the chord system, $F_{Yc} = 61441.9525214$ N

Computed Reactions in the Chord System, in N and N-m:

	3 Elements	10 Elements
F_{Xc}	7.4058016×10^{-3}	7.4058016×10^{-3}

F_{Yc}	-61441.9525233	-61441.9525233
F_{Zc}	1.9445444×10^{-4}	1.9445444×10^{-4}
M_{Xc}	-0.7405821	-0.7405804
M_{Yc}	$-7.4658299 \times 10^{-5}$	$-7.4650474 \times 10^{-5}$
M_{Zc}	$-1.9591481 \times 10^{-2}$	$-1.9458587 \times 10^{-2}$

Displacements in the Chord System, in m and deg:

	Exact Solution	3 Elements	10 Elements
$\triangle X_c$	6.5383257×10^{-4}	6.5382582×10^{-4}	6.5383147×10^{-4}
$\triangle Y_c$	3.6873849×10^{-3}	3.6873676×10^{-3}	3.6873678×10^{-3}
$\triangle Z_c$	1.1442295×10^{-6}	1.4901627×10^{-5}	1.4873416×10^{-5}
$\triangle\theta_{Xc}$	$5.5909964 \times 10^{-16}$	3.7456808×10^{-4}	3.7456666×10^{-4}
$\triangle\theta_{Yc}$	$-4.5889408 \times 10^{-9}$	2.3109602×10^{-7}	2.3127627×10^{-7}
$\triangle\theta_{Zc}$	$-1.4271180 \times 10^{-2}$	$-1.4286921 \times 10^{-2}$	$-1.4287038 \times 10^{-2}$

Comparing cases 3 and 5, we see that an increase in the torsion has very little effect on the accuracy of finite element solution. On the other hand, comparing cases 3 and 4, we see that increasing the curvature of the gun tube reduces the accuracy of the solution. This is consistent with the intuitive notion that when the curvature is small, the effect of torsion is to twist the beam about its centroidal axis without changing its geometry significantly.

Note that even though the displacements $\triangle Z_c$, $\triangle\theta_{Xc}$ and $\triangle\theta_{Yc}$ which correspond to w, α_x and α_y are inaccurate, their values are at least an order of magnitude smaller than the other "in-plane" displacements and so the error becomes less severe. In the next and final chapter, we present the conclusions of this investigation.

CHAPTER 8

CONCLUSIONS

In chapters 2 through 4, we presented an exact solution to the problem of finding the displacement of the end of the gun tube in terms of the imposed temperature change that causes the thermal shroud to expand. In Chapter 5, we performed a parametric study of the exact solution by plotting the components of force and displacement against different initial curvatures and torsions of the gun tube for different axial and flexural rigidities of the thermal shroud.

A brief summary of the conclusions of the parametric study follows. It was found that for a constant curvature, increasing the torsion of the gun tube had very little effect on the in-plane force and displacement components, while it caused an increase in the out-of-plane force and displacement components. It was observed that for high and low EA, displacements were minimal. For high EI, the increased lateral resistance to bending prevented large lateral displacements of the gun tube. However, this did not alleviate the problem of relatively large angular displacements. For low EI, the compatibility condition 2 reduced to condition 1, which yielded fairly large displacements. Thus, it appears that it would be most advantageous to have a thermal shroud with a low EA for the following reasons: Firstly, the displacements are smallest in this case. Secondly, the forces are also small. This second reason makes the low EA case preferable to the high EA case since it not only reduces displacements but also the forces on the connection between the gun tube and the shroud. It would be easier to construct an axially flexible shroud than one which is rigid; in addition, the gun tube-shroud joint could be designed for lesser loads. This would lead to a saving of material.

An alternative method of solution employing a general space-curved finite element was developed in Chapter 6. In the preceding section, we compared the two proposed solutions. The finite element solution yielded fairly accurate results as compared to the exact solution. However, despite its relative inaccuracy, the flexibility of the finite element approach makes it highly attractive. The particular advantages referred to are the fact that variable curvature and torsion can be accomodated within an element, and also the numerous possibilities afforded in modeling a structure with an assemblage of different elements. One such example was provided in Chapter 6, in which the cross-sections of different pieces of the gun tube were of different sizes. Thus it would be possible to model a variety of highly complex structures, provided that the curvature and torsion of the elements would be small.

APPENDIX A

THE COMPLEMENTARY STRAIN ENERGY OF THE HELICAL ROD

The complete expression for the strain energy of deformation, U, of the helical rod, expressed in terms of the XYZ components of applied force and moment, is as follows:

$$
\begin{aligned}
U \;=\; & \frac{1}{2EI}\left(\frac{L}{4\phi}\,(2\phi - \sin 2\phi)\left(M_y{}^2 + \frac{F_z{}^2 a^2}{\phi^2}\cos{}^2\phi + F_x{}^2 b^2 \right.\right. \\
& - \frac{2M_y F_z a}{\phi}\cos\phi - \frac{2F_x F_z ab}{\phi}\cos\phi + 2M_y F_x b \\
& - \frac{b^2}{L^2}\left(M_x{}^2 + \frac{F_z{}^2 a^2}{\phi^2}\sin{}^2\phi + F_y{}^2 b^2 \right. \\
& \left. + \frac{2M_x F_z a}{\phi}\sin\phi - \frac{2F_y F_z ab}{\phi}\sin\phi - 2M_x F_y b \right) \\
& - \frac{a^2}{L^2}\left(\frac{F_z{}^2 a^2}{\phi^2} \right) - \frac{2ab}{L^2}\left(\frac{M_z F_z a}{\phi} - \frac{M_z F_z a}{\phi} - \frac{F_y F_z a^2}{\phi^2}\cos\phi \right. \\
& \left.\left. + \frac{2F_x F_z a^2}{\phi^2}\sin\phi - \frac{F_x F_y ab}{\phi} \right) \right) \\
& + \frac{L}{4\phi}\,(2\phi + \sin 2\phi)\left(M_x{}^2 + \frac{F_z{}^2 a^2}{\phi^2}\sin{}^2\phi + F_y{}^2 b^2 \right. \\
& + \frac{2M_x F_z a}{\phi}\sin\phi - \frac{2F_y F_z ab}{\phi}\sin\phi - 2M_x F_y b + \frac{b^2}{L^2}\left(\frac{F_z{}^2 a^2}{\phi^2}\cos{}^2\phi \right.
\end{aligned}
$$

$$- M_y^2 - F_z^2 b^2 - \frac{2M_y F_z a}{\phi}\cos\phi - \frac{2F_z F_z ab}{\phi}\cos\phi + 2M_y F_z b \Big)$$

$$- \frac{a^2}{L^2}\left(\frac{F_y^2 a^2}{\phi^2}\right) - \frac{2ab}{L^2}\Big(- \frac{M_y F_y a}{\phi} + \frac{M_z F_z a}{\phi}$$

$$+ \frac{2F_y F_z a^2}{\phi^2}\cos\phi - \frac{F_z F_z a^2}{\phi^2}\sin\phi - \frac{F_z F_y ab}{\phi}\Big)\Big)$$

$$+ \frac{L}{3\phi}(2 - \cos^3\phi - 3\cos\phi)\left(\frac{b^2}{L^2}\Big(- \frac{2F_z^2 a^2}{\phi^2}\sin\phi - \frac{2M_z F_z a}{\phi}\right.$$

$$\left. - \frac{2F_y F_z ab}{\phi}\Big) + \frac{2ab}{L^2}\Big(- \frac{F_z F_z a^2}{\phi^2}\Big)\right)$$

$$- \frac{L}{3\phi}(3\sin\phi - \sin^3\phi)\left(\frac{b^2}{L^2}\Big(- \frac{2F_z^2 a^2}{\phi^2}\cos\phi + \frac{2M_y F_z a}{\phi}\right.$$

$$\left. - \frac{2F_z F_z ab}{\phi}\Big) - \frac{2ab}{L^2}\Big(- \frac{F_y F_z a^2}{\phi^2}\Big)\right)$$

$$- \frac{L}{32\phi}(12\phi - 8\sin 2\phi + \sin 4\phi)\left(\frac{b^2}{L^2}\left(\frac{F_z^2 a^2}{\phi^2}\right)\right)$$

$$+ \frac{L}{32\phi}(12\phi - 8\sin 2\phi + \sin 4\phi)\left(\frac{b^2}{L^2}\left(\frac{F_z^2 a^2}{\phi^2}\right)\right)$$

$$+ \frac{L}{\phi}(1 - \cos\phi)\left(\frac{a^2}{L^2}\Big(- \frac{2F_z^2 a^2}{\phi^2}\sin\phi + \frac{2M_z F_z a}{\phi} + \frac{2F_z F_y a^2}{\phi^2}\cos\phi\Big)\right.$$

$$+ \frac{2ab}{L^2}\Big(M_z M_z + \frac{M_z F_y a}{\phi}\cos\phi - \frac{M_z F_z a}{\phi}\sin\phi$$

$$\left. + \frac{M_z F_z a}{\phi}\sin\phi + \frac{F_y F_z a^2}{\phi^2}\cos\phi\sin\phi - \frac{F_z F_z a^2}{\phi^2}\sin^2\phi\right.$$

$$- M_x F_y b - \frac{F_y{}^2 ab}{\phi}\cos\phi + \frac{F_x F_y ab}{\phi}\sin\phi \Big) \Big)$$

$$+ \frac{L}{\phi}\sin\phi \left(\frac{a^2}{L^2}\left(- \frac{2F_y{}^2 a^2}{\phi^2}\cos\phi - \frac{2M_x F_y a}{g(f)} + \frac{2F_x F_y a^2}{\phi^2}\sin\phi \right) \right.$$

$$\left. - \frac{2ab}{L^2}\right) M_y M_z - \frac{M_y F_y a}{\phi}\cos\phi - \frac{M_y F_z a}{\phi}\sin\phi - \frac{M_z F_z a}{\phi}\cos\phi$$

$$- \frac{F_y F_z a^2}{\phi^2}\cos^2\phi + \frac{F_z F_z a^2}{\phi^2}\cos\phi\sin\phi + M_z F_z b$$

$$- \frac{F_z F_y ab}{\phi}\cos\phi - \frac{F_z{}^2 ab}{\phi}\sin\phi \Big) \Big)$$

$$- \frac{L}{8\phi^2}(2\phi^2 - 2\phi\sin 2\phi - \cos 2\phi + 1)\left(- 2F_z{}^2 b^2 + \frac{2F_z F_z ab}{\phi}\cos\phi \right.$$

$$\left. - 2M_y F_z b - \frac{b^2}{L^2}\left(- 2F_y{}^2 b^2 + \frac{2F_y F_z ab}{\phi}\sin\phi + 2M_z F_y b \right) \right.$$

$$\left. + \frac{2ab}{L^2}\left(\frac{F_z F_y ab}{\phi}\right)\right)$$

$$- \frac{L}{8\phi^2}(2\phi^2 + 2\phi\sin 2\phi - \cos 2\phi - 1)\left(- 2F_y{}^2 b^2 - \frac{2F_y F_z ab}{\phi}\sin\phi \right.$$

$$\left. + 2M_z F_y b + \frac{b^2}{L^2}\left(- 2F_z{}^2 b^2 + \frac{2F_z F_z ab}{\phi}\cos\phi - 2M_y F_z b \right) \right.$$

$$\left. - \frac{2ab}{L^2}\left(\frac{F_z F_y ab}{\phi}\right)\right)$$

$$+ \frac{L}{24\phi^3}[\,4\phi^3 + 3(1 - 2\phi^2)\sin 2\phi - 6\phi\cos 2\phi\,]\left(F_z{}^2 b^2 + \frac{F_y{}^2 b^4}{L^2}\right)$$

$$+ \frac{L}{24\phi^3}\left[4\phi^3 - 3(1-2\phi^2)\sin 2\phi + 6\phi\cos 2\phi\right]\left(F_y{}^2b^2 + \frac{F_z{}^2b^4}{L^2}\right)$$

$$- \frac{L}{9\phi^2}(6\sin\phi - \sin{}^3\phi - 9\phi\cos\phi + 3\phi\cos{}^3\phi)\left(\frac{2F_yF_zab^3}{\phi L^2}\right)$$

$$- \frac{L}{9\phi^2}(-7 - 6\cos\phi + \cos{}^3\phi + 9\phi\sin\phi - 3\phi\sin{}^3\phi)\left(\frac{2F_zF_yab^3}{\phi L^2}\right)$$

$$+ L\left(\frac{a^2}{L^2}\left(M_z{}^2 + \frac{F_y{}^2a^2}{\phi^2}\cos{}^2\phi + \frac{F_z{}^2a^2}{\phi^2}\sin{}^2\phi + \frac{2M_zF_ya}{\phi}\cos\phi\right.\right.$$

$$\left.\left. - \frac{2M_zF_za}{\phi}\sin\phi - \frac{2F_zF_ya^2}{\phi^2}\cos\phi\sin\phi\right)\right)$$

$$- \frac{L}{2\phi}\sin{}^2\phi\left(2\left(M_xM_y - \frac{M_xF_za}{\phi}\cos\phi + M_xF_zb + \frac{M_yF_za}{\phi}\sin\phi\right.\right.$$

$$- \frac{F_z{}^2a^2}{\phi^2}\sin\phi\cos\phi + \frac{F_xF_zab}{\phi}\sin\phi - M_yF_yb$$

$$\left.\left. - \frac{F_yF_zab}{\phi}\cos\phi - F_xF_yb^2\right) - \frac{a^2}{L^2}\left(\frac{2F_zF_ya^2}{\phi^2}\right)\right.$$

$$- \frac{2b^2}{L^2}\left(M_xM_y - \frac{M_xF_za}{\phi}\cos\phi + M_xF_zb + \frac{M_yF_za}{\phi}\sin\phi\right.$$

$$- \frac{F_z{}^2a^2}{\phi^2}\sin\phi\cos\phi + \frac{F_xF_zab}{\phi}\sin\phi - M_yF_yb$$

$$\left. - \frac{F_yF_zab}{\phi}\cos\phi - F_xF_yb^2\right) + \frac{2ab}{L^2}\left(-\frac{M_yF_za}{\phi}\right.$$

$$\left. + \frac{F_xF_za^2}{\phi^2}\cos\phi - \frac{F_z{}^2ab}{\phi} - \frac{M_zF_ya}{\phi}\right.$$

$$- \frac{F_y F_z a^2}{\phi^2} \sin\phi + \frac{F_y{}^2 ab}{\phi} \Big) \Big)$$

$$+ \frac{L}{8\phi^2} (4\phi \sin^2\phi - 2\phi + \sin 2\phi) \Big(\frac{2a^2}{L^2} \Big(- M_z F_z b - \frac{F_z F_z ab}{\phi} \sin\phi$$

$$- M_y F_y b - \frac{F_y F_z ab}{\phi} \cos\phi + 2F_z F_y b^2 \Big)$$

$$- \frac{2ab}{L^2} \Big(\frac{F_z{}^2 ab}{\phi} - \frac{F_y{}^2 ab}{\phi} \Big) \Big)$$

$$- \frac{L}{8\phi^3} (- 1 - 2\phi^2 + \cos 2\phi + 2\phi \sin 2\phi + 4\phi^2 \sin^2\phi)$$

$$\times \Big(2F_z F_y b^2 - \frac{2F_z F_y b^4}{L^2} \Big)$$

$$- \frac{L}{3\phi} \sin^3\phi \Big(- \frac{2b^2}{L^2} \Big(- \frac{M_y F_z a}{\phi} - \frac{F_z{}^2 a^2}{\phi^2} \cos\phi - \frac{F_z F_z ab}{\phi} \Big)$$

$$- \frac{2ab}{L^2} \Big(\frac{F_z F_z a^2}{\phi^2} \Big) \Big)$$

$$+ \frac{L}{3\phi} (1 - \cos^3\phi) \Big(- \frac{2b^2}{L^2} \Big(\frac{M_z F_z a}{\phi} + \frac{F_z{}^2 a^2}{\phi^2} \sin\phi - \frac{F_y F_z ab}{\phi} \Big)$$

$$- \frac{2ab}{L^2} \Big(\frac{F_z F_z a^2}{\phi^2} \Big) \Big)$$

$$+ \frac{L}{32\phi} (4\phi - \sin 4\phi) \Big(\frac{2b^2}{L^2} \Big(\frac{F_z{}^2 a^2}{\phi^2} \Big) \Big)$$

$$+ \frac{L}{9\phi^2} (3\phi \sin^3\phi - 2 - \cos^3\phi + 3\cos\phi) \Big(- \frac{2b^2}{L^2} \Big(\frac{F_z F_z ab}{\phi} \Big) \Big)$$

$$- \frac{L}{9\phi^2}(-3\phi\cos^3\phi + 3\sin\phi - \sin^3\phi)\left(-\frac{2b^2}{L^2}\left(\frac{F_yF_xab}{\phi}\right)\right)$$

$$- \frac{L}{\phi^2}(\phi\sin\phi - 1 + \cos\phi)$$

$$\times \left(\frac{2ab}{L^2}\left(-M_xF_xb - \frac{F_xF_yab}{\phi}\cos\phi + \frac{F_x^2ab}{\phi}\sin\phi\right)\right)$$

$$- \frac{L}{\phi^2}(-\phi\cos\phi + \sin\phi) \times$$

$$\left(\frac{2ab}{L^2}\left(M_xF_yb - \frac{F_y^2ab}{\phi}\cos\phi - \frac{F_xF_yab}{\phi}\sin\phi\right)\right)\Bigg)$$

$$- \frac{L}{4GJ}\Bigg(\frac{L}{4\phi}(2\phi - \sin 2\phi)\left(\frac{a^2}{L^2}\left(M_x^2 + \frac{F_x^2a^2}{\phi^2}\sin^2\phi\right.\right.$$

$$\left. - F_y^2b^2 - \frac{2M_xF_xa}{\phi}\sin\phi - \frac{2F_yF_xab}{\phi}\sin\phi - 2M_xF_yb\right)$$

$$- \frac{b^2}{L^2}\left(\frac{F_x^2a^2}{\phi^2}\right) - \frac{2ab}{L^2}\left(\frac{M_xF_xa}{\phi} - \frac{M_xF_xa}{\phi} - \frac{F_yF_xa^2}{\phi^2}\cos\phi\right.$$

$$\left.\left. - \frac{2F_xF_xa^2}{\phi^2}\sin\phi - \frac{F_xF_yab}{\phi}\right)\right)$$

$$- \frac{L}{4\phi}(2\phi + \sin 2\phi)\left(\frac{a^2}{L^2}\left(M_y^2 + \frac{F_x^2a^2}{\phi^2}\cos^2\phi + F_x^2b^2\right.\right.$$

$$\left.\left. - \frac{2M_yF_xa}{\phi}\cos\phi - \frac{2F_xF_xab}{\phi}\cos\phi + 2M_yF_xb\right)\right.$$

$$+\frac{b^2}{L^2}\left(\frac{F_y{}^2a^2}{\phi^2}\right)+\frac{2ab}{L^2}\left(-\frac{M_yF_ya}{\phi}+\frac{M_xF_xa}{\phi}\right.$$

$$\left.+\frac{2F_yF_xa^2}{\phi^2}\cos\phi-\frac{F_xF_xa^2}{\phi^2}\sin\phi-\frac{F_xF_yab}{\phi}\right)\Bigg)$$

$$-\frac{L}{3\phi}(2-\cos^3\phi-3\cos\phi)\left(\frac{a^2}{L^2}\left(-\frac{2F_z{}^2a^2}{\phi^2}\sin\phi-\frac{2M_xF_xa}{\phi}\right.\right.$$

$$\left.+\frac{2F_yF_xab}{\phi}\right)+\frac{2ab}{L^2}\left(\frac{F_xF_xa^2}{\phi^2}\right)\Bigg)$$

$$-\frac{L}{3\phi}(3\sin\phi-\sin^3\phi)\left(\frac{a^2}{L^2}\left(-\frac{2F_z{}^2a^2}{\phi^2}\cos\phi+\frac{2M_yF_xa}{\phi}\right.\right.$$

$$\left.+\frac{2F_xF_xab}{\phi}\right)-\frac{2ab}{L^2}\left(\frac{F_yF_xa^2}{\phi^2}\right)\Bigg)$$

$$-\frac{L}{32\phi}(12\phi-8\sin 2\phi+\sin 4\phi)\left(\frac{a^2}{L^2}\left(\frac{F_z{}^2a^2}{\phi^2}\right)\right)$$

$$-\frac{L}{32\phi}(12\phi+8\sin 2\phi-\sin 4\phi)\left(\frac{a^2}{L^2}\left(\frac{F_z{}^2a^2}{\phi^2}\right)\right)$$

$$-\frac{L}{\phi}(1-\cos\phi)\left(\frac{b^2}{L^2}\left(-\frac{2F_z{}^2a^2}{\phi^2}\sin\phi+\frac{2M_xF_xa}{\phi}\right.\right.$$

$$\left.+\frac{2F_xF_ya^2}{\phi^2}\cos\phi\right)-\frac{2ab}{L^2}\left(M_xM_x+\frac{M_xF_ya}{\phi}\cos\phi\right.$$

$$-\frac{M_xF_xa}{\phi}\sin\phi+\frac{M_xF_xa}{\phi}\sin\phi+\frac{F_yF_xa^2}{\phi^2}\cos\phi\sin\phi$$

$$\left.\left.-\frac{F_xF_xa^2}{\phi^2}\sin^2\phi-M_xF_yb-\frac{F_y{}^2ab}{\phi}\cos\phi+\frac{F_xF_yab}{\phi}\sin\phi\right)\right)$$

$$- \frac{L}{\phi}\sin\phi\left(\frac{b^2}{L^2}\left(-\frac{2F_y{}^2a^2}{\phi^2}\cos\phi - \frac{2M_zF_ya}{\phi}\right.\right.$$

$$\left.- \frac{2F_zF_ya^2}{\phi^2}\sin\phi\right) + \frac{2ab}{L^2}\left(M_yM_z + \frac{M_yF_ya}{\phi}\cos\phi\right.$$

$$- \frac{M_yF_za}{\phi}\sin\phi - \frac{M_zF_za}{\phi}\cos\phi - \frac{F_yF_za^2}{\phi^2}\cos^2\phi$$

$$\left.\left.- \frac{F_zF_za^2}{\phi^2}\cos\phi\sin\phi + M_zF_zb + \frac{F_zF_yab}{\phi}\cos\phi - \frac{F_z{}^2ab}{\phi}\sin\phi\right)\right)$$

$$- \frac{L}{8\phi^2}(2\phi^2 - 2\phi\sin 2\phi - \cos 2\phi + 1)\left(\frac{a^2}{L^2}\left(-2F_y{}^2b^2\right.\right.$$

$$\left.\left.- \frac{2F_yF_zab}{\phi}\sin\phi - 2M_zF_yb\right) - \frac{2ab}{L^2}\left(\frac{F_zF_yab}{\phi}\right)\right)$$

$$- \frac{L}{8\phi^2}(2\phi^2 + 2\phi\sin 2\phi + \cos 2\phi - 1)\left(\frac{a^2}{L^2}\left(-2F_z{}^2b^2\right.\right.$$

$$\left.\left.- \frac{2F_zF_zab}{\phi}\cos\phi - 2M_yF_zb\right) + \frac{2ab}{L^2}\left(\frac{F_zF_yab}{\phi}\right)\right)$$

$$- \frac{L}{24\phi^3}(4\phi^3 + 3(1 - 2\phi^2)\sin 2\phi - 6\phi\cos 2\phi)\left(\frac{a^2}{L^2}\left(F_y{}^2b^2\right)\right)$$

$$- \frac{L}{24\phi^3}(4\phi^3 - 3(1 - 2\phi^2)\sin 2\phi + 6\phi\cos 2\phi)\left(\frac{a^2}{L^2}\left(F_z{}^2b^2\right)\right)$$

$$- \frac{L}{9\phi^2}(6\sin\phi + \sin^3\phi - 9\phi\cos\phi + 3\phi\cos^3\phi)\left(\frac{a^2}{L^2}\left(\frac{2F_yF_zab}{\phi}\right)\right)$$

$$+ \frac{L}{9\phi^2}(7 - 6\cos\phi - \cos^3\phi - 9\phi\sin\phi + 3\phi\sin^3\phi)\left(\frac{a^2}{L^2}\left(\frac{2F_zF_zab}{\phi}\right)\right)$$

$$- L\left(\frac{b^2}{L^2}\left(M_z^2 - \frac{F_y^2 a^2}{\phi^2}\cos^2\phi + \frac{F_z^2 a^2}{\phi^2}\sin^2\phi \right.\right.$$

$$\left.\left. - \frac{2M_z F_y a}{\phi}\cos\phi - \frac{2M_z F_z a}{\phi}\sin\phi - \frac{2F_z F_y a^2}{\phi^2}\cos\phi\sin\phi \right)\right)$$

$$- \frac{L}{2\phi}\sin^2\phi\left(\frac{b^2}{L^2}\left(- \frac{2F_z F_y a^2}{\phi^2}\right) - \frac{2a^2}{L^2}\left(M_x M_y \right.\right.$$

$$- \frac{M_x F_z a}{\phi}\cos\phi - M_x F_z b + \frac{M_y F_z a}{\phi}\sin\phi$$

$$- \frac{F_z^2 a^2}{\phi^2}\sin\phi\cos\phi - \frac{F_x F_z a b}{\phi}\sin\phi - M_y F_y b$$

$$\left.\left. - \frac{F_y F_z a b}{\phi}\cos\phi - F_x F_y b^2\right) + \frac{2ab}{L^2}\left(\frac{M_y F_z a}{\phi} \right.\right.$$

$$- \frac{F_x F_z a^2}{\phi^2}\cos\phi - \frac{F_z^2 a b}{\phi} - \frac{M_x F_y a}{\phi}$$

$$\left.\left. - \frac{F_y F_z a^2}{\phi^2}\sin\phi - \frac{F_y^2 a b}{\phi}\right)\right)$$

$$- \frac{L}{8\phi^2}(4\phi\sin^2\phi - 2\phi + \sin 2\phi)\left(- \frac{2a^2}{L^2}\left(- M_x F_z b \right.\right.$$

$$- \frac{F_x F_z a b}{\phi}\sin\phi + M_y F_y b - \frac{F_y F_z a b}{\phi}\cos\phi + 2F_x F_y b^2\Big)$$

$$\left.\left. + \frac{2ab}{L^2}\left(- \frac{F_z^2 a b}{\phi} - \frac{F_y^2 a b}{\phi}\right)\right)\right)$$

$$+ \frac{L}{8\phi^3}(-1 - 2\phi^2 + \cos 2\phi + 2\phi\sin 2\phi + 4\phi^2\sin^2\phi)\left(\frac{2F_z F_y a^2 b^2}{L^2} \right)$$

$$+ \frac{L}{3\phi}\sin^3\phi\left(- \frac{2a^2}{L^2}\left(- \frac{M_yF_za}{\phi} + \frac{F_z^2a^2}{\phi^2}\cos\phi - \frac{F_xF_zab}{\phi}\right)\right.$$

$$\left. - \frac{2ab}{L^2}\left(\frac{F_yF_za^2}{\phi^2}\right)\right)$$

$$+ \frac{L}{3\phi}(1 - \cos^3\phi)\left(- \frac{2a^2}{L^2}\left(\frac{M_xF_za}{\phi} + \frac{F_z^2a^2}{\phi^2}\sin\phi - \frac{F_yF_zab}{\phi}\right)\right.$$

$$\left. + \frac{2ab}{L^2}\left(\frac{F_xF_za^2}{\phi^2}\right)\right)$$

$$- \frac{L}{32\phi}(4\phi - \sin 4\phi)\left(\frac{2a^2}{L^2}\left(\frac{F_z^2a^2}{\phi^2}\right)\right)$$

$$+ \frac{L}{9\phi^2}(3\phi\sin^3\phi - 2 - \cos^3\phi + 3\cos\phi)\left(- \frac{2a^2}{L^2}\left(\frac{F_xF_zab}{\phi}\right)\right)$$

$$+ \frac{L}{9\phi^2}(- 3\phi\cos^3\phi + 3\sin\phi - \sin^3\phi)\left(- \frac{2a^2}{L^2}\left(\frac{F_yF_zab}{\phi}\right)\right)$$

$$+ \frac{L}{\phi^2}(\phi\sin\phi - 1 + \cos\phi) \times$$

$$\left(\frac{2ab}{L^2}\left(- M_xF_xb - \frac{F_xF_yab}{\phi}\cos\phi + \frac{F_z^2ab}{\phi}\sin\phi\right)\right)$$

$$+ \frac{L}{\phi^2}(- \phi\cos\phi + \sin\phi) \times$$

$$\left(- \frac{2ab}{L^2}\left(M_xF_yb + \frac{F_y^2ab}{\phi}\cos\phi - \frac{F_xF_yab}{\phi}\sin\phi\right)\right)\Bigg)$$

$$+ \frac{1}{4GA}\left(\frac{L}{4\phi}(2\phi - \sin 2\phi)\left(F_y^2 + \frac{F_z^2b^2}{L^2}\right)\right.$$

$$
\begin{aligned}
&- \frac{L}{4\phi}(2\phi - \sin 2\phi)\left(F_x{}^2 + \frac{F_y{}^2 b^2}{L^2} \right) \\
&- \frac{L}{2\phi}\sin{}^2\phi \left(2F_xF_y - \frac{2F_xF_y b^2}{L^2} \right) \\
&- \frac{F_x{}^2 a^2}{L} - \frac{L}{\phi}(1 - \cos\phi)\left(\frac{2F_xF_x ab}{L^2} \right) - \frac{L}{\phi}\sin\phi \left(\frac{2F_yF_x ab}{L^2} \right) \Bigg) \\
&- \frac{1}{2EA}\left(\frac{L}{4\phi}(2\phi - \sin 2\phi)\left(\frac{F_x{}^2 a^2}{L^2} \right) \right. \\
&- \frac{L}{4\phi}(2\phi - \sin 2\phi)\left(\frac{F_y{}^2 a^2}{L^2} \right) \\
&- \frac{L}{2\phi}\sin{}^2\phi \left(- \frac{2F_xF_y a^2}{L^2} \right) + \frac{F_x{}^2 b^2}{L} \\
&\left. - \frac{L}{\phi}(1 - \cos\phi)\left(\frac{2F_xF_x ab}{L^2} \right) + \frac{L}{\phi}\sin\phi \left(\frac{2F_yF_x ab}{L^2} \right) \right)
\end{aligned}
$$

APPENDIX B

THE STRAIN ENERGY OF DEFORMATION OF THE FINITE ELEMENT

The strain energy of deformation of the space-curved finite element is a function of the nodal values of displacement, namely,

$$U = U(u_1, v_1, w_1, u_1', v_1', \phi_1, u_2, v_2, w_2, u_2', v_2', \phi_2).$$

The complete expression for the strain energy is,

```
U    =   a3*(l*w2**2+l*w1*w2+l*w1**2)/3.0-a29*((3*l**2*v2p-21*l
*v2-2*l**2*v1p-9*l*v1)*w2+(2*l**2*v2p-9*l*v2-3*l**2*v1p-21*l*v1
)*w1)/60.0+a30*((l*v2p+6*v2-l*v1p-6*v1)*w2+(-l*v2p+6*v2+l*v1p-6
*v1)*w1)/12.0+a35*((l*v2p-v2+v1)*w2+(v2-l*v1p-v1)*w1)/l-a25*((3
*l**2*u2p-21*l*u2-2*l**2*u1p-9*l*u1)*w2+(2*l**2*u2p-9*l*u2-3*l*
*2*u1p-21*l*u1)*w1)/60.0+a26*((l*u2p+6*u2-l*u1p-6*u1)*w2+(-l*u2
p+6*u2+l*u1p-6*u1)*w1)/12.0+a33*((l*u2p-u2+u1)*w2+(u2-l*u1p-u1)
*w1)/l+a49*((2*l*p2+l*p1)*w2+(l*p2+2*l*p1)*w1)/6.0+a38*(w2-w1)*
(l*w2+l*w1)/l/2.0+a51*(p2-p1)*(l*w2+l*w1)/l/2.0+a7*(w2-w1)**2/l
-a31*(l**2*v2p-6*l*v2-l**2*v1p-6*l*v1)*(w2-w1)/l/12.0+a36*(v2p-
v1p)*(w2-w1)/l+a32*(v2-v1)*(w2-w1)/l-a27*(l**2*u2p-6*l*u2-l**2*
u1p-6*l*u1)*(w2-w1)/l/12.0+a34*(u2p-u1p)*(w2-w1)/l+a28*(u2-u1)*
(w2-w1)/l+a50*(l*p2+l*p1)*(w2-w1)/l/2.0+a2*(2*l**3*v2p**2+(-22*
l**2*v2-3*l**3*v1p-13*l**2*v1)*v2p+78*l*v2**2+(13*l**2*v1p+54*l
*v1)*v2+2*l**3*v1p**2+22*l**2*v1*v1p+78*l*v1**2)/210.0+a10*(4*l
**2*v2p**2+(-12*l*v2+4*l**2*v1p+12*l*v1)*v2p+12*v2**2+(-12*l*v1
p-24*v1)*v2+4*l**2*v1p**2+12*l*v1*v1p+12*v1**2)/l**3+a6*(2*l**2
*v2p**2+(-3*l*v2-l**2*v1p+3*l*v1)*v2p+18*v2**2+(-3*l*v1p-36*v1)
*v2+2*l**2*v1p**2+3*l*v1*v1p+18*v1**2)/l/15.0-a18*(2*l**2*v2p**
2+(-18*l*v2-l**2*v1p+3*l*v1)*v2p+18*v2**2+(-3*l*v1p-36*v1)*v2+2
*l**2*v1p**2+18*l*v1*v1p+18*v1**2)/l/15.0+a19*(v2p**2/2.0-v1p**
2/2.0)+a11*((4*l**3*u2p-22*l**2*u2-3*l**3*u1p-13*l**2*u1)*v2p+(
-22*l**2*u2p+156*l*u2+13*l**2*u1p+54*l*u1)*v2+(-3*l**3*u2p+13*l
**2*u2+4*l**3*u1p+22*l**2*u1)*v1p+(-13*l**2*u2p+54*l*u2+22*l**2
*u1p+156*l*u1)*v1)/420.0+a20*((4*l**2*u2p-3*l*u2-l**2*u1p+3*l*u
1)*v2p+(-3*l*u2p+36*u2-3*l*u1p-36*u1)*v2+(-l**2*u2p-3*l*u2+4*l*
```

```
*2*u1p+3*l*u1)*v1p+(3*l*u2p-36*u2+3*l*u1p+36*u1)*v1)/l/30.0-a22
*((4*l**2*u2p-3*l*u2-l**2*u1p+3*l*u1)*v2p+(-33*l*u2p+36*u2-3*l*
u1p-36*u1)*v2+(-l**2*u2p-3*l*u2+4*l**2*u1p+3*l*u1)*v1p+(3*l*u2p
-36*u2+33*l*u1p+36*u1)*v1)/l/30.0+a37*((4*l**2*u2p-6*l*u2+2*l**
2*u1p+6*l*u1)*v2p+(-6*l*u2p+12*u2-6*l*u1p-12*u1)*v2+(2*l**2*u2p
-6*l*u2+4*l**2*u1p+6*l*u1)*v1p+(6*l*u2p-12*u2+6*l*u1p+12*u1)*v1
)/l**3-a21*((4*l**2*u2p-33*l*u2-l**2*u1p+3*l*u1)*v2p+(-3*l*u2p+
36*u2-3*l*u1p-36*u1)*v2+(-l**2*u2p-3*l*u2+4*l**2*u1p+33*l*u1)*v
1p+(3*l*u2p-36*u2+3*l*u1p+36*u1)*v1)/l/30.0+a23*((l*u2p+2*u2-l*
u1p-2*u1)*v2p+(2*u1p-2*u2p)*v2+(l*u2p-2*u2-l*u1p+2*u1)*v1p+(2*u
2p-2*u1p)*v1)/l/2.0+a24*((l*u2p-2*u2+l*u1p+2*u1)*v2p+(2*u2p-2*u
1p)*v2+(-l*u2p+2*u2-l*u1p-2*u1)*v1p+(2*u1p-2*u2p)*v1)/l/2.0+a13
*((6*l*u2-l**2*u1p-6*l*u1)*v2p+(-6*l*u2p+30*u2+6*l*u1p+30*u1)*v
2+(l**2*u2p-6*l*u2+6*l*u1)*v1p+(6*l*u2p-30*u2-6*l*u1p-30*u1)*v1
)/60.0-a12*((6*l*u2-l**2*u1p-6*l*u1)*v2p+(-6*l*u2p-30*u2+6*l*u1
p+30*u1)*v2+(l**2*u2p-6*l*u2+6*l*u1)*v1p+(6*l*u2p-30*u2-6*l*u1p
+30*u1)*v1)/60.0-a44*((3*l**2*p2+2*l**2*p1)*v2p+(-21*l*p2-9*l*p
1)*v2+(-2*l**2*p2-3*l**2*p1)*v1p+(-9*l*p2-21*l*p1)*v1)/60.0+a45
*((l*p2-l*p1)*v2p+(6*p2+6*p1)*v2+(l*p1-l*p2)*v1p+(-6*p2-6*p1)*v
1)/12.0+a48*(l*p2*v2p+(p1-p2)*v2-l*p1*v1p+(p2-p1)*v1)/l-a46*(p2
-p1)*(l**2*v2p-6*l*v2-l**2*v1p-6*l*v1)/l/12.0+a17*(v2**2-v1**2)
/2.0+a47*(p2-p1)*(v2-v1)/l+a1*(2*l**3*u2p**2+(-22*l**2*u2-3*l**
3*u1p-13*l**2*u1)*u2p+78*l*u2**2+(13*l**2*u1p+54*l*u1)*u2+2*l**
3*u1p**2+22*l**2*u1*u1p+78*l*u1**2)/210.0+a9*(4*l**2*u2p**2+(-1
2*l*u2+4*l**2*u1p+12*l*u1)*u2p+12*u2**2+(-12*l*u1p-24*u1)*u2+4*
l**2*u1p**2+12*l*u1*u1p+12*u1**2)/l**3+a5*(2*l**2*u2p**2+(-3*l*
u2-l**2*u1p+3*l*u1)*u2p+18*u2**2+(-3*l*u1p-36*u1)*u2+2*l**2*u1p
**2+3*l*u1*u1p+18*u1**2)/l/15.0-a15*(2*l**2*u2p**2+(-18*l*u2-l*
*2*u1p+3*l*u1)*u2p+18*u2**2+(-3*l*u1p-36*u1)*u2+2*l**2*u1p**2+1
8*l*u1*u1p+18*u1**2)/l/15.0+a16*(u2p**2/2.0-u1p**2/2.0)-a39*((3
*l**2*p2+2*l**2*p1)*u2p+(-21*l*p2-9*l*p1)*u2+(-2*l**2*p2-3*l**2
*p1)*u1p+(-9*l*p2-21*l*p1)*u1)/60.0+a40*((l*p2-l*p1)*u2p+(6*p2+
6*p1)*u2+(l*p1-l*p2)*u1p+(-6*p2-6*p1)*u1)/12.0+a43*(l*p2*u2p+(p
1-p2)*u2-l*p1*u1p+(p2-p1)*u1)/l-a41*(p2-p1)*(l**2*u2p-6*l*u2-l*
*2*u1p-6*l*u1)/l/12.0+a14*(u2**2-u1**2)/2.0+a42*(p2-p1)*(u2-u1)
/l+a4*(l*p2**2+l*p1*p2+l*p1**2)/3.0+a8*(p2-p1)**2/l
```

where u1 = u_1, u1p = u_1', p = ϕ, etc., and the coefficients a_1, a_2, . . . , a_{51} depend on geometric and material properties of the element, such as the length of the element, l, the moments of inertia of its cross-section, ixx, iyy and ixy, the curvature, k (kappa), the rate of change of curvature of the element, kp (kappa prime), the torsion, la (lambda), the rate of change of torsion, lap (lambda prime), and modulus of elasticity e, and finally, shear

modulus g. These coefficients are listed below:

```
a1 = (e*(ixx*lap**2+a*k**2)+g*ixx*k**2*la**2)/2.0

a2 = iyy*(e*lap**2+g*k**2*la**2)/2.0

a3 = iyy*(e*kp**2+g*k**4)/2.0

a4 = (ixx*(g*la**2+e*k**2)+g*iyy*la**2)/2.0

a5 = (e*ixx*la**2+g*iyy*k**2)/2.0

a6 = (e*iyy*la**2+g*ixx*k**2)/2.0

a7 = e*(iyy*k**2+a)/2.0

a8 = g*(iyy+ixx)/2.0

a9 = e*iyy/2.0

a10 = e*ixx/2.0

a11 = -ixy*(e*lap**2+g*k**2*la**2)

a12 = -e*ixy*la*lap-g*iyy*k**2*la

a13 = g*ixx*k**2*la-e*ixy*la*lap

a14 = e*ixx*la*lap+g*ixy*k**2*la

a15 = e*ixy*lap

a16 = e*ixy*la

a17 = e*iyy*la*lap-g*ixy*k**2*la

a18 = -e*ixy*lap

a19 = -e*ixy*la

a20 = ixy*(g*k**2-e*la**2)

a21 = e*ixx*lap

a22 = -e*iyy*lap
```

```
a23 = e*ixx*la

a24 = -e*iyy*la

a25 = ixy*(e*kp*lap+g*k**3*la)

a26 = e*ixy*kp*la+g*iyy*k**3

a27 = e*ixy*k*lap-a*e*k

a28 = e*ixy*k*la

a29 = -iyy*(e*kp*lap+g*k**3*la)

a30 = g*ixy*k**3-e*iyy*kp*la

a31 = -e*iyy*k*lap

a32 = -e*iyy*k*la

a33 = e*iyy*kp

a34 = e*iyy*k

a35 = e*ixy*kp

a36 = e*ixy*k

a37 = e*ixy

a38 = e*iyy*k*kp

a39 = g*ixy*k*la**2-e*ixx*k*lap

a40 = g*iyy*k*la-e*ixx*k*la

a41 = g*ixx*k*la

a42 = g*ixy*k

a43 = -e*ixy*k

a44 = e*ixy*k*lap-g*iyy*k*la**2

a45 = ixy*(g*k*la+e*k*la)
```

```
a46 = -g*ixy*k*la

a47 = g*ixx*k

a48 = -e*ixx*k

a49 = g*iyy*k**2*la-e*ixy*k*kp

a50 = -e*ixy*k**2

a51 = g*ixy*k**2
```

APPENDIX C

COMPUTER IMPLEMENTATION OF THE EXACT SOLUTION

```
C-----------------------------------------------------------------------
C
C     THIS PROGRAM COMPUTES DISPLACEMENTS AT THE END OF THE GUN TUBE
C     DUE TO THE FORCE EXERTED BY THE EXPANSION OF THE THERMAL SHROUD
C     FOR VARYING INITIAL CURVATURE AND TORSION OF THE GUN TUBE.
C-----------------------------------------------------------------------
C
C
      INTEGER KOUNT1, KOUNT2, KOUNT3, KOUNT4, IA, IDGT, IER
      REAL*8 ELAST, G, AC, AS, IXX, JP, ALPHA, TMPR, L, PI, CUR, TOR
      REAL*8 RATIO, A, B, P, R, C1, S1, C, S, EI, GJ, EA, GA
      REAL*8 DENOM1, DENOM2, DENOM3, LS, CVAL, TVAL
      REAL*8 DIST1, DIST2, DISTANCE
      REAL*8 RAD1, RAD2, RAD3, RAD4, ISHROUD, EASHROUD, EISHROUD
C
C     DOUBLE PRECISION CONSTANTS ABBREVIATED FOR USE IN THE COMPUTATION
C     OF FLEXIBILITY MATRIX ELEMENTS
C
      REAL*8 TO, TR, FO, FI, SI, SE, ET, NI, TE, EV, TW, FF, SX, TF
      REAL*8 TT, FE, ST, NS, ONE, ZERO, START, FACTOR
C
C     ARRAYS USED:
C     F             FLEXIBILITY MATRIX IN GLOBAL COORDINATE SYSTEM
C     FBAR          FLEXIBILITY MATRIX IN CHORD SYSTEM
C     COMPAT        MATRIX USED TO SOLVE COMPATIBILITY EQUATIONS
C     INVCOMPAT     INVERSE OF COMPAT
C     FORCE3        FORCE VECTOR IN COMPATIBILITY EQUATIONS
C     RHS           RIGHT HAND SIDE OF COMPATIBILITY EQUATIONS
C     DELTABAR, DELTA, DELTATAN
C                   DISPLACEMENTS IN CHORD, GLOBAL AND TANGENT SYSTEMS
C     FORCEBAR, FORCE, FORCETAN
C                   FORCES IN CHORD, GLOBAL AND TANGENT SYSTEMS
C     CG            CHORD TO GLOBAL TRANSFORMATION MATRIX
C     GC            GLOBAL TO CHORD TRANSFORMATION MATRIX
C     TG            TANGENT TO GLOBAL TRANSFORMATION MATRIX
```

```
C     GT            GLOBAL TO TANGENT TRANSFORMATION MATRIX
C     TC            TANGENT TO CHORD TRANSFORMATION MATRIX
C     TEMP6         TEMPORARY STORAGE
C     WKAREA        USED BY IMSL INVERSION ROUTINE
C
      REAL*8 F(6,6), FBAR(6,6), COMPAT(3,3), INVCOMPAT(3,3)
      REAL*8 DELTABAR(6,1), DELTA(6,1), DELTATAN(6,1)
      REAL*8 FORCEBAR(6,1), FORCE(6,1), FORCETAN(6,1), FORCE3(3,1)
      REAL*8 CG(6,6), TG(6,6), CT(6,6), GC(6,6), GT(6,6)
      REAL*8 TEMP6(6,6), RHS(3,1), WKAREA(500)
C
      DATA ELAST/4.35097D9/
      DATA G/1.67345D9/
      DATA RAD1, RAD2, RAD3, RAD4/6.0D-2, 1.0D-1, 1.1D-1, 1.45D-1/
      DATA ALPHA/1.206D-5/
      DATA TMPR/1.0D2/
      DATA L/5.25D0/
C
C     DATA FOR CONSTANTS
C
      DATA TO,TR,FO,FI,SI,SE/2.0D0,3.0D0,4.0D0,5.0D0,6.0D0,7.0D0/
      DATA ET,NI,TE,EV,TW,FF/8.0D0,9.0D0,10.0D0,11.0D0,12.0D0,15.0D0/
      DATA SX,TF,TT,FE,ST/16.0D0,24.0D0,33.0D0,48.0D0,72.0D0/
      DATA NS,ONE,ZERO,START/96.0D0,1.0D0,0.0D0,1.0D-4/
C
C     OPEN OUTPUT FILES
C
      OPEN(UNIT=12,FILE='delxbar.dat',STATUS='NEW')
      OPEN(UNIT=13,FILE='delybar.dat',STATUS='NEW')
      OPEN(UNIT=14,FILE='delzbar.dat',STATUS='NEW')
      OPEN(UNIT=15,FILE='thexbar.dat',STATUS='NEW')
      OPEN(UNIT=16,FILE='theybar.dat',STATUS='NEW')
      OPEN(UNIT=17,FILE='thezbar.dat',STATUS='NEW')
      OPEN(UNIT=34,FILE='forcexbar.dat',STATUS='NEW')
      OPEN(UNIT=18,FILE='forceybar.dat',STATUS='NEW')
      OPEN(UNIT=37,FILE='forcezbar.dat',STATUS='NEW')
      OPEN(UNIT=33,FILE='distance.dat',STATUS='NEW')
C
C     ASSIGN VALUES OF PI AND FACTOR (FOR MULTIPLYING CURVATURE)
C
      PI = DATAN(ONE)*FO
      FACTOR = DSQRT(DSQRT(DSQRT(DSQRT(TE))))
C
C     COMPUTE SECTION PROPERTIES OF GUN TUBE AND THERMAL SHROUD
C
```

```
C     GUN TUBE:
C
      AC = PI*(RAD2**2-RAD1**2)
      IXX = PI*(RAD2**4-RAD1**4)/FO
      JP = TO*IXX
      EI = ELAST*IXX
      GJ = G*JP
      EA = ELAST*AC
      GA = G*AC
C
C     THERMAL SHROUD:
C
      AS = PI*(RAD4**2-RAD3**2)
      ISHROUD = PI*(RAD4**4-RAD3**4)/FO
      EISHROUD = ELAST*ISHROUD
      EASHROUD = ELAST*AS
C
C     INITIALIZE TOR AND TVAL
C
      TOR = ZERO
      TVAL = ZERO
C
C     LOOP TO COMPUTE DISPLACEMENTS FOR VARYING CURVATURES AND TORSIONS
C
      DO 100 KOUNT3 = 1, 50
      CUR = START
      CVAL = ONE
      IF (KOUNT3.EQ.2) THEN
         TOR = START
         TVAL = ONE
      ENDIF
      DO 200 KOUNT4 = 1, 49
C
C     COMPUTE HELIX GEOMETRY FROM CUR AND TOR AND INITIALIZE ARRAYS
C
      RATIO = TOR/CUR
      A = L/DSQRT(ONE+RATIO**2)
      B = DSQRT(L**2-A**2)
      C1 = A/L
      S1 = B/L
      R = C1**2/CUR
      P = A/R
      C = DCOS(P)
      S = DSIN(P)
      LS = DSQRT((R*C-R)**2+(R*S)**2+B**2)
```

```
C
C     INITIALIZE TRANSFORMATION MATRICES TO ZEROES
C
      DO 101 KOUNT1 = 1, 6
      DO 101 KOUNT2 = 1, 6
         CG(KOUNT1, KOUNT2) = ZERO
         TG(KOUNT1, KOUNT2) = ZERO
         CT(KOUNT1, KOUNT2) = ZERO
         GC(KOUNT1, KOUNT2) = ZERO
         GT(KOUNT1, KOUNT2) = ZERO
  101 CONTINUE
C
C     INITIALIZE FORCE VECTORS IN ALL 3 COORDINATE SYSTEMS TO ZEROES
C
      DO 102 KOUNT1 = 1, 6
         FORCEBAR(KOUNT1, 1) = ZERO
         FORCE(KOUNT1, 1) = ZERO
         FORCETAN(KOUNT1, 1) = ZERO
  102 CONTINUE
C
C     COMPUTE ALL 6 TRANSFORMATION MATRICES
C     FIRST, ASSIGN ELEMENTS OF CG (CHORD TO GLOBAL TRANSFORMATION MATRIX)
C
      DENOM1 = DSQRT(TO*(ONE-C))
      DENOM2 = DSQRT(TO*(ONE-C)+(P*B/A)**2)
      DENOM3 = DENOM1*DENOM2
      CG(1,1) = S/DENOM1
      CG(1,2) = (C-ONE)/DENOM2
      CG(1,3) = (ONE-C)*(P*B/A)/DENOM3
      CG(2,1) = (ONE-C)/DENOM1
      CG(2,2) = S/DENOM2
      CG(2,3) = -(S*P*B/A)/DENOM3
      CG(3,1) = ZERO
      CG(3,2) = (P*B/A)/DENOM2
      CG(3,3) = TO*(ONE-C)/DENOM3
      DO 103 KOUNT1 = 1, 3
      DO 103 KOUNT2 = 1, 3
         CG(KOUNT1+3, KOUNT2+3) = CG(KOUNT1, KOUNT2)
  103 CONTINUE
C
C     ASSIGN ELEMENTS OF TG (TANGENT TO GLOBAL TRANSFORMATION MATRIX)
C
      TG(1,1) = -C
      TG(1,2) = S1*S
      TG(1,3) = -C1*S
```

```
      TG(2,1) = -S
      TG(2,2) = -S1*C
      TG(2,3) = C1*C
      TG(3,1) = ZERO
      TG(3,2) = C1
      TG(3,3) = S1
      DO 104 KOUNT1 = 1, 3
      DO 104 KOUNT2 = 1, 3
         TG(KOUNT1+3, KOUNT2+3) = TG(KOUNT1, KOUNT2)
  104 CONTINUE
C
C     INVERT CG TO GET GC (GLOBAL TO CHORD TRANSFORMATION MATRIX)
C     AND TG TO GET GT (GLOBAL TO TANGENT TRANSFORMATION MATRIX)
C
      DO 105 KOUNT1 = 1, 6
      DO 105 KOUNT2 = 1, 6
         TEMP6(KOUNT1, KOUNT2) = CG(KOUNT1, KOUNT2)
  105 CONTINUE
      IDGT = 0
      IA = 6
      KOUNT1 = 6
      CALL LINV1F(TEMP6,KOUNT1,IA,GC,IDGT,WKAREA,IER)

      DO 106 KOUNT1 = 1, 6
      DO 106 KOUNT2 = 1, 6
         TEMP6(KOUNT1, KOUNT2) = TG(KOUNT1, KOUNT2)
  106 CONTINUE
      IDGT = 0
      IA = 6
      KOUNT1 = 6
      CALL LINV1F(TEMP6,KOUNT1,IA,GT,IDGT,WKAREA,IER)
C
C     COMPUTE CT (CHORD TO TANGENT TRANSFORMATION MATRIX) = GT * CG
C
      KOUNT1 = 6
      CALL MULMATX(GT, CG, CT, KOUNT1, KOUNT1, KOUNT1)
C
C     ASSIGN ELEMENTS OF F MATRIX
C
      F(1,1) = L**3/(TW*EI)*(SI*C1**4*(TR*S*C-FO*S+TO*P*S**2+P)
     1         +S1**4*(TR*P+TO*P**3-TR*S*C)+SI*C1**2*S1**2*(FO*S-
     2         TR*S*C-P)+S1**2*(-TR*P+TO*P**3+TR*S*C))/P**3
     3         -L**3/(TF*GJ)*C1**2*S1**2/P**3*(-FF*P-TW*P*S**2
     4         -TO*P**3+FE*S-TT*S*C)
     5         +L/(TO*EA)*C1**2*(P-S*C)/P + L/(FO*GA)*(C1**2*(P+
```

```
6         S*C)/P+TO*S1**2)

 F(1,2) = L**3/(FO*EI)*(TO*C1**4*(TR*S**2-TO*P*S*C+TO*C-TO)+
1         S1**4*(P**2-S**2)+TO*C1**2*S1**2*(-TR*S**2+TO*P*S
2         -TO*C+TO)+S1**2*(S**2-P**2))/P**3
3         -L**3/(ET*GJ)*C1**2*S1**2*(ET-ET*C-EV*S**2+FO*P*S*C
4         +FO*P*S-P**2)/P**3
5         -L/(TO*EA)*C1**2*S**2/P + L/(FO*GA)*C1**2*S**2/P

 F(1,3) = L**3/(FO*EI)*(C1*S1*P*(S-P*C)+TO*C1**3*S1*(-TO+TO*C
1         -TO*S**2+TR*P*S)+C1*S1**3*(FO-FO*C-P*S-P**2*C))/P**3
2         -L**3/(ET*GJ)*C1**3*S1*(P**2*C+SE*P*S-FO*S**2+ET*C-
3         ET)/P**3-L/EA*C1*S1*(ONE-C)/P+L/(TO*GA)*C1*S1*(ONE-
4         C)/P

 F(1,4) = L**2/(FO*EI)*(S1*(P-S*C)+TO*C1**2*S1*(P+S*C-TO*S)+
1         S1**3*(S*C-P))/P**2
2         -L**2/(ET*GJ)*C1**2*S1*(S*C-FO*S+TR*P)/P**2

 F(1,5) = L**2/(FO*EI)*(S1*(P**2-S**2)+TO*C1**2*S1*S**2+S1**3
1         *(P**2+S**2))/P**2
2         -L**2/(ET*GJ)*C1**2*S1*(S**2-P**2)/P**2

 F(1,6) = L**2/EI*(C1**3*(ONE-C-P*S)+C1*S1**2*(C-ONE))/P**2
1         -L**2/(TO*GJ)*C1*S1**2*(P*S+TO*C-TO)/P**2

 F(2,2) = L**3/(TW*EI)*(SI*C1**4*(P-TR*S*C+TO*P*C**2)+SI*
1         C1**2*S1**2*(P+TR*S*C-FO*P*C)+S1**4*(-TR*P+TO*P**3+
2         TR*S*C)+S1**2*(TR*P+TO*P**3-TR*S*C))/P**3
3         -L**3/(TF*GJ)*C1**2*S1**2*(-NI*P-TO*P**3-TF*P*C+TW*
4         P*S**2+TT*S*C)/P**3
5         +L/(TO*EA)*C1**2*(P+S*C)/P + L/(FO*GA)*(C1**2*(P-S
6         *C)/P+TO*S1**2)

 F(2,3) = L**3/(FO*EI)*(C1*S1*(P*C-S-P**2*S)+TO*C1**3*S1*(S+
1         TO*S*C-TR*P*C)+C1*S1**3*(-TR*S-P*C-P**2*S+FO*P))/
2         P**3
3         -L**3/(ET*GJ)*C1**3*S1*(FI*S-FI*P*C+FO*S*C+P**2*S
4         -FO*P)/P**3 + L/EA*C1*S1*S/P - L/(TO*GA)*C1*S1*S/P

 F(2,4) = L**2/(FO*EI)*(S1*(-S**2-P**2)+TO*C1**2*S1*(-C**2+TO
1         *C-ONE)+S1**3*(S**2-P**2))/P**2
2         -L**2/(ET*GJ)*C1**2*S1*(-FO+FO*C+S**2+P**2)/P**2

 F(2,5) = L**2/(FO*EI)*(-S1+TO*C1**2*S1+S1**3)*(P-S*C)/P**2
```

```
     1          -L**2/(ET*GJ)*C1**2*S1*(P-S*C)/P**2

      F(2,6) = L**2/EI*(C1**3*(P*C-S)+C1*S1**2*(S-P))/P**2
     1          -L**2/(TO*GJ)*C1*S1**2*(-P*C-P+TO*S)/P**2

      F(3,3) = L**3/(TO*EI)*(C1**2*(P-S*C)+C1**2*S1**2*(TR*P+S*C-
     1          FO*S))/P**3
     2          -L**3/(FO*GJ)*C1**4*(FO*S-TR*P-S*C)/P**3
     3          +L/EA*S1**2 + L/(TO*GA)*C1**2

      F(3,4) = L**2/(TO*EI)*(C1*P*S+C1*S1**2*(TO*C-TO+P*S))/P**2
     1          -L**2/(FO*GJ)*C1**3*(-TO*C+TO-P*S)/P**2

      F(3,5) = L**2/(TO*EI)*(C1+C1*S1**2)*(S-P*C)/P**2
     1          -L**2/(FO*GJ)*C1**3*(P*C-S)/P**2

      F(3,6) = L**2*(ONE/EI-ONE/(TO*GJ))*C1**2*S1*(S-P)/P**2

      F(4,4) = L/(TO*EI*P)*(S*C*C1**2+P*(ONE+S1**2))
     1          -L*C1**2/(FO*GJ*P)*(S*C-P)

      F(4,5) = (L/(TO*EI)-L/(FO*GJ))*(C1**2*S**2/P)

      F(4,6) = (L/EI-L/(TO*GJ))*(C1*S1*(ONE-C)/P)

      F(5,5) = L/(TO*EI*P)*(-C1**2*S*C+P*(ONE+S1**2))
     1          -L/(FO*GJ*P)*(C1**2*(-S*C-P))

      F(5,6) = (L/(TO*GJ)-L/EI)*(C1*S1*S/P)

      F(6,6) = L*C1**2/EI+L*S1**2/(TO*GJ)

      DO 108 KOUNT1 = 2, 6
      DO 108 KOUNT2 = 1, KOUNT1-1
         F(KOUNT1, KOUNT2) = F(KOUNT2, KOUNT1)
  108 CONTINUE
C
C     PRE & POSTMULTIPLY ORIGINAL F WITH GC & CG RESPECTIVELY TO
C     OBTAIN THE TRANSFORMED FLEXIBILITY MATRIX, FBAR, IN THE CHORD SYSTEM
C
      KOUNT1 = 6
      CALL MULMATX(GC,F,TEMP6,KOUNT1,KOUNT1,KOUNT1)
      KOUNT1 = 6
      CALL MULMATX(TEMP6,CG,FBAR,KOUNT1,KOUNT1,KOUNT1)
C
```

```
C     APPLY COMPATIBILITY OF DISPLACEMENTS TO FIND FORCES EXERTED ON
C     GUN TUBE DUE TO EXPANSION OF SHROUD
C
C     COMPATIBILITY IS EXPRESSED AS A SET OF 3 SIMULTANEOUS EQUATIONS
C     IN THE 3 FORCE COMPONENTS, FXBAR, FYBAR, FZBAR
C
      COMPAT(1,1) = FBAR(1,1)+LS**3/(TR*EISHROUD)
      COMPAT(1,2) = FBAR(1,2)
      COMPAT(1,3) = FBAR(1,3)
      COMPAT(2,1) = FBAR(2,1)
      COMPAT(2,2) = FBAR(2,2)+LS/(EASHROUD)
      COMPAT(2,3) = FBAR(2,3)
      COMPAT(3,1) = FBAR(3,1)
      COMPAT(3,2) = FBAR(3,2)
      COMPAT(3,3) = FBAR(3,3)+LS**3/(TR*EISHROUD)

      RHS(1,1) = ZERO
      RHS(2,1) = LS*ALPHA*TMPR
      RHS(3,1) = ZERO

      IDGT = 0
      IA = 3
      KOUNT1 = 3
      CALL LINV1F(COMPAT,KOUNT1,IA,INVCOMPAT,IDGT,WKAREA,IER)

      KOUNT1 = 3
      KOUNT2 = 1
      CALL MULMATX(INVCOMPAT,RHS,FORCE3,KOUNT1,KOUNT1,KOUNT2)

      DO 110 KOUNT1 = 1, 3
         FORCEBAR(KOUNT1,1) = FORCE3(KOUNT1,1)
  110 CONTINUE
C
C     OBTAIN DISPLACEMENTS VECTOR AS DELTABAR = FBAR * FORCEBAR
C
      KOUNT1 = 6
      KOUNT2 = 1
      CALL MULMATX(FBAR,FORCEBAR,DELTABAR,KOUNT1,KOUNT1,KOUNT2)
C
C     CONVERT DISPLACEMENTS AND FORCES INTO DIFFERENT SYSTEMS
C
      KOUNT1 = 6
      KOUNT2 = 1
      CALL MULMATX(CG,FORCEBAR,FORCE,KOUNT1,KOUNT1,KOUNT2)
      CALL MULMATX(CT,FORCEBAR,FORCETAN,KOUNT1,KOUNT1,KOUNT2)
```

```
      CALL MULMATX(CG,DELTABAR,DELTA,KOUNT1,KOUNT1,KOUNT2)
      CALL MULMATX(CT,DELTABAR,DELTATAN,KOUNT1,KOUNT1,KOUNT2)
C
C     CONVERT ANGULAR DISPLACEMENTS INTO DEGREES
C
      DO 109 KOUNT1 = 4, 6
         DELTABAR(KOUNT1,1) = DELTABAR(KOUNT1,1)*1.8D2/PI
         DELTA(KOUNT1,1) = DELTA(KOUNT1,1)*1.8D2/PI
         DELTATAN(KOUNT1,1) = DELTATAN(KOUNT1,1)*1.8D2/PI
  109 CONTINUE
      DISTANCE = DSQRT(DELTABAR(1,1)**2 + DELTABAR(2,1)**2 +
     1                 DELTABAR(3,1)**2)
      DIST1 = DSQRT(DELTA(1,1)**2 + DELTA(2,1)**2 +
     1                 DELTA(3,1)**2)
      DIST2 = DSQRT(DELTATAN(1,1)**2 + DELTATAN(2,1)**2 +
     1                 DELTATAN(3,1)**2)
C
C     WRITE THE RESULTS IN THE OUTPUT FILES OPENED
C
      WRITE(12,*) CVAL, TVAL, DELTABAR(1,1)
      WRITE(13,*) CVAL, TVAL, DELTABAR(2,1)
      WRITE(14,*) CVAL, TVAL, DELTABAR(3,1)
      WRITE(15,*) CVAL, TVAL, DELTABAR(4,1)
      WRITE(16,*) CVAL, TVAL, DELTABAR(5,1)
      WRITE(17,*) CVAL, TVAL, DELTABAR(6,1)
      WRITE(34,*) CVAL, TVAL, FORCEBAR(1,1)
      WRITE(18,*) CVAL, TVAL, FORCEBAR(2,1)
      WRITE(37,*) CVAL, TVAL, FORCEBAR(3,1)
      WRITE(33,*) CVAL, TVAL, DISTANCE
C
C     START OVER WITH NEW CUR AND TOR VALUES
C
      CUR = CUR*FACTOR
      CVAL = CVAL + 6.25D-2
  200 CONTINUE
      TOR = TOR*FACTOR
      TVAL = TVAL + 6.25D-2
  100 CONTINUE
      STOP
      END
C
C     MULMATX SUBROUTINE BEGINS
C
      SUBROUTINE MULMATX(MAT1,MAT2,MAT3,L1,L2,L3)
      INTEGER L1, L2, L3, KNT1, KNT2, KNT3
```

```
      REAL*8 MAT1(L1,L2), MAT2(L2,L3), MAT3(L1,L3)
      DO 111 KNT1 = 1, L1
      DO 111 KNT2 = 1, L3
         MAT3(KNT1,KNT2) = 0.0D0
         DO 112 KNT3 = 1, L2
            MAT3(KNT1,KNT2) = MAT3(KNT1,KNT2)+MAT1(KNT1,KNT3)*
     1      MAT2(KNT3,KNT2)
  112    CONTINUE
  111 CONTINUE
      RETURN
      END
C
C     END OF PROGRAM
C
C-----------------------------------------------------------------------
```

APPENDIX D

COMPUTER IMPLEMENTATION OF THE FINITE ELEMENT METHOD

```
C-----------------------------------------------------------------------
C
C                        D E C L A R A T I O N S
C
C-----------------------------------------------------------------------
C
C
      INTEGER I, IA, IDGT, IER, J, NELEM, NI, NJ, NK

      REAL*8 K, KP, LA, LAP, A, IXX, IYY, IXY, E, G
      REAL*8 AA, BB, RATIO, P, PP, R, S, C, S1, C1, L, LTUBE
      REAL*8 DENOM1, DENOM2, DENOM3, PI, RINNER, ROUTER
C
      REAL*8 X0, X1, X2, X3, X4, X5, X6, X7, X9, X10, X11
      REAL*8 X12, X13, X15, X20, X30, X35, X60, X70, X105
      REAL*8 X140, X180, X210, X420
C
C     ARRAYS USED:
C
C     CG         CHORD TO GLOBAL TRANSFORMATION MATRIX
C     GC         GLOBAL TO CHORD TRANSFORMATION MATRIX
C     TG         TANGENT TO GLOBAL TRANSFORMATION MATRIX
C     TC         TANGENT TO CHORD TRANSFORMATION MATRIX
C     TCINV      INVERSE OF TC
C     TRANS      GLOBAL TC MATRIX
C     TRANSINV   INVERSE OF GLOBAL TC MATRIX
C     ELSTIF     ELEMENT STIFFNESS MATRIX
C     GLSTIF     GLOBAL STIFFNESS MATRIX
C     CHDSTF     GLOBAL STIFFNESS MATRIX IN CHORD SYSTEM
C     REDFLEX    REDUCED FLEXIBILITY MATRIX
C     FKNOWN     GLOBAL FORCE VECTOR IN CHORD SYSTEM
C     DELCHD     GLOBAL DISPLACEMENT VECTOR IN CHORD SYSTEM
C
      REAL*8 CG(3,3), GC(3,3), TG(3,3), TC(3,3), TCINV(3,3)
      REAL*8 TRANS(24,24), TRANSINV(24,24), ELSTIF(12,12)
```

```
      REAL*8 GLSTIF(24,24), CHDSTF(24,24), REDFLEX(18,18)
      REAL*8 WKAREA(100), TEMP61(6,1), TEMP18(18,18), TEMP24(24,24)
      REAL*8 FKNOWN(18,1), DELCHD(18,1), CHECK(18,18)
      REAL*8 KBETAALPHA(6,18)
C
C     DOUBLE PRECISION CONSTANTS USED IN STIFFNESS MATRIX DEFINITION
C
      DATA X0,X1,X2,X3,X4/0.0D0,1.0D0,2.0D0,3.0D0,4.0D0/
      DATA X5,X6,X7,X9,X10/5.0D0,6.0D0,7.0D0,9.0D0,1.0D1/
      DATA X11,X12,X13,X15,X20/1.1D1,1.2D1,1.3D1,1.5D1,2.0D1/
      DATA X30,X35,X60,X70,X105/3.0D1,3.5D1,6.0D1,7.0D1,1.05D2/
      DATA X140,X180,X210,X420/1.4D2,1.8D2,2.1D2,4.2D2/
C
      OPEN(UNIT=11,FILE='femdata',STATUS='OLD')
      OPEN(UNIT=12,FILE='femoutput',STATUS='NEW')
C-----------------------------------------------------------------------
C
C     ASSIGN VALUE OF PI USING THE FACT THAT TAN(PI/4) = 1
C
      PI = DATAN(X1)*X4
C
C-----------------------------------------------------------------------
C
C     (I)     READ MATERIAL AND GEOMETRIC PROPERTIES OF EACH ELEMENT
C     (II)    COMPUTE  ELEMENT STIFFNESS MATRIX
C     (III)   ADD THE CONTRIBUTION OF THE ELEMENT TO THE GLOBAL
C             STIFFNESS MATRIX
C
C     THIS ASSUMES CONNECTIVITY INFORMATION, I.E., THE ELEMENTS ARE
C     CONNECTED TO EACH OTHER END TO END IN THE ORDER GIVEN
C
C-----------------------------------------------------------------------
C
C
C     READ GEOMETRICAL AND MATERIAL PROPERTIES
C
      READ(11,*) NELEM, K, KP, LA, LAP, E, G, LTUBE
C
C     COMPUTE GEOMETRICAL PARAMETERS OF THE HELIX
C
      RATIO = LA/K
      AA = LTUBE/DSQRT(X1 + RATIO**2)
      BB = DSQRT(LTUBE**2 - AA**2)
      C1 = AA/LTUBE
      S1 = BB/LTUBE
```

```
      R = C1**2/K
      P = AA/R
      C = DCOS(P)
      S = DSIN(P)
C
C     ASSIGN VALUES TO CG (CHORD TO GLOBAL TRANSFORMATION MATRIX)
C
      DENOM1 = DSQRT(X2*(X1-C))
      DENOM2 = DSQRT(X2*(X1-C) + (P*BB/AA)**2)
      DENOM3 = DENOM1*DENOM2
      CG(1,1) = S/DENOM1
      CG(1,2) = (C-X1)/DENOM2
      CG(1,3) = (X1-C)*(P*BB/AA)/DENOM3
      CG(2,1) = (X1-C)/DENOM1
      CG(2,2) = S/DENOM2
      CG(2,3) = -(S*P*BB/AA)/DENOM3
      CG(3,1) = XO
      CG(3,2) = (P*BB/AA)/DENOM2
      CG(3,3) = X2*(X1-C)/DENOM3
C
C     INVERT CG TO OBTAIN GC (GLOBAL TO CHORD TRANSFORMATION MATRIX)
C
      IDGT = 0
      IA = 3
      NI = 3
      CALL LINV1F(CG, NI, IA, GC, IDGT, WKAREA, IER)
C
C     INITIALIZE ELEMENT AND GLOBAL STIFFNESS MATRICES, TRANSFORMATION
C     MATRICES, GLOBAL FORCE VECTOR, CONNECTIVES I AND J, AND ANGLE PP
C     SUBTENDED BY ARC AT GLOBAL ORIGIN
C
      DO 100 NI = 1, 12
      DO 100 NJ = 1, 12
         ELSTIF(NI,NJ) = XO
  100 CONTINUE
      DO 101 NI = 1, 6*(NELEM+1)
      DO 101 NJ = 1, 6*(NELEM+1)
         GLSTIF(NI,NJ) = XO
         TRANS(NI,NJ) = XO
         TRANSINV(NI,NJ) = XO
  101 CONTINUE
      DO 102 NI = 1, 6*NELEM
         FKNOWN(NI,1) = XO
  102 CONTINUE
      I = 0
```

```
      J = 0
      PP = XO
C
C     READ APPLIED FORCES AND MOMENTS
C
      READ(11,*) (FKNOWN(6*(NELEM-1)+NI,1), NI = 1, 6)
C
C     FOR EACH ELEMENT, DO THE FOLLOWING:
C
      DO 200 NK = 1, NELEM

         READ(11,*) RINNER, ROUTER, L

         A = PI*(ROUTER**2-RINNER**2)
         IXX = PI*(ROUTER**4-RINNER**4)/X4
         IYY = IXX
         IXY = XO

       ELSTIF(1,1) = X13*L*(E*(IXX*LAP**2+A*K**2)+G*IXX*K**2*LA**2)/X35
     1   +X12*((E*IXX*LA**2+G*IYY*K**2)/X2-E*IXY*LAP)/(X5*L)-E*IXX*LA
     2   *LAP-G*IXY*K**2*LA+X12*E*IYY/L**3

       ELSTIF(1,2) = (-X13)*IXY*L*(E*LAP**2+G*K**2*LA**2)/X35-(-X2*E*
     1   IXY*LA*LAP-G*IYY*K**2*LA+G*IXX*K**2*LA)/X2+(-X6)*(-E*IYY*LAP+
     2   E*IXX*LAP-IXY*(G*K**2-E*LA**2))/(X5*L)+X12*E*IXY/L**3

       ELSTIF(1,3) = X7*IXY*L*(E*KP*LAP+G*K**3*LA)/X20-(E*IXY*K*LAP+E*
     1   IXY*KP*LA+G*IYY*K**3-A*E*K)/X2+(E*IXY*K*LA-E*IYY*KP)/L

       ELSTIF(1,4) = X11*IXY*L**2*(E*LAP**2+G*K**2*LA**2)/X210-(E*IYY*
     1   LAP-X11*E*IXX*LAP+IXY*(G*K**2-E*LA**2))/X10-L*(G*IYY*K**2*LA
     2   +G*IXX*K**2*LA)/X10-(E*IYY*LA+E*IXX*LA)/L-X6*E*IXY/L**2

       ELSTIF(1,5) = X11*L**2*(E*(IXX*LAP**2+A*K**2)+G*IXX*K**2*LA**2)
     1   /X210+((E*IXX*LA**2+G*IYY*K**2)/X2-X6*E*IXY*LAP)/X5+X6*E*IYY
     2   /L**2

       ELSTIF(1,6) = X7*L*(G*IXY*K*LA**2-E*IXX*K*LAP)/X20-(G*IYY*K*LA+
     1   G*IXX*K*LA-E*IXX*K*LA)/X2+(G*IXY*K+E*IXY*K)/L

       ELSTIF(1,7) = X9*L*(E*(IXX*LAP**2+A*K**2)+G*IXX*K**2*LA**2)/X70+
     1   X12*(E*IXY*LAP-(E*IXX*LA**2+G*IYY*K**2)/X2)/(X5*L)-X12*E*IYY/
     2   L**3

       ELSTIF(1,8) = (-X9)*IXY*L*(E*LAP**2+G*K**2*LA**2)/X70+X6*(-E*IYY
```

```
     1    *LAP+E*IXX*LAP-IXY*(G*K**2-E*LA**2))/(X5*L)+(G*IYY*K**2*LA+G*
     2    IXX*K**2*LA)/X2-X12*E*IXY/L**3

      ELSTIF(1,9) = X3*IXY*L*(E*KP*LAP+G*K**3*LA)/X20+(E*IXY*K*LAP-E*
     1    IXY*KP*LA-G*IYY*K**3-A*E*K)/X2+(E*IYY*KP-E*IXY*K*LA)/L

      ELSTIF(1,10) = (-X13)*IXY*L**2*(E*LAP**2+G*K**2*LA**2)/X420-(E*
     1    IYY*LAP-E*IXX*LAP+IXY*(G*K**2-E*LA**2))/X10-L*(-G*IYY*K**2*LA
     2    -G*IXX*K**2*LA)/X10-(-E*IYY*LA-E*IXX*LA)/L-X6*E*IXY/L**2

      ELSTIF(1,11) = (-X13)*L**2*(E*(IXX*LAP**2+A*K**2)+G*IXX*K**2*
     1    LA**2)/X420+((E*IXX*LA**2+G*IYY*K**2)/X2-E*IXY*LAP)/X5+X6*E
     2    *IYY/L**2

      ELSTIF(1,12) = X3*L*(G*IXY*K*LA**2-E*IXX*K*LAP)/X20+(-G*IYY*K*LA
     1    +G*IXX*K*LA+E*IXX*K*LA)/X2+(-G*IXY*K-E*IXY*K)/L

      ELSTIF(2,2) = X13*IYY*L*(E*LAP**2+G*K**2*LA**2)/X35+X12*(E*IXY*
     1    LAP+(E*IYY*LA**2+G*IXX*K**2)/X2)/(X5*L)-E*IYY*LA*LAP+G*IXY*
     2    K**2*LA+X12*E*IXX/L**3

      ELSTIF(2,3) = (-X7)*IYY*L*(E*KP*LAP+G*K**3*LA)/X20-(-E*IYY*K*LAP
     1    -E*IYY*KP*LA+G*IXY*K**3)/X2+(-E*IYY*K*LA-E*IXY*KP)/L

      ELSTIF(2,4) = (-X11)*IYY*L**2*(E*LAP**2+G*K**2*LA**2)/X210-(X6*E*
     1    IXY*LAP+(E*IYY*LA**2+G*IXX*K**2)/X2)/X5-X6*E*IXX/L**2

      ELSTIF(2,5) = (-X11)*IXY*L**2*(E*LAP**2+G*K**2*LA**2)/X210+(X11*E
     1    *IYY*LAP-E*IXX*LAP+IXY*(G*K**2-E*LA**2))/X10+L*(-G*IYY*K**2*LA
     2    -G*IXX*K**2*LA)/X10+(-E*IYY*LA-E*IXX*LA)/L+X6*E*IXY/L**2

      ELSTIF(2,6) = X7*L*(E*IXY*K*LAP-G*IYY*K*LA**2)/X20-(IXY*(G*K*LA+
     1    E*K*LA)-G*IXY*K*LA)/X2+(G*IXX*K+E*IXX*K)/L

      ELSTIF(2,7) = (-X9)*IXY*L*(E*LAP**2+G*K**2*LA**2)/X70+X6*(-E*IYY
     1    *LAP+E*IXX*LAP-IXY*(G*K**2-E*LA**2))/(X5*L)+(-G*IYY*K**2*LA-G
     2    *IXX*K**2*LA)/X2-X12*E*IXY/L**3

      ELSTIF(2,8) = X9*IYY*L*(E*LAP**2+G*K**2*LA**2)/X70+X12*(-E*IXY*
     1    LAP-(E*IYY*LA**2+G*IXX*K**2)/X2)/(X5*L)-X12*E*IXX/L**3

      ELSTIF(2,9) = (-X3)*IYY*L*(E*KP*LAP+G*K**3*LA)/X20+(-E*IYY*K*LAP
     1    +E*IYY*KP*LA-G*IXY*K**3)/X2+(E*IYY*K*LA+E*IXY*KP)/L

      ELSTIF(2,10) = X13*IYY*L**2*(E*LAP**2+G*K**2*LA**2)/X420-(E*IXY*
```

```
1    LAP+(E*IYY*LA**2+G*IXX*K**2)/X2)/X5-X6*E*IXX/L**2

 ELSTIF(2,11) = X13*IXY*L**2*(E*LAP**2+G*K**2*LA**2)/X420+(E*IYY*
1    LAP-E*IXX*LAP+IXY*(G*K**2-E*LA**2))/X10+L*(G*IYY*K**2*LA+G*IXX
2    *K**2*LA)/X10+(E*IYY*LA+E*IXX*LA)/L+X6*E*IXY/L**2

 ELSTIF(2,12) = X3*L*(E*IXY*K*LAP-G*IYY*K*LA**2)/X20+(-IXY*(G*K*
1    LA+E*K*LA)-G*IXY*K*LA)/X2+(-G*IXX*K-E*IXX*K)/L

 ELSTIF(3,3) = IYY*(E*KP**2+G*K**4)*L/X3+E*(IYY*K**2+A)/L-E*IYY*K
1    *KP

 ELSTIF(3,4) = IYY*L**2*(E*KP*LAP+G*K**3*LA)/X20-L*(E*IYY*K*LAP-E*
1    IYY*KP*LA+G*IXY*K**3)/X12-E*IXY*K/L+E*IXY*KP

 ELSTIF(3,5) = IXY*L**2*(E*KP*LAP+G*K**3*LA)/X20+L*(-E*IXY*K*LAP+E
1    *IXY*KP*LA+G*IYY*K**3+A*E*K)/X12+E*IYY*K/L-E*IYY*KP

 ELSTIF(3,6) = L*(G*IYY*K**2*LA-E*IXY*K*KP)/X3-(G*IXY*K**2-E*IXY*
1    K**2)/X2

 ELSTIF(3,7) = X3*IXY*L*(E*KP*LAP+G*K**3*LA)/X20+(-E*IXY*K*LAP+E*
1    IXY*KP*LA+G*IYY*K**3+A*E*K)/X2+(E*IYY*KP-E*IXY*K*LA)/L

 ELSTIF(3,8) = (-X3)*IYY*L*(E*KP*LAP+G*K**3*LA)/X20+(E*IYY*K*LAP-
1    E*IYY*KP*LA+G*IXY*K**3)/X2+(E*IYY*K*LA+E*IXY*KP)/L

 ELSTIF(3,9) = IYY*(E*KP**2+G*K**4)*L/X6-E*(IYY*K**2+A)/L

 ELSTIF(3,10) = -IYY*L**2*(E*KP*LAP+G*K**3*LA)/X30-L*(-E*IYY*K*LAP
1    +E*IYY*KP*LA-G*IXY*K**3)/X12+E*IXY*K/L

 ELSTIF(3,11) = -IXY*L**2*(E*KP*LAP+G*K**3*LA)/X30+L*(E*IXY*K*LAP-
1    E*IXY*KP*LA-G*IYY*K**3-A*E*K)/X12-E*IYY*K/L

 ELSTIF(3,12) = L*(G*IYY*K**2*LA-E*IXY*K*KP)/X6+(G*IXY*K**2+E*IXY*
1    K**2)/X2

 ELSTIF(4,4) = IYY*L**3*(E*LAP**2+G*K**2*LA**2)/X105+X4*L*(E*IXY*
1    LAP+(E*IYY*LA**2+G*IXX*K**2)/X2)/X15+E*IXY*LA+X4*E*IXX/L

 ELSTIF(4,5) = IXY*L**3*(E*LAP**2+G*K**2*LA**2)/X105+(-X2)*L*(E*
1    IYY*LAP-E*IXX*LAP+IXY*(G*K**2-E*LA**2))/X15+(E*IXX*LA-E*IYY*
2    LA)/X2-X4*E*IXY/L
```

```
 ELSTIF(4,6) = -L**2*(E*IXY*K*LAP-G*IYY*K*LA**2)/X20-L*(IXY*(G*K*
1    LA+E*K*LA)+G*IXY*K*LA)/X12-E*IXX*K

 ELSTIF(4,7) = X13*IXY*L**2*(E*LAP**2+G*K**2*LA**2)/X420-(-E*IYY*
1    LAP+E*IXX*LAP-IXY*(G*K**2-E*LA**2))/X10-L*(-G*IYY*K**2*LA-G*
2    IXX*K**2*LA)/X10-(-E*IYY*LA-E*IXX*LA)/L+X6*E*IXY/L**2

 ELSTIF(4,8) = (-X13)*IYY*L**2*(E*LAP**2+G*K**2*LA**2)/X420-(-E*
1    IXY*LAP-(E*IYY*LA**2+G*IXX*K**2)/X2)/X5+X6*E*IXX/L**2

 ELSTIF(4,9) = IYY*L**2*(E*KP*LAP+G*K**3*LA)/X30-L*(-E*IYY*K*LAP+E
1    *IYY*KP*LA-G*IXY*K**3)/X12+E*IXY*K/L

 ELSTIF(4,10) = -IYY*L**3*(E*LAP**2+G*K**2*LA**2)/X140+L*(-E*IXY*
1    LAP-(E*IYY*LA**2+G*IXX*K**2)/X2)/X15+X2*E*IXX/L

 ELSTIF(4,11) = -IXY*L**3*(E*LAP**2+G*K**2*LA**2)/X140-L*(-E*IYY*
1    LAP+E*IXX*LAP-IXY*(G*K**2-E*LA**2))/X30-L**2*(G*IYY*K**2*LA+G*
2    IXX*K**2*LA)/X60-(E*IYY*LA+E*IXX*LA)/X2-X2*E*IXY/L

 ELSTIF(4,12) = -L**2*(E*IXY*K*LAP-G*IYY*K*LA**2)/X30-L*(-IXY*(G*K
1    *LA+E*K*LA)-G*IXY*K*LA)/X12

 ELSTIF(5,5) = L**3*(E*(IXX*LAP**2+A*K**2)+G*IXX*K**2*LA**2)/X105+
1    X4*L*((E*IXX*LA**2+G*IYY*K**2)/X2-E*IXY*LAP)/X15-E*IXY*LA+X4*
2    E*IYY/L

 ELSTIF(5,6) = L**2*(G*IXY*K*LA**2-E*IXX*K*LAP)/X20+L*(G*IYY*K*LA-
1    G*IXX*K*LA-E*IXX*K*LA)/X12+E*IXY*K

 ELSTIF(5,7) = X13*L**2*(E*(IXX*LAP**2+A*K**2)+G*IXX*K**2*LA**2)/
1    X420+(E*IXY*LAP-(E*IXX*LA**2+G*IYY*K**2)/X2)/X5-X6*E*IYY/L**2

 ELSTIF(5,8) = (-X13)*IXY*L**2*(E*LAP**2+G*K**2*LA**2)/X420+(-E*
1    IYY*LAP+E*IXX*LAP-IXY*(G*K**2-E*LA**2))/X10+L*(G*IYY*K**2*LA
2    +G*IXX*K**2*LA)/X10+(E*IYY*LA+E*IXX*LA)/L-X6*E*IXY/L**2

 ELSTIF(5,9) = IXY*L**2*(E*KP*LAP+G*K**3*LA)/X30+L*(E*IXY*K*LAP-E*
1    IXY*KP*LA-G*IYY*K**3-A*E*K)/X12-E*IYY*K/L

 ELSTIF(5,10) = -IXY*L**3*(E*LAP**2+G*K**2*LA**2)/X140-L*(-E*IYY*
1    LAP+E*IXX*LAP-IXY*(G*K**2-E*LA**2))/X30-L**2*(-G*IYY*K**2*LA-
2    G*IXX*K**2*LA)/X60-(-E*IYY*LA-E*IXX*LA)/X2-X2*E*IXY/L

 ELSTIF(5,11) = -L**3*(E*(IXX*LAP**2+A*K**2)+G*IXX*K**2*LA**2)/X140
```

```
1    +L*(E*IXY*LAP-(E*IXX*LA**2+G*IYY*K**2)/X2)/X15+X2*E*IYY/L

 ELSTIF(5,12) = L**2*(G*IXY*K*LA**2-E*IXX*K*LAP)/X30+L*(-G*IYY*K*
1    LA+G*IXX*K*LA+E*IXX*K*LA)/X12

 ELSTIF(6,6) = L*(IXX*(G*LA**2+E*K**2)+G*IYY*LA**2)/X3+G*(IYY+IXX)
1    /L

 ELSTIF(6,7) = X3*L*(G*IXY*K*LA**2-E*IXX*K*LAP)/X20+(G*IYY*K*LA-G
1    *IXX*K*LA-E*IXX*K*LA)/X2+(-G*IXY*K-E*IXY*K)/L

 ELSTIF(6,8) = X3*L*(E*IXY*K*LAP-G*IYY*K*LA**2)/X20+(IXY*(G*K*LA+
1    E*K*LA)+G*IXY*K*LA)/X2+(-G*IXX*K-E*IXX*K)/L

 ELSTIF(6,9) = L*(G*IYY*K**2*LA-E*IXY*K*KP)/X6+(-G*IXY*K**2-E*IXY*
1    K**2)/X2

 ELSTIF(6,10) = L**2*(E*IXY*K*LAP-G*IYY*K*LA**2)/X30-L*(-IXY*(G*K*
1    LA+E*K*LA)-G*IXY*K*LA)/X12

 ELSTIF(6,11) = L*(-G*IYY*K*LA+G*IXX*K*LA+E*IXX*K*LA)/X12-L**2*(G*
1    IXY*K*LA**2-E*IXX*K*LAP)/X30

 ELSTIF(6,12) = L*(IXX*(G*LA**2+E*K**2)+G*IYY*LA**2)/X6-G*(IYY+IXX
1    )/L

 ELSTIF(7,7) = X13*L*(E*(IXX*LAP**2+A*K**2)+G*IXX*K**2*LA**2)/X35
1    +X12*((E*IXX*LA**2+G*IYY*K**2)/X2-E*IXY*LAP)/(X5*L)+E*IXX*LA
2    *LAP+G*IXY*K**2*LA+X12*E*IYY/L**3

 ELSTIF(7,8) = (-X13)*IXY*L*(E*LAP**2+G*K**2*LA**2)/X35+(-X2*E*IXY
1    *LA*LAP-G*IYY*K**2*LA+G*IXX*K**2*LA)/X2+X6*(E*IYY*LAP-E*IXX*
2    LAP+IXY*(G*K**2-E*LA**2))/(X5*L)+X12*E*IXY/L**3

 ELSTIF(7,9) = X7*IXY*L*(E*KP*LAP+G*K**3*LA)/X20+(E*IXY*K*LAP+E*
1    IXY*KP*LA+G*IYY*K**3-A*E*K)/X2+(E*IXY*K*LA-E*IYY*KP)/L

 ELSTIF(7,10) = (-X11)*IXY*L**2*(E*LAP**2+G*K**2*LA**2)/X210-(-E*
1    IYY*LAP+X11*E*IXX*LAP-IXY*(G*K**2-E*LA**2))/X10-L*(G*IYY*K**2
2    *LA+G*IXX*K**2*LA)/X10-(E*IYY*LA+E*IXX*LA)/L+X6*E*IXY/L**2

 ELSTIF(7,11) = (-X11)*L**2*(E*(IXX*LAP**2+A*K**2)+G*IXX*K**2*
1    LA**2)/X210+(X6*E*IXY*LAP-(E*IXX*LA**2+G*IYY*K**2)/X2)/X5-X6*E
2    *IYY/L**2
```

```
      ELSTIF(7,12) = X7*L*(G*IXY*K*LA**2-E*IXX*K*LAP)/X20+(G*IYY*K*LA+
     1   G*IXX*K*LA-E*IXX*K*LA)/X2+(G*IXY*K+E*IXY*K)/L

      ELSTIF(8,8) = X13*IYY*L*(E*LAP**2+G*K**2*LA**2)/X35+X12*(E*IXY*
     1   LAP+(E*IYY*LA**2+G*IXX*K**2)/X2)/(X5*L)+E*IYY*LA*LAP-G*IXY*
     2   K**2*LA+X12*E*IXX/L**3

      ELSTIF(8,9) = (-X7)*IYY*L*(E*KP*LAP+G*K**3*LA)/X20+(-E*IYY*K*LAP
     1   -E*IYY*KP*LA+G*IXY*K**3)/X2+(-E*IYY*K*LA-E*IXY*KP)/L

      ELSTIF(8,10) = X11*IYY*L**2*(E*LAP**2+G*K**2*LA**2)/X210-(-X6*E*
     1   IXY*LAP-(E*IYY*LA**2+G*IXX*K**2)/X2)/X5+X6*E*IXX/L**2

      ELSTIF(8,11) = X11*IXY*L**2*(E*LAP**2+G*K**2*LA**2)/X210+(-X11*E*
     1   IYY*LAP+E*IXX*LAP-IXY*(G*K**2-E*LA**2))/X10+L*(-G*IYY*K**2*LA-
     2   G*IXX*K**2*LA)/X10+(-E*IYY*LA-E*IXX*LA)/L-X6*E*IXY/L**2

      ELSTIF(8,12) = X7*L*(E*IXY*K*LAP-G*IYY*K*LA**2)/X20+(IXY*(G*K*LA
     1   +E*K*LA)-G*IXY*K*LA)/X2+(G*IXX*K+E*IXX*K)/L

      ELSTIF(9,9) = IYY*(E*KP**2+G*K**4)*L/X3+E*(IYY*K**2+A)/L+E*IYY*K*
     1   KP

      ELSTIF(9,10) = -IYY*L**2*(E*KP*LAP+G*K**3*LA)/X20-L*(E*IYY*K*LAP-
     1   E*IYY*KP*LA+G*IXY*K**3)/X12-E*IXY*K/L-E*IXY*KP

      ELSTIF(9,11) = -IXY*L**2*(E*KP*LAP+G*K**3*LA)/X20+L*(-E*IXY*K*LAP
     1   +E*IXY*KP*LA+G*IYY*K**3+A*E*K)/X12+E*IYY*K/L+E*IYY*KP

      ELSTIF(9,12) = L*(G*IYY*K**2*LA-E*IXY*K*KP)/X3+(G*IXY*K**2-E*IXY*
     1   K**2)/X2

      ELSTIF(10,10) = IYY*L**3*(E*LAP**2+G*K**2*LA**2)/X105+X4*L*(E*
     1   IXY*LAP+(E*IYY*LA**2+G*IXX*K**2)/X2)/X15-E*IXY*LA+X4*E*IXX/L

      ELSTIF(10,11) = IXY*L**3*(E*LAP**2+G*K**2*LA**2)/X105+(-X2)*L*(E
     1   *IYY*LAP-E*IXX*LAP+IXY*(G*K**2-E*LA**2))/X15-(E*IXX*LA-E*IYY*
     2   LA)/X2-X4*E*IXY/L

      ELSTIF(10,12) = L**2*(E*IXY*K*LAP-G*IYY*K*LA**2)/X20-L*(IXY*(G*K*
     1   LA+E*K*LA)+G*IXY*K*LA)/X12+E*IXX*K

      ELSTIF(11,11) = L**3*(E*(IXX*LAP**2+A*K**2)+G*IXX*K**2*LA**2)/
     1   X105+X4*L*((E*IXX*LA**2+G*IYY*K**2)/X2-E*IXY*LAP)/X15+E*IXY*
     2   LA+X4*E*IYY/L
```

```
      ELSTIF(11,12) = -L**2*(G*IXY*K*LA**2-E*IXX*K*LAP)/X20+L*(G*IYY*K*
     1   LA-G*IXX*K*LA-E*IXX*K*LA)/X12-E*IXY*K

      ELSTIF(12,12) = L*(IXX*(G*LA**2+E*K**2)+G*IYY*LA**2)/X3+G*(IYY+
     1   IXX)/L
C
C        ASSIGN REMAINING ELEMENTS IN SYMMETRIC FASHION
C
         DO 300 NI = 2, 12
         DO 300 NJ = 1, NI-1
            ELSTIF(NI,NJ) = ELSTIF(NJ,NI)
  300    CONTINUE
C
C        COMPUTE GLOBAL STIFFNESS MATRIX (IN THE TANGENT SYSTEM)
C
         DO 301 NI = 1, 12
         DO 301 NJ = 1, 12
            GLSTIF(I+NI,J+NJ) = GLSTIF(I+NI,J+NJ) + ELSTIF(NI,NJ)
  301    CONTINUE
C
C        ASSIGN VALUES TO TG (TANGENT TO GLOBAL TRANSFORMATION MATRIX)
C        EVALUATED FOR NODE# 1 OF THE ELEMENT
C
         TG(1,1) = -DCOS(PP)
         TG(1,2) = S1*DSIN(PP)
         TG(1,3) = -C1*DSIN(PP)
         TG(2,1) = -DSIN(PP)
         TG(2,2) = -S1*DCOS(PP)
         TG(2,3) = C1*DCOS(PP)
         TG(3,1) = XO
         TG(3,2) = C1
         TG(3,3) = S1
C
C        COMPUTE TC (TANGENT TO CHORD TRANSFORMATION MATRIX) FOR
C        NODE# 1 OF THE ELEMENT
C
         NI = 3
         CALL MULMATX(GC, TG, TC, NI, NI, NI)
C
C        FILL IN CORRESPONDING ELEMENTS OF TRANS
C
         DO 302 NI = 1, 3
         DO 302 NJ = 1, 3
            TRANS(I+NI,J+NJ) = TRANS(I+NI,J+NJ) + TC(NI,NJ)
            TRANS(I+NI+3,J+NJ+3) = TRANS(I+NI+3,J+NJ+3) + TC(NI,NJ)
```

```
  302    CONTINUE
C
C        INVERT TC TO OBTAIN TCINV FOR NODE# 1 OF THE ELEMENT
C
         IDGT = 0
         IA = 3
         NI = 3
         CALL LINV1F(TC, NI, IA, TCINV, IDGT, WKAREA, IER)
C
C        FILL IN CORRESPONDING ELEMENTS OF TRANSINV
C
         DO 303 NI = 1, 3
         DO 303 NJ = 1, 3
            TRANSINV(I+NI,J+NJ) = TRANSINV(I+NI,J+NJ) + TCINV(NI,NJ)
            TRANSINV(I+NI+3,J+NJ+3) = TRANSINV(I+NI+3,J+NJ+3)
     1                              + TCINV(NI,NJ)
  303    CONTINUE
C
C        COMPUTE PP FOR NODE# 2 OF THE ELEMENT
C
         PP = PP + P*L/LTUBE
C
C        ASSIGN VALUES TO TG (TANGENT TO GLOBAL TRANSFORMATION MATRIX)
C        EVALUATED FOR NODE# 1 OF THE ELEMENT
C
         TG(1,1) = -DCOS(PP)
         TG(1,2) = S1*DSIN(PP)
         TG(1,3) = -C1*DSIN(PP)
         TG(2,1) = -DSIN(PP)
         TG(2,2) = -S1*DCOS(PP)
         TG(2,3) = C1*DCOS(PP)
         TG(3,1) = XO
         TG(3,2) = C1
         TG(3,3) = S1
C
C        COMPUTE TC (TANGENT TO CHORD TRANSFORMATION MATRIX) FOR
C        NODE# 2 OF THE ELEMENT
C
         NI = 3
         CALL MULMATX(GC, TG, TC, NI, NI, NI)
C
C        FILL IN CORRESPONDING ELEMENTS OF TRANS
C
         DO 304 NI = 1, 3
         DO 304 NJ = 1, 3
```

```
            TRANS(I+NI+6,J+NJ+6) = TRANS(I+NI+6,J+NJ+6) + TC(NI,NJ)
            TRANS(I+NI+9,J+NJ+9) = TRANS(I+NI+9,J+NJ+9) + TC(NI,NJ)
  304    CONTINUE
C
C        INVERT TC TO OBTAIN TCINV FOR NODE# 2 OF THE ELEMENT
C
         IDGT = 0
         IA = 3
         NI = 3
         CALL LINV1F(TC, NI, IA, TCINV, IDGT, WKAREA, IER)
C
C        FILL IN CORRESPONDING ELEMENTS OF TRANSINV
C
         DO 305 NI = 1, 3
         DO 305 NJ = 1, 3
            TRANSINV(I+NI+6,J+NJ+6) = TRANSINV(I+NI+6,J+NJ+6)
     1                               + TCINV(NI,NJ)
            TRANSINV(I+NI+9,J+NJ+9) = TRANSINV(I+NI+9,J+NJ+9)
     1                               + TCINV(NI,NJ)
  305    CONTINUE
C
C        INCREMENT CONNECTIVES I AND J BY DOF/NODE = 6
C
         I = I + 6
         J = J + 6
C
C        LOOP BACK
C
  200 CONTINUE
C
C     OBTAIN CHDSTF, GLOBAL STIFFNESS MATRIX IN THE CHORD SYSTEM, AS:
C                    CHDSTF = TRANS * GLSTIF *  TRANSINV
C
      NI = 6*(NELEM+1)
      CALL MULMATX(TRANS, GLSTIF, TEMP24, NI, NI, NI)
      NI = 6*(NELEM+1)
      CALL MULMATX(TEMP24, TRANSINV, CHDSTF, NI, NI, NI)
C
C     OBTAIN REDFLEX, A SUBMATRIX OF THE GLOBAL FLEXIBILITY
C     MATRIX BY INVERTING A SUBMATRIX OF CHDSTF OF DIMENSIONS
C     6*NELEM x 6*NELEM, I.E., WHICH EXCLUDES ELEMENTS
C     CORRESPONDING TO THE FIRST NODE WHOSE DISPLACEMENTS ARE
C     KNOWN TO BE ZERO
C
      DO 210 NI = 7, 6*(NELEM+1)
```

```
      DO 210 NJ = 7, 6*(NELEM+1)
         TEMP18(NI-6,NJ-6) = CHDSTF(NI,NJ)
  210 CONTINUE
      IDGT = 0
      IA = 6*NELEM
      NI = 6*NELEM
      CALL LINV1F(TEMP18, NI, IA, REDFLEX, IDGT, WKAREA, IER)
      DO 900 NI = 7, 6*(NELEM+1)
      DO 900 NJ = 7, 6*(NELEM+1)
         TEMP18(NI-6,NJ-6) = CHDSTF(NI,NJ)
  900 CONTINUE
      NI = 6*NELEM
      CALL MULMATX(REDFLEX,TEMP18,CHECK,NI,NI,NI)
C
C     OBTAIN DISPLACEMENTS DELCHD = REDFLEX * FKNOWN IN CHORD SYSTEM
C
      NI = 6*NELEM
      NJ = 1
      CALL MULMATX(REDFLEX, FKNOWN, DELCHD, NI, NI, NJ)
C
C     COMPUTE REACTIONS FROM THE ABOVE DISPLACEMENTS
C
      DO 903 NI = 1, 6
      DO 903 NJ = 7, 6*(NELEM+1)
         KBETAALPHA(NI,NJ-6) = CHDSTF(NI,NJ)
  903 CONTINUE
      NI = 6
      NJ = 6*NELEM
      NK = 1
      CALL MULMATX(KBETAALPHA,DELCHD,TEMP61,NI,NJ,NK)
C
C     WRITE COMPUTED REACTIONS IN CHORD SYSTEM TO FILE "FEMOUTPUT"
C
      WRITE(12,*)
      WRITE(12,*) 'COMPUTED REACTIONS IN CHORD SYSTEM'
      WRITE(12,*)
      WRITE(12,*) (TEMP61(NI,1), NI = 1, 6)
      WRITE(12,*)
C
C     CONVERT RADIANS INTO DEGREES
C
      DO 212 NI = 1, NELEM
      DO 212 NJ = 1, 3
         DELCHD((6*NI-NJ+1),1) = DELCHD((6*NI-NJ+1),1)*X180/PI
  212 CONTINUE
```

```
C
C     WRITE CHECK TO FILE "FEMOUTPUT"
C
C     WRITE(12,*) 'FLEX CHECK:'
C     DO 901 NI = 1, 6*NELEM
C        WRITE(12,*) (CHECK(NI,NJ), NJ = 1, 6*NELEM)
C 901 CONTINUE
C
C     WRITE END DISPLACEMENT TO FILE "FEMOUTPUT"
C
      WRITE(12,*)
      WRITE(12,*) 'END DISPLACEMENT IN CHORD SYSTEM:'
      WRITE(12,*)
      WRITE(12,*) 'Delx = ', DELCHD(6*(NELEM-1)+1,1), 'm'
      WRITE(12,*) 'Dely = ', DELCHD(6*(NELEM-1)+2,1), 'm'
      WRITE(12,*) 'Delz = ', DELCHD(6*(NELEM-1)+3,1), 'm'
      WRITE(12,*) 'Thex = ', DELCHD(6*(NELEM-1)+4,1), 'deg'
      WRITE(12,*) 'They = ', DELCHD(6*(NELEM-1)+5,1), 'deg'
      WRITE(12,*) 'Thez = ', DELCHD(6*(NELEM-1)+6,1), 'deg'
C
C     WRITE GLOBAL STIFFNESS MATRIX INTO FILE "FEMOUTPUT"
C
C     WRITE(12,*)
C     WRITE(12,*) 'GLSTIF:'
C     WRITE(12,*)
C     DO 214 NI = 1, 6*(NELEM+1)
C        WRITE(12,*) (INT(GLSTIF(NI,NJ)), NJ = 1, 6*(NELEM+1))
C 214 CONTINUE
C
C     WRITE FKNOWN, GLOBAL FORCE VECTOR TO FILE "FEMOUTPUT"
C
      WRITE(12,*)
      WRITE(12,*) 'FKNOWN VECTOR:'
      WRITE(12,*)
      WRITE(12,*) (FKNOWN(NI,1), NI = 1, 6*NELEM)
C
      STOP
      END
C
C     MULMATX SUBROUTINE BEGINS
C
      SUBROUTINE MULMATX(MAT1,MAT2,MAT3,L1,L2,L3)
      INTEGER L1, L2, L3, KNT1, KNT2, KNT3
      REAL*8 MAT1(L1,L2), MAT2(L2,L3), MAT3(L1,L3)
      DO 10 KNT1 = 1, L1
```

```
      DO 10 KNT2 = 1, L3
        MAT3(KNT1,KNT2) = 0.0D0
         DO 11 KNT3 = 1, L2
            MAT3(KNT1,KNT2) = MAT3(KNT1,KNT2)+MAT1(KNT1,KNT3)*
     1      MAT2(KNT3,KNT2)
   11       CONTINUE
   10    CONTINUE
         RETURN
         END
C
C        END OF PROGRAM
C-------------------------------------------------------------------
```

References

[Kingsbury 84] Kingsbury, Herbert B.
On the Motion of Rods with Initial Space Curvature.
Technical Report BRL-TR-2658, US Army Ballistics Research Laboratory, Maryland, September, 1984.

[Sokolnikoff 66] Sokolnikoff, I. S. and Redheffer, R. M.
Mathematics of Physics and Modern Engineering.
McGraw-Hill Book Company, New York, 1966.

[Tsay 86] Tsay, H. and Kingsbury, H. B.
On the Vibration of Helical Rods.
Master's thesis, University of Delaware, 1986.

[Zienkiewicz 77] Zienkiewicz, O. C.
The Finite Element Method.
McGraw-Hill Book Company (UK) Limited, Berkshire, England, 1977.

DISTRIBUTION LIST

No of Copies	Organization
12	Administrator Defense Technical Info Center ATTN: DTIC-DDA Cameron Station Alexandria, VA 22304-6145
1	HQDA (SARD-TR) Washington, DC 20310-0001
1	Commander US Army Materiel Command ATTN: AMCDRA-ST 5001 Eisenhower Avenue Alexandria, VA 22333-0001
1	Commander US Army Laboratory Command ATTN: AMSLC-DL Adelphi, MD 20783-1145
2	Commander Armament RD&E Center US Army AMCCOM ATTN: SMCAR-MSI Picatinny Arsenal, NJ 07806-5000
2	Commander Armament RD&E Center US Army AMCCOM ATTN: SMCAR-TDC Picatinny Arsenal, NJ 07806-5000
1	Director Benet Weapons Laboratory Armament RD&E Center US Army AMCCOM ATTN: SMCAR-LCB-TL Watervliet, NY 12189-4050
1	Commander US Army Armament, Munitions and Chemical Command ATTN: SMCAR-ESP-L Rock Island, IL 61299-5000
1	Commander US Army Aviation Systems Command ATTN: AMSAV-DACL 4300 Goodfellow Blvd. St. Louis, MO 63120-1798
1	Director US Army Aviation Research and Technology Activity Ames Research Center Moffett Field, CA 94035-1099

No of Copies	Organization
1	Commander US Army Missile Command ATTN: AMSMI-RD-CS-R (DOC) Redstone Arsenal, AL 35898-5241
1	Commander US Army Tank Automotive Command ATTN: AMSTA-TSL Warren, MI 48397-5000
1	Director US Army TRADOC Analysis Command ATTN: ATAA-SL White Sands Missile Range, NM 88002-5502
1	Commandant US Army Infantry School ATTN: ATSH-CD-CSO-OR Fort Benning, GA 31905-5660
1	AFWL/SUL Kirtland AFB, NM 87117-5800
1	Air Force Armament Laboratory ATTN: AFATL/DLODL Eglin AFB, FL 32542-5000
	Aberdeen Proving Ground Dir, USAMSAA ATTN: AMXSY-D AMXSY-MP, H. Cohen Cdr, USATECOM ATTN: AMSTE-TO-F Cdr, CRDEC, AMCCOM ATTN: SMCCR-RSP-A SMCCR-MU SMCCR-MSI

DISTRIBUTION LIST

No of Copies	Organization
1	Commander, ARDEC ATTN: SMCAR-CCH-V B. Kowalski Picatinny Arsenal, NJ 07806-5000
1	Commander, ARDEC ATTN: SMCAR-CCH-V B. Konrad Picatinny Arsenal, NJ 07806-5000
1	Commander, ARDEC ATTN: SMCAR-CCH-T J. Hedderich Picatinny Arsenal, NJ 07806-5000
1	Commander, ARDEC ATTN: SMCAR-CCH-V Ed Fennell Picatinny Arsenal, NJ 07806-5000
1	Commander, ARDEC ATTN: SMCAR-CCH-T S. Musalli Picatinny Arsenal, NJ 07806-5000
1	Commander, ARDEC ATTN: SMCAR-CCH-W Renata Price Picatinny Arsenal, NJ 07806-5000
1	Commander, ARDEC ATTN: SMCAR-TD V. Lindner Picatinny Arsenal, NJ 07806-5000
2	Director Benet Weapons Laboratory, ARDEC ATTN: SMCAR-LCB-DA T. Simkins Watervliet Arsenal Watervliet, NY 12189
2	Director Benet Weapons Laboratory, ARDEC ATTN: SMCAR-LCB-DA L. Johnson Watervliet Arsenal Watervliet, NY 12189
2	Sandia National Laboratory Applied Mechanics Department Engineering Design Division Livermore, CA 94550
1	Project Manager, TMAS ATTN: AMCPM-TMA-120 K. Russell Picatinny Arsenal, NJ 07806-5000
1	Project Manager, TMAS ATTN: AMCPM-TMA-105 C. Kemker Picatinny Arsenal, NJ 07806-5000
1	Project Manager, TMAS ATTN: AMCPM-TMA-105 Ken Rubin Picatinny Arsenal, NJ 07806-5000
1	Project Manager, TMAS ATTN: AMCPM-TMA-105 R. Billington Picatinny Arsenal, NJ 07806-5000
1	Commander U.S. Army Laboratory Command ATTN: AMSLC-DL R. Vitali 2800 Powder Mill Road Adelphi, MD 20783-1145

USER EVALUATION SHEET/CHANGE OF ADDRESS

This laboratory undertakes a continuing effort to improve the quality of the reports it publishes. Your comments/answers below will aid us in our efforts.

1. Does this report satisfy a need? (Comment on purpose, related project, or other area of interest for which the report will be used.) _____

2. How, specifically, is the report being used? (Information source, design data, procedure, source of ideas, etc.) _____

3. Has the information in this report led to any quantitative savings as far as man-hours or dollars saved, operating costs avoided, or efficiencies achieved, etc? If so, please elaborate. _____

4. General Comments. What do you think should be changed to improve future reports? (Indicate changes to organization, technical content, format, etc.) _____

BRL Report Number _____ Division Symbol _____

Check here if desire to be removed from distribution list. ____

Check here for address change. ____

Current address: Organization _____
Address _____

----------FOLD AND TAPE CLOSED----------

Director
U.S. Army Ballistic Research Laboratory
ATTN: SLCBR-DD-T(NEI)
Aberdeen Proving Ground, MD 21005-5066

OFFICIAL BUSINESS
PENALTY FOR PRIVATE USE $300

BUSINESS REPLY LABEL
FIRST CLASS PERMIT NO. 12062 WASHINGTON D.C.
POSTAGE WILL BE PAID BY DEPARTMENT OF THE ARMY

NO POSTAGE NECESSARY IF MAILED IN THE UNITED STATES

Director
U.S. Army Ballistic Research Laboratory
ATTN: SLCBR-DD-T(NEI)
Aberdeen Proving Ground, MD 21005-9989